University of Alberta

Single Drop Microextraction: Principles and Application

by

Michael Andrew Jeannot

A thesis submitted to the Faculty of Graduate Studies and Research in partial fulfillment of the requirements for the degree of Doctor of Philosophy

Department of Chemistry

Edmonton, Alberta

Fall 1997

National Library of Canada

Acquisitions and Bibliographic Services

395 Wellington Street
Ottawa ON K1A 0N4
Canada

Bibliothèque nationale du Canada

Acquisitions et services bibliographiques

395, rue Wellington
Ottawa ON K1A 0N4
Canada

Your file Votre référence

Our file Notre référence

The author has granted a non-exclusive licence allowing the National Library of Canada to reproduce, loan, distribute or sell copies of this thesis in microform, paper or electronic formats.

L'auteur a accordé une licence non exclusive permettant à la Bibliothèque nationale du Canada de reproduire, prêter, distribuer ou vendre des copies de cette thèse sous la forme de microfiche/film, de reproduction sur papier ou sur format électronique.

The author retains ownership of the copyright in this thesis. Neither the thesis nor substantial extracts from it may be printed or otherwise reproduced without the author's permission.

L'auteur conserve la propriété du droit d'auteur qui protège cette thèse. Ni la thèse ni des extraits substantiels de celle-ci ne doivent être imprimés ou autrement reproduits sans son autorisation.

0-612-22996-3

Canada

University of Alberta

Library Release Form

Name of Author: Michael Andrew Jeannot

Title of Thesis: Single Drop Microextraction: Principles and Application

Degree: Doctor of Philosophy

Year this Degree Granted: 1997

Permission is hereby granted to the University of Alberta Library to reproduce single copies of this thesis and to lend or sell such copies for private, scholarly, or scientific research purposes only.

The author reserves all other publication and other rights in association with the copyright in the thesis, and except as hereinbefore provided, neither the thesis nor any substantial portion thereof may be printed or otherwise reproduced in any material form whatever without the author's prior written permission.

63 Newton Crescent
Regina, Saskatchewan, Canada
S4S 2V9

July 21, 1997

University of Alberta

Faculty of Graduate Studies and Research

The undersigned certify that they have read, and recommend to the Faculty of Graduate Studies and Research for acceptance, a thesis entitled Single Drop Microextraction: Principles and Application submitted by Michael Andrew Jeannot in partial fulfillment of the requirements for the degree of Doctor of Philosophy.

Dr. F. Cantwell

Dr. B. Kratochvil

Dr. S. Bergens

Dr. M. McDermott

Dr. R. Batycky

July 18, 1997

Dr. P. Dasgupta
(External examiner)

This work is dedicated to my wife Lori and my parents

for their love and support

Abstract

An analytical technique has been developed using a very small volume of organic solvent to selectively extract and concentrate semi-volatile organic compounds from aqueous samples for analysis by gas chromatography (GC). Two techniques are described in which the single drop of water-immiscible organic solvent (n-octane) is contained either at the end of a Teflon rod or directly on the tip of the GC microsyringe needle in a stirred aqueous sample solution. After stirring for a prescribed time, part or all of the organic phase is injected into the GC for quantification. An internal standard such as n-dodecane is present in the drop at a fixed concentration to correct for post-extraction solvent evaporation and variable GC injection volumes. The methodology has been shown to be reproducible (~2% relative standard deviation), fast (analysis times of 1-10 minutes), simple to perform, and inexpensive.

Both equilibrium and kinetic aspects of the extraction process have been characterized extensively. Extraction rate curves (plots of concentration in the drop versus stirring time) are used to obtain both equilibrium and kinetic data. The dependence of the mass transfer rate on stirring rate has been elucidated for both the Teflon rod system and the microsyringe needle system. It is linear for the latter system. The extraction kinetics have been interpreted in terms of two mass transfer models, film theory and penetration theory. It has been found experimentally that the aqueous phase mass transfer coefficient is directly proportional to the aqueous phase diffusion coefficient using model compounds 4-nitrotoluene, 4-methylacetophenone, malathion, and progesterone. This is consistent with the film theory of convective-diffusive mass transfer. Both theory and experiment show that it is not necessary to reach equilibrium in an analytical application, thus greatly reducing the analysis time.

The solvent microextraction technique has been successfully applied to speciation studies of the steroid hormone progesterone in an aqueous protein (bovine

serum albumin) matrix, where only the unbound species of progesterone extracts. The binding of progesterone by protein has some interesting implications for both the equilibrium and kinetic aspects of the extraction process. A mass transfer model which incorporates diffusion of both free and bound forms of progesterone in the aqueous Nernst diffusion film explains the increased rate constant for extraction with protein present, and agrees quantitatively with experimental data. At a protein concentration of 1% (w/v), 20% of the progesterone is in the free (unbound) form. The measured binding constant (2.5×10^4 L/mol) is in agreement with other values reported in the literature using more traditional approaches, such as equilibrium dialysis.

The method described here shows great potential as a tool for rapid analysis by solvent extraction/GC. The advantages of a liquid-liquid method combined with the simplicity of the single drop technique make this method a promising alternative to other sample cleanup/preconcentration approaches.

Acknowledgements

I would like to thank my supervisor, Dr. Fred Cantwell, for his patience and dedication throughout the past four years. I would also like to acknowledge Dr. J. W. Lown for kindly allowing the use of his HP5840A gas chromatograph for these studies. Many thanks to the staff of the machine shop and electronics shop for their invaluable assistance.

Finally, I would like to thank the Natural Sciences and Engineering Research Council (NSERC) and the University of Alberta for financial assistance.

Table of Contents

CHAPTER 1 - INTRODUCTION		1
1.1	Conventional sample preparation approaches	1
	1.1.1 Conventional solvent extraction	1
	1.1.2 Solvent extraction - flow injection analysis	2
	1.1.3 Solid phase extraction	3
	1.1.4 Solid phase microextraction	4
	1.1.5 Gas phase methods	5
	1.1.6 Membrane techniques	7
1.2	Solvent microextraction into a single drop	8
CHAPTER 2 - THEORY		12
2.1	Introduction	12
2.2	Equilibrium considerations	12
2.3	Kinetic considerations	13
2.4	Mass transfer models	18
	2.4.1 Film theory	18
	2.4.2 Penetration theory	20
2.5	Analytical methodology	23
CHAPTER 3 - MEASUREMENT OF DIFFUSION COEFFICIENTS		28
3.1	The Taylor dispersion method	28
3.2	Experimental details	31
3.3	Results and discussion	33
CHAPTER 4 - TEFLON ROD SYSTEM		42
4.1	Introduction	42
4.2	Experimental details	43
	4.2.1 Chemicals	43

4.2.2 Apparatus 43
4.2.3 Extraction studies 44
4.3 Results and discussion 45
4.3.1 Flow pattern 45
4.3.2 Kinetics 45
4.3.3 Dissolution of n-octane 50
4.3.4 Analytical methodology 51
4.3.4.1 Distribution isotherm 51
4.3.4.2 Calibration and precision 52
CHAPTER 5 - SYRINGE NEEDLE SYSTEM AND MASS TRANSFER MODEL 63
5.1 Introduction 63
5.2 Experimental details 64
5.2.1 Chemicals 64
5.2.2 Apparatus 64
5.2.3 Extraction procedure 66
5.2.4 Carryover study 67
5.3 Results and discussion 68
5.3.1 Practical considerations 68
5.3.2 Kinetics 70
5.3.3 Mass transfer model 73
5.3.4 Analytical application 76
CHAPTER 6 - SPECIATION: DETERMINATION OF FREE PROGESTERONE IN A PROTEIN SOLUTION 96
6.1 Introduction 96
6.2 Binding of steroids to protein 97
6.3 Modifications to the mass transfer model 98

6.4 Drop-volume method of interfacial tension measurement 103
6.5 Experimental details 104
6.5.1 Chemicals 104
6.5.2 Extraction apparatus and procedure 104
6.5.3 Interfacial tension measurement 106
6.5.4 Solutions 107
6.6 Results and discussion 107
6.6.1 Extraction rate curves 107
6.6.2 Equilibrium extractions 108
6.6.3 Non-equilibrium extractions 111
6.6.4 Agreement with modified mass transfer model 113
6.6.5 Protein adsorption at the liquid-liquid interface 116
CHAPTER 7 - CONCLUSIONS AND FUTURE WORK 126
7.1 Conclusions 126
7.2 Future work 128
BIBLIOGRAPHY 133
APPENDIX 141

List of Tables

2.1	Concentrations immediately adjacent to the interface for the data in Figure 2.1, according to film theory	25
3.1	Calibration of the tubing radius with caffeine ($D = 6.3 \times 10^{-6}$ cm^2/s)	36
3.2	Measurement of diffusion coefficients for 4-NT, 4-MAP, malathion, and progesterone in water at 25°C	37
3.3	Verification of assumptions (equations 3.6 and 3.7) for the experimental conditions employed in the determination of diffusion coefficients	38
4.1	Equilibrium and kinetic parameters for extraction of 4-MAP from water into 8.0 µL of n-octane at four stirring rates, plus diffusion film thicknesses in the water phase	54
4.2	GC data for replicate non-equilibrium (5-min) extractions of 0.177 mmol/L 4-MAP, illustrating the role of the internal standard (IS)	55
5.1	Equilibrium and kinetic parameters for extraction of 2.06×10^{-4} mol/L 4-MAP from water into 1.00 µL of n-octane at four stirring rates	78
5.2	Equilibrium and kinetic parameters for extraction of four compounds from water into 1.00 µL of n-octane at 1500 rpm, plus diffusion coefficients from Table 3.2	79
5.3	GC data for replicate non-equilibrium (1-min) extractions of 0.182 mmol/L 4-MAP, illustrating the role of the internal standard (IS)	80
6.1	Speciation and binding constant data for the steroid progesterone (S) in the presence of 0.16 mol/L NaCl + 1% BSA	119
6.2	Interfacial tension data for aqueous - octane systems using the drop-volume method	120

List of Figures

1.1	Schematic diagram of a typical solvent extraction - flow injection analysis (SE-FIA) system	11
2.1	Concentration profiles near the interface according to film theory	26
2.2	Concentration profiles near the interface according to penetration theory	27
3.1	Taylor dispersion in laminar flow	39
3.2	Experimental apparatus for the determination of diffusion coefficients	40
3.3	Typical 4-MAP peak from the Taylor dispersion apparatus	41
4.1	Side view illustration of the solvent microextraction system	56
4.2	Enlarged view of the end of the Teflon probe showing the organic drop immersed in the aqueous phase	57
4.3	Calibration of GC response with standard solutions of 4-MAP in n-octane / internal standard solution	58
4.4	Plots of concentration of 4-methylacetophenone in n-octane versus stirring time at various aqueous phase stirring rates	59
4.5	Plot of log $\bar{\beta}_o$ versus log s (s in rpm) for the data in Table 4.1	60
4.6	Equilibrium distribution isotherm for 4-MAP between water (aq) and n-octane (o)	61
4.7	Calibration of the solvent microextraction system using aqueous standards	62
5.1	Photograph showing a 1-μL drop of n-octane suspended from the needle tip in aqueous solution	81
5.2	Carryover study to determine the number of syringe flushing cycles necessary to avoid contamination from one injection to the next	82
5.3	Calibration of GC response with standard solutions of 4-MAP in n-octane / internal standard solution	83

5.4 Plots of observed concentration of 4-MAP in n-octane versus stirring time at various stirring rates 84

5.5 Structures of the four compounds used in the mass transfer model study 85

5.6 Calibration of GC response with standard solutions of 4-NT in n-octane / internal standard solution 86

5.7 Calibration of GC response with standard solutions of 4-MAP in n-octane / internal standard solution 87

5.8 Calibration of GC response with standard solutions of malathion in n-octane / internal standard solution 88

5.9 Calibration of GC response with standard solutions of progesterone in n-octane / internal standard solution 89

5.10 Plot of observed concentration versus stirring time at 1500 rpm for 4-nitrotoluene (4-NT) 90

5.11 Plot of observed concentration versus stirring time at 1500 rpm for 4-methylacetophenone (4-MAP) 91

5.12 Plot of observed concentration versus stirring time at 1500 rpm for malathion 92

5.13 Plot of observed concentration versus stirring time at 1500 rpm for progesterone 93

5.14 Plot of aqueous mass transfer coefficient β_{aq} versus aqueous diffusion coefficient D_{aq} for four compounds 94

5.15 Plot of film thickness in the aqueous phase versus reciprocal stirring rate for the data in Table 5.1 95

6.1 Sketch of the steady-state concentration profiles for S and SP at a total aqueous phase steroid concentration of 1.60×10^{-5} mol/L, early in the extraction experiment 121

6.2 Normalized extraction rate curves for: (a) $[S]_{T,aq} = 2._5$ μmol/L progesterone in 0.16 mol/L NaCl, and (b) $[S]_{T,aq} = 6._1$ μmol/L progesterone in 0.16 mol/L NaCl + 1.00% BSA 122

6.3 Calibration curve for the determination of free progesterone 123

6.4 Standard addition plot for the data in Table 6.1 124

6.5 Microscopic association scheme for steroid (S) and protein (P) with two protein binding sites 125

7.1 Microliter drop solvent double-extraction apparatus (not to scale) 132

List of Symbols

a	radius (cm)
A	area (cm^2)
C	concentration (mol/L or mol/cm^3)
D	diffusion coefficient (cm^2/s)
$^1f_{aq}$	fraction of analyte remaining in the aqueous phase at equilibrium
F	volumetric flow rate (cm^3/s)
F′	correction factor in drop-volume method
g	acceleration due to gravity (981 cm/s^2)
k	first order extraction rate constant (s^{-1})
k_1, k_2	microscopic equilibrium constants in Figure 6.5
k_{12}, k_{21}	microscopic equilibrium constants in Figure 6.5
K_1, K_2	macroscopic equilibrium constants
K	Taylor dispersion coefficient (cm^2/s)
K_a	steroid-protein binding constant (L/mol)
l_1, l_2	semi- major and minor axes of an ellipse or ellipsoid (cm)
L	length of tubing or stirring bar (cm)
m	number of binding sites per protein molecule
M	total amount of solute injected in Taylor dispersion apparatus (mol or g)
n	number of moles (mol)
p	power dependence of $\bar{\beta}_o$ on s
P	pressure (atm)
r	radial distance variable (cm)
R	GC response (peak area ratio)
Re	dimensionless stirring Reynolds number = $sL^2\rho/\mu$

s	stirring rate (rpm or rps)
Sc	dimensionless Schmidt number = $\mu/(\rho D)$
t	time variable, or elution time (s)
t_e	exposure or contact time in penetration theory (s)
$t_{1/2}$	half-time of extraction (min)
T	temperature (K)
U	velocity of flow (cm/s)
$\overline{U}$	average velocity of flow (cm/s)
U_t	terminal velocity (falling/rising drops) (cm/s)
V	volume (cm^3)
w_t	peak width at the baseline in time units (s)
W	weight (g)
x	distance variable (cm)
β	single-phase mass transfer coefficient (cm/s)
$\bar{\beta}_o$	overall mass transfer coefficient (cm/s)
γ	interfacial tension (dynes/cm = g/s^2)
δ	Nernst diffusion film thickness (cm)
ε	eccentricity of an ellipsoid (dimensionless)
κ	distribution coefficient (L/L)
λ_{max}	wavelength of maximum absorption (nm)
μ	viscosity (g / (cm s))
ν	integrating factor in Chapter 2

ρ	density (g/cm^3)
$\Re$	universal gas constant (0.0821 L atm / (mol K))
σ_x^2	variance of the distribution in distance units (cm^2)
σ_t^2	variance of the distribution in time units (s^2)
τ	characteristic time (e.g. associated with the injection volume) (s)

Subscripts

aq	aqueous phase
eff	effective
eq	equilibrium
i	interfacial
inj	injector
o	organic phase
P	protein
S	steroid
SP	steroid-protein complex
std	standard
T	total
unk	unknown
∞	bulk

Chapter 1

INTRODUCTION

1.1 Conventional sample preparation approaches.

Quantitative analysis of one or more sample components in a complex aqueous mixture is often complicated by two factors. First, the sample component(s) of interest may be present at a concentration below the detection limit of the instrument. Second, the sample matrix (other components present in the sample) may interfere with the analysis. The first limitation can be overcome by *preconcentration* of the analyte (increasing its concentration by some means). The second limitation requires a *sample cleanup* step to separate the analyte from interfering matrix components. Various techniques have been devised to address one or both of these problems:[1-4]

1.1.1 Conventional solvent extraction.

Solvent extraction or liquid-liquid extraction refers to the partitioning of one or more analytes between the aqueous sample phase and an immiscible organic phase.[5-8] This is often performed in a separatory funnel or other piece of equipment where the bulk phases are agitated to enhance mass transfer and reach distribution equilibrium in a reasonable amount of time. If there is sufficient agitation, one of the phases (dispersed phase) will break up into droplets which are dispersed in the other phase (continuous phase).[9] Greater agitation enhances the rate of mass transfer through (1) smaller droplets and hence greater interfacial area, and (2) enhanced convective-diffusive mass transfer, as discussed in Chapter 2.

Conditions are chosen such that the analyte of interest has a large distribution coefficient, κ between the organic and aqueous phases, while interfering matrix components have a small κ, defined by

$$\kappa = \frac{C_{o,eq}}{C_{aq,eq}} \qquad (1.1)$$

where $C_{o,eq}$ and $C_{aq,eq}$ are equilibrium concentrations in the organic and aqueous phases respectively. Sample cleanup is achieved in this way. At equilibrium, a certain fraction of analyte will remain in the aqueous phase. If desired, ***exhaustive*** extraction can be achieved by repeatedly contacting the aqueous phase with fresh portions of organic phase, and combining the organic extracts. Preconcentration of semi-volatile or non-volatile components can be achieved by evaporating most or all of the solvent, and dissolving the residue in a small, known volume of solvent for analysis.

The bulk partitioning nature of liquid-liquid extraction has the advantage that κ is constant over a large concentration range. Furthermore, liquid-liquid extraction is widely applicable to a large number of analytes, including drugs, surfactants (ion-pairs), and metal ions (metal chelates). However, there are a number of disadvantages to liquid-liquid extraction. The formation of stable emulsions can be problematic during phase coalescence. Also, liquid-liquid extraction tends to be labour-intensive, and the use of large volumes of solvents is costly in terms of obtaining the solvents and disposing of them properly.

1.1.2 Solvent extraction - flow injection analysis

Automation of liquid-liquid extraction can be achieved in a flowing system in which the sample is injected into a flowing aqueous stream.[10,11] This technique, usually referred to as solvent extraction - flow injection analysis (SE-FIA), was first introduced by Karlberg and Thelander[12] and Bergamin *et al.*[13] SE-FIA systems generally have three basic components: (1) a segmentor where the aqueous and organic streams meet, forming alternating segments of aqueous and organic phases, (2) an

extraction coil in which analyte transfer from the aqueous phase to the organic phase occurs, and (3) a phase separator to isolate the organic phase for analysis (e.g. by UV absorption in a flow cell). A schematic diagram of a typical SE-FIA system is shown in Figure 1.1.

There are several consequences of segmented flow. Sample zone dispersion is minimized since the laminar flow profile is disrupted by segmentation. Also, circulation within the segments facilitates both reagent mixing (in one phase) and extractive mass transfer of the analyte (from aqueous phase to organic phase). SE-FIA has been well characterized in terms of kinetics and mechanism of extraction[14-16] and has been applied to a broad range of analytical problems.[11] SE-FIA without phase separation has also recently been described.[17] Preconcentration is generally not achieved with SE-FIA, since the phase ratio (organic volume/aqueous volume) is generally close to unity.[10]

1.1.3 Solid phase extraction

An increasingly popular alternative to liquid-liquid extraction is solid phase extraction (SPE).[1-4,18-24] The solid phase can be inorganic (e.g. alumina, silica), activated carbon, polyurethane, ion-exchange resin, porous polymer (e.g. Amberlite XAD resins), or bonded-phase material, but the latter two are currently the most commonly used phases owing to their inertness and high sorptive capacity.

The solid phase particles are generally contained either within a small column[19-22] (e.g. Waters Sep-Pak cartridges) or enmeshed in Teflon fibers in a thin disk[23,24] (e.g. 3-M Empore extraction disks). The cartridge-type systems typically contain several hundred milligrams of 30-60μm particles, while the disk-type systems contain a similar mass of smaller (8μm) particles in a 25-47mm diameter, 0.5mm thick disk. Large volumes of aqueous sample can be passed through the sorbent bed to exhaustively

extract trace organic compounds from the sample. The sorbent is then usually washed (e.g. with water or buffer) to remove unretained components. Elution of the organic compound(s) of interest can be achieved by passing an appropriate organic solvent (e.g. acetone, diethyl ether, hexane, methylene chloride) through the sorbent and collecting the eluate, which can be evaporated down to a very small volume if necessary. Thus, significant preconcentration or enrichment can be attained by this method. Furthermore, SPE is relatively inexpensive and simple to perform, and uses smaller amounts of solvents than liquid-liquid extraction.

There are a number of disadvantages to SPE, however. Because SPE involves surface sorption as opposed to bulk partitioning, sample capacity is greatly reduced compared to liquid-liquid extraction. Furthermore, sorbed impurities can compete with analyte molecules for sorption sites. Column plugging and pore blockage can also be a problem if samples contain particulate material. Also, contamination, carryover, and batch-to-batch variation are problematic in SPE.

1.1.4 Solid-phase microextraction

Solid-phase microextraction (SPME) is a relative newcomer to the field of sample preparation. Much of the development of the solventless SPME technique is attributed to Pawliszyn and co-workers.[25-28] In SPME, a fused silica fiber which has been coated with an appropriate stationary phase such as poly(dimethylsiloxane) is immersed in an aqueous sample during which time analytes partition into the coating. After a certain time, the analytes are thermally desorbed in a gas chromatographic (GC) injection port for analysis by GC. The fiber is contained within a conventional microsyringe needle and is exposed by depressing the plunger. Commercial SPME devices are available from Supelco (Bellefonte, PA) for use with conventional GC systems.

SPME overcomes some of the disadvantages of SPE, such as plugging of cartridges and solvent use. Unlike SPE, extraction is generally not exhaustive. The system is either allowed to reach distribution equilibrium, or in the interest of analysis time, the extraction may be stopped before equilibrium is reached, in which case timing and other factors must be carefully controlled. In either case, the system must be calibrated.

SPME extractions are simple to perform and amenable to automation.[29] Thin coatings (10-100μm) and vigorous agitation of the aqueous phase speed-up mass transfer rates and provide short analysis times on the order of several minutes, depending on the mass transfer scheme. The kinetics of the extraction process have been studied extensively.[30-33] Selectivity can be controlled by the choice of coating material, and sensitivity can be enhanced by using a thicker coating or longer fiber. Reproducability of ~5% relative standard deviation is typical.[26]

The main drawback to SPME appears to be the slow desorption step which can lead to tailed peaks and a poor separation in the GC. Recent modifications of SPME accelerate the desorption rate, but at the cost of a more complex SPME injection system.[34]

In addition to direct immersion in the aqueous sample, SPME is amenable to headspace analysis,[35] since headspace vapors will partition into the SPME fiber. Thus, SPME a suitable technique for very dirty or complex samples which contain volatile organic compounds. Additionally, SPME has recently been coupled to high performance liquid chromatography (HPLC), extending its application to the analysis of semi- and non-volatile compounds.[36]

1.1.5 Gas phase methods

A number of closely-related gas phase methods have been developed for the analysis of volatile organic compounds (VOC's) in aqueous samples.[1-4, 37, 38] These

methods take advantage of the partitioning of VOC's between the aqueous matrix and a gas (e.g. air, He). In this way, isolation of the VOC's from a complex aqueous matrix can be achieved, and the gas phase can either be analyzed directly or passed through a sorbent trap to collect and concentrate the VOC's.

Static headspace analysis involves the direct sampling of the headspace over an aqueous sample in a sealed vessel.[39-41] Solution-vapor equilibrium is a prerequisite and experimental conditions such as temperature, sample volume, and vapor sampling method must be carefully controlled to obtain reproducible results. While this method works well for compounds that are present at high concentration and/or are highly volatile, problems such as slow equilibration, adsorption of analytes on septa, and the requirement for rigid control of experimental conditions limit the application of this technique.

Dynamic headspace analysis overcomes some of the disadvantages of the static technique by passing a stream of gas over the sample and trapping the volatile components in a suitable sorbent or cryogenic trap.[42] In this way, VOC's that are less volatile and/or present at trace concentrations can be enriched on the trapping medium for subsequent analysis (e.g. by GC). The rate of enrichment can be enhanced by vigorous stirring of the aqueous phase.

More efficient gas phase extractions can be performed by introducing the gas below the water surface in the form of finely dispersed bubbles. In this way, greater surface contact between the aqueous sample and the gas is achieved, and mass transfer is much more rapid. The gas is then collected and passed through a suitable trapping medium. However, for solid samples, or liquid samples which tend to foam (e.g biological fluids), the dynamic headspace technique is necessary.[42] Systems involving the sparging of aqueous samples with a gas below the surface are of two types: (1) open systems (purge and trap, PT) in which the gas is vented to waste after exiting the trap,[43-46] and (2) closed systems (closed loop stripping analysis, CLSA) in which the

gas is recycled through the system after exiting the trap.[47-50] Exhaustive extraction is possible only for sample components that have very low water solubility and high volatility, and requires long sampling times. Desorption of analytes from the trap is performed either thermally (directly onto the GC) or by elution with an appropriate solvent.

1.1.6 Membrane techniques

There are a number of sample cleanup techniques which utilize a membrane to separate the analyte of interest from a complex aqueous matrix.[2] Traditional techniques include dialysis and ultrafiltration. Dialysis involves the selective permeation (diffusion) of small molecules across a thin membrane as a result of a concentration gradient. Macromolecules (e.g. proteins) are prevented from diffusing into the membrane because of their molecular size. Ultrafiltration differs from dialysis in that solution is forced to flow through the membrane either by pressure or centrifugation. Membranes for ultrafiltration are commercially available with molecular mass limits of 10^3 - 10^6 (ref. 2).

A number of miniaturized membrane techniques have recently been developed. Microdialysis is a sampling technique in which hollow dialysis fibers are used to sample low molecular weight compounds from a complex matrix (e.g. blood, tissue) *in vivo*.[51-52] The fluid which is pumped through the dialysis fiber is the ***perfusate***, an aqueous solution of similar ionic composition and pH as the material being sampled. After passing through the fiber, the fluid (now enriched with low molecular weight compounds of interest) is referred to as the ***dialysate***. The dialysate can then be analyzed by high-performance liquid chromatography (HPLC) or capillary electrophoresis (CE) either off-line or on-line. The main advantage of microdialysis is that it can be performed on awake, freely moving animals or human subjects, thus eliminating artifacts from anesthesia or blood withdrawal.

Supported liquid membranes (SLM's), which consist of a hydrophobic polymer membrane with an organic solvent filling the pores of the membrane, have been described for sample cleanup and preconcentration in flow systems.[53-54] The technique has also recently been miniaturized using a hollow fiber membrane in a cylindrical flow channel.[55] The system differs from microdialysis in that the acceptor phase is a small volume of stagnant fluid, and the sample fluid is pumped around the membrane. Conditions are chosen to favor both the partitioning of analyte from the sample into the membrane, and from the membrane into the acceptor fluid. For example, preconcentration of amines can be achieved by using a high pH in the sample (amine in neutral form) to favor partition into the membrane, and a low pH in the acceptor fluid (amine in protonated form) to "trap" it in the acceptor fluid. The acceptor fluid can be analyzed on-line by UV absorbance with or without chromatographic separation.

Hollow fiber membranes have also been used for the extraction of volatile or semi-volatile organic compounds from aqueous samples using flowing gas[56-58] or supercritical carbon dioxide[59] as acceptor phase. The use of a cryogenic trap at the GC inlet to collect analytes and a thermal desorption module to rapidly desorb them for GC analysis is required. This system has been referred to as membrane extraction with a sorbent interface (MESI) by Pawliszyn and co-workers.[58]

1.2 Solvent microextraction into a single drop

The purpose of the present work is to develop a complimentary sample cleanup/preconcentration method based on solvent extraction employing very small solvent volumes. In this way, the advantages of liquid-liquid extraction (such as linear distribution isotherms and minimal sample carryover by using fresh solvent) can be retained while many of the disadvantages (such as the formation of emulsions and use of large volumes of solvent) are eliminated. Speed, convenience, low cost, precision, and accuracy are the driving forces throughout this work.

The traditional liquid-liquid extraction approach is to first extract with a large volume of solvent (comparable to the volume of aqueous sample) and second to evaporate most of the solvent to increase the concentration of the analyte. There are two major problems with the second step, however. If the analyte is semi-volatile, significant losses can occur. Also, impurities which are inevitably present in the solvent are concentrated along with the analyte. Thus, methods which involve extraction into very small volumes of solvent and require no solvent evaporation are preferable.

The use of a liquid droplet or film as a gas sampling interface has recently been described by Dasgupta and co-workers.[60-63] Gas sampling interfaces using capillary format sequential injection analysis,[60] direct absorbance measurement with optical fibers,[61] collection of gases on a thin film of liquid formed on a wire loop at the tip of a capillary,[62] and a dynamically growing and falling droplet system[63] have been reported.

A drop-within-a-drop liquid-liquid extraction system has also recently been described.[64] In this system, a ~1.3-μL drop of chloroform was contained within a 25-45 μL aqueous drop. The aqueous drop was continuously renewed by flow. The authors applied the system to the analysis of sodium dodecylsulfate (SDS) which extracts as an ion-pair with methylene blue (MB). Colorimetric determination was made with in-situ LED/fiber optic detection system. This system offers several advantages over solvent extraction-flow injection analysis (SE-FIA): the phase ratio can be adjusted over a wide range, only a single drop of solvent is required, and the optical detection system is windowless.

Several "micro" extraction methods have been described in the literature for extraction into small volumes of solvent.[65-67] These methods are basically modifications of a conventional separatory funnel type extraction in that the organic phase is dispersed as droplets in the continuous aqueous phase, followed by phase

separation. After phase separation, the solvent layer is drawn into a narrow capillary neck where most of the solvent can be withdrawn by a syringe needle for analysis by GC. However, the mass transfer kinetics are ill-defined in these systems since agitation is performed manually and the interfacial area is not known or reproducible.

In the solvent microextraction method described in this work, there is no dispersion of the organic phase and therefore no phase coalescence step required after extraction. Furthermore, the interfacial area can be measured with reasonable accuracy, and is approximately independent of stirring rate and solution composition, facilitating the development of a theoretical model of mass transfer kinetics. Reproducible results can be conveniently obtained under both equilibrium and non-equilibrium conditions in a reasonable time. Furthermore, if the volume of the aqueous phase is very much larger than the volume of the organic drop, the amount of analyte removed from the aqueous phase is negligible, and speciation studies can be performed without perturbing homogeneous aqueous phase equilibria.

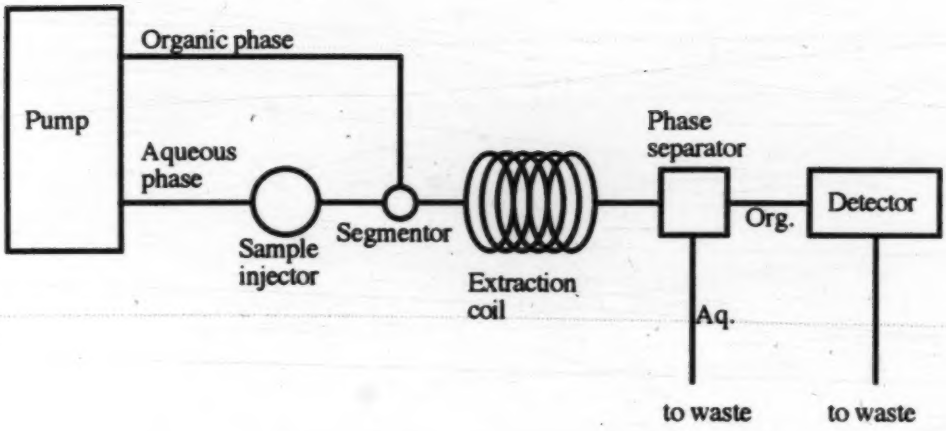

Figure 1.1 Schematic diagram of a typical solvent extraction - flow injection analysis (SE-FIA) system. See text for details.

Chapter 2

THEORY[a]

2.1 Introduction

In this chapter, some important equations describing the equilibrium and kinetic aspects of solvent extraction are detailed. The equations are applicable to any two-phase liquid system approaching partition equilibrium under constant agitation conditions, with analyte initially present in only one phase. Mass transfer modelling, while not necessary in an analytical application, where simple calibration suffices, does allow for prediction of extraction rates from knowledge of analyte diffusion coefficients.

2.2 Equilibrium considerations

The limit of detection in the system is ultimately that of the GC detector. Thus, the concentration of analyte in the organic phase after stirring must be above this detection limit. The equilibrium concentration in the organic phase is given by

$$C_{o,eq} = \kappa C_{aq,eq} = \frac{\kappa C_{aq,initial}}{1 + \kappa V_o / V_{aq}} \qquad (2.1)$$

where $C_{aq,\,initial}$ and $C_{aq,\,eq}$ are the initial and equilibrium aqueous phase concentrations, V_o and V_{aq} are the organic and aqueous phase volumes, and κ is the distribution coefficient, defined by

$$\kappa = C_{o,eq} / C_{aq,eq} \qquad (2.2)$$

---

[a] A version of this chapter has been published. Jeannot, M.A.; Cantwell, F.F. 1996. Analytical Chemistry. 68: 2236-2240.

Thus, κ and/or $C_{aq,\,initial}$ must be sufficiently large, and the phase ratio, V_o/V_{aq}, must be reasonably small to avoid detection problems. Also, in the interest of time, equilibrium may not be reached in an analytical application, so the organic phase concentration may be somewhat lower than $C_{o,\,eq}$.

2.3 Kinetic considerations

The general rate equation for liquid-liquid extraction can be written as[68-74]

$$\frac{dC_o}{dt} = \frac{A_i}{V_o}\bar{\beta}_o\left(\kappa C_{aq} - C_o\right) \tag{2.3}$$

where C_o is the concentration of analyte in the organic phase at time t, A_i is the interfacial area, $\bar{\beta}_o$ is the overall mass transfer coefficient with respect to the organic phase (in cm/s), and C_{aq} is the analyte concentration in the aqueous phase at time t. Equation 2.3 has the form of a reversible first order reaction.

Assuming rapid transfer across the liquid-liquid interface, the overall mass transfer coefficient can be expressed as

$$\frac{1}{\bar{\beta}_o} = \frac{1}{\beta_o} + \frac{\kappa}{\beta_{aq}} \tag{2.4}$$

where β_o and β_{aq} are the individual mass transfer coefficients for the organic and aqueous phases, respectively, defined by the flux at the interface:

$$\frac{1}{A_i}\frac{dn}{dt} = \beta_{aq}\left(C_{aq} - C_{aq,i}\right) = \beta_o\left(C_{o,i} - C_o\right) \tag{2.5}$$

The subscript i refers to concentrations immediately adjacent to, but not adsorbed at, the interface, while C_{aq} and C_o refer to bulk concentrations. Equation 2.5 requires that there be no accumulation or depletion of analyte at the interface (i.e. steady-state at the interface).

Furthermore, it is assumed that equilibrium prevails at the interface at all times,[68-74] so

$$C_{o,i}/C_{aq,i} = \kappa \tag{2.6}$$

To solve eq 2.3, C_{aq} can be written in terms of C_o from mass-balance considerations:

$$C_{aq} = \frac{C_{aq,initial}V_{aq} - C_oV_o}{V_{aq}} \tag{2.7}$$

After substitution from eq 2.7, eq 2.3 can be rewritten as a first-order linear differential equation:

$$\frac{dC_o}{dt} + P(t)\cdot C_o = Q(t) \tag{2.8}$$

where P(t) and Q(t) are given by:

$$P(t) = \frac{A_i}{V_o}\bar{\beta}_o\left(\kappa\frac{V_o}{V_{aq}} + 1\right) \tag{2.9}$$

$$Q(t) = \frac{A_i}{V_o}\bar{\beta}_o \kappa C_{aq,initial} \tag{2.10}$$

The general solution to eq 2.8 is

$$C_o = \frac{1}{\nu}\int \nu Q(t)dt + \frac{const}{\nu} \tag{2.11}$$

where ν is the integrating factor:

$$\nu = e^{\int P(t)dt} \tag{2.12}$$

Equation 2.11 becomes

$$C_o = \frac{\kappa C_{aq,initial}}{\left(\kappa V_o / V_{aq} + 1\right)} + \frac{const}{e^{k \cdot t}} \tag{2.13}$$

where k is the observed rate constant (s^{-1}),

$$k = \frac{A_i}{V_o}\bar{\beta}_o\left(\kappa \frac{V_o}{V_{aq}} + 1\right) \tag{2.14}$$

and the first term on the right-hand-side in eq 2.13 is simply $C_{o,\,eq}$ (from eq 2.1). The constant term can be evaluated by substitution of the initial conditions (i.e. $C_o = 0$ at $t = 0$):

$$\text{const} = -C_{o,eq} \tag{2.15}$$

Thus, with this initial condition, eq 2.13 can be written as

$$C_o = C_{o,eq}\left(1 - e^{-k\cdot t}\right) \tag{2.16}$$

Experimental values of C_o versus time can be fit to equation 2.16 to obtain both $C_{o,eq}$ and k, which yield both equilibrium (κ) and kinetic ($\bar{\beta}_o$) parameters. From eqs 2.2 and 2.7, at equilibrium, the distribution coefficient, κ, can be calculated:

$$\kappa = \frac{C_{o,eq} V_{aq}}{C_{aq,initial} V_{aq} - C_{o,eq} V_o} \tag{2.17}$$

The overall mass transfer coefficient $\bar{\beta}_o$ can then be estimated by equation 2.14 since A_i can be estimated with reasonable accuracy, from geometrical considerations. For a particular combination of analyte and solvents, $\bar{\beta}_o$ will be a constant, provided that stirring rate and temperature are constant.

Note that if κ is large (i.e. for hydrophobic molecules), eq 2.4 reduces to

$$\bar{\beta}_o \approx \beta_{aq} / \kappa \tag{2.18}$$

and β_{aq} can be evaluated directly. In this case, resistance to mass transfer in the aqueous phase is rate-limiting. If κ is not so large, then both terms in equation 2.4 are

significant, and independent evaluation of β_{aq} and β_o is not possible without additional experiments using compounds with different κ's.

Equations 2.4 and 2.14 reveal the influence of the experimental variables A_i, V_o, V_{aq}, β_o, β_{aq}, and κ on analysis time. From eq 2.14, the rate constant depends directly on A_i. The effects of V_o and V_{aq} depend on the magnitude of the capacity factor, $\kappa V_o/V_{aq}$, relative to 1 (eq 2.14). The effects of β_o and β_{aq} depend on κ, as discussed above. Finally, the effect of κ on the rate constant depends on both the magnitude of κ (eq 2.4) and the magnitude of the capacity factor (eq 2.14). For example, if κ is large so that eq 2.18 applies, and the phase ratio is very small such that $\kappa V_o/V_{aq} << 1$, eq 2.14 simply reduces to

$$k \approx \frac{A_i \beta_{aq}}{V_o \kappa} \tag{2.19}$$

In this case, the rate constant is inversely proportional to both V_o and κ, is directly proportional to β_{aq}, and is independent of V_{aq} and β_o. However, if these approximations are not valid, then the dependence of k on the experimental parameters becomes more complicated (eqs 2.4 and 2.14).

It may be noted that it is difficult to experimentally verify these dependencies, since the variables cannot be independently controlled. For example, changing V_o will also alter the interfacial area A_i and possibly the hydrodynamics ($\bar{\beta}_o$) in a way that may be difficult to measure or predict accurately. Similarly, varying κ (e.g. by changing the

sample molecule, solvent, or temperature) will also vary the diffusion coefficient and/or the hydrodynamics.

2.4 Mass transfer models

Up to this point, the mass transfer coefficient has been treated as an empirical parameter relating the mass flux to the concentration difference, which serves as the driving force. The interpretation of the mass transfer coefficient entails modelling the system by, for example, Whitman two-film theory[68, 69, 72, 74] or Higbie's penetration theory.[69, 71, 72, 74] The discussion will focus on β_{aq}, since a large κ is generally a sought-for analyte property in which case eq 2.18 is applicable.

2.4.1 Film theory

This theory, first proposed by Nernst[75] and further developed by Lewis and Whitman,[76] assumes no movement of the solution immediately adjacent to the interface (e.g. one molecule thick) and a gradually increasing vigorousness of convection (i.e. mixing flow) of the solution at locations farther away from the interface. This condition, which is difficult to treat mathematically, is approximated in film theory by postulating that uniform, instantaneous, and complete convective mixing exists throughout the bulk solution up to some small distance δ cm away from the liquid-liquid interface. The liquid layer of thickness δ, called the Nernst diffusion film, is postulated to be completely stagnant and nonconvected, so that a sample molecule crosses it by pure diffusion only. At steady state in the film, the aqueous phase mass transfer coefficient is given by

$$\beta_{aq} = D_{aq}/\delta_{aq} \qquad (2.20)$$

where D_{aq} is the diffusion coefficient in the aqueous phase. At faster stirring rates, β_{aq} increases because δ_{aq} decreases. According to eq 2.20, there is a direct proportionality between β_{aq} and D_{aq}.

Equation 2.20 can be derived from Fick's first law of diffusion:

$$\frac{1}{A_i}\frac{dn}{dt} = -D_{aq}\frac{\partial C}{\partial x} \qquad (2.21)$$

where x is distance (cm). At steady state in the film, the concentration gradient $\partial C/\partial x$ is linear and is given by

$$\frac{\partial C}{\partial x} = \frac{C_{aq,i} - C_{aq}}{\delta_{aq}} \qquad (2.22)$$

Substitution of eq 2.22 into eq 2.21 gives

$$\frac{1}{A_i}\frac{dn}{dt} = D_{aq}\frac{C_{aq} - C_{aq,i}}{\delta_{aq}} \qquad (2.23)$$

Analogy with eq 2.5 yields eq 2.20 for the aqueous phase mass transfer coefficient.

A sketch of concentration profiles according to film theory is shown in Figure 2.1 (aqueous phase at x<0, organic phase at x>0). Equations 2.5 (taking $\beta_{aq} = D_{aq}/\delta_{aq}$ and $\beta_o = D_o/\delta_o$) and 2.6 are solved simultaneously with typical parameters given in the figure caption to obtain the interfacial concentrations (shown in Table 2.1). The plots

illustrate how mass transfer control resides in the aqueous phase for $\kappa = 40$. If δ_o is doubled (dashed lines in Figure 2.1), the concentration gradients (and hence the flux) remain essentially unchanged. However, if δ_{aq} is doubled (dotted lines in Figure 2.1), the absolute value of the concentration gradients are approximately halved. Thus, when κ is large, changes in δ_o have almost no effect on the observed rate of mass transfer, while changes in δ_{aq} have a direct effect.

2.4.2 Penetration theory

This theory was first proposed by Higbie[77] and later modified by Danckwerts.[78] It postulates fluid convection right up to the interface. At the interface, a small fluid volume element of one phase is momentarily in contact with the other phase for some exposure time, t_e, after which the volume element is mixed back into the bulk fluid. Mass transfer of solute occurs via unsteady-state semi-infinite linear diffusion for the time increment t_e. The resulting expression for the aqueous phase mass transfer coefficient is

$$\beta_{aq} = 2\sqrt{D_{aq}/\pi t_e} \qquad (2.24)$$

where t_e is a constant at a constant stirring rate. At a faster stirring rate, the value of t_e is smaller. In contrast to the linear dependence predicted from film theory, a square-root dependence of β_{aq} on D_{aq} is predicted from penetration theory.

Equation 2.24 can be derived from a solution to Fick's second law of diffusion:

$$\frac{\partial C}{\partial t} = D\frac{\partial^2 C}{\partial x^2} \tag{2.25}$$

which can be applied to both phases. Here we are considering unsteady-state diffusion from an aqueous fluid element of initially uniform concentration $C_{aq,\infty}$ to an organic fluid element of initially uniform concentration $C_{o,\infty}$. The aqueous phase is at x<0, and the organic phase is at x>0. Equilibrium is assumed to prevail at the interface, so that eq 2.6 applies. Since no material may accumulate at the interface itself, from Fick's first law we can write

$$D_{aq}\frac{\partial C_{aq}}{\partial x} = D_o\frac{\partial C_o}{\partial x} \tag{2.26}$$

at x=0. Based on the treatment of Crank,[79] the solution to eq 2.25 with boundary conditions given by eq 2.6 and 2.26 is[b]

$$C_{aq} = \left(C_{aq,\infty} - C_{aq,i}\right)\mathrm{erf}\frac{|x|}{2\sqrt{D_{aq}t}} + C_{aq,i} \tag{2.27}$$

and

$$C_o = \left(C_{o,\infty} - C_{o,i}\right)\mathrm{erf}\frac{x}{2\sqrt{D_o t}} + C_{o,i} \tag{2.28}$$

The aqueous interfacial concentration $C_{aq,i}$ is constant and is given by

---

[b] $\mathrm{erf}(u) = \frac{2}{\sqrt{\pi}}\int_0^u e^{-y^2}dy$

$$C_{aq,i} = \frac{\sqrt{D_{aq}}C_{aq,\infty} + \sqrt{D_o}C_{o,\infty}}{\sqrt{D_{aq}} + \kappa\sqrt{D_o}} \qquad (2.29)$$

and the organic interfacial concentration is simply

$$C_{o,i} = \kappa\frac{\sqrt{D_{aq}}C_{aq,\infty} + \sqrt{D_o}C_{o,\infty}}{\sqrt{D_{aq}} + \kappa\sqrt{D_o}} \qquad (2.30)$$

Equations 2.27 and 2.28 with interfacial concentrations given by eqs 2.29 and 2.30 are solutions to Fick's second law (eq 2.25) which satisfy the boundary conditions given by eqs 2.6 and 2.26. Concentration profiles according to penetration theory are shown at two different times in Figure 2.2 for typical values of κ and D. $C_{aq,i}$ and $C_{o,i}$ are 9.9×10^{-3} and 9.9×10^{-1} respectively (arbitrary units) from eqs 2.29 and 2.30.

The *instantaneous* flux (as a function of time) at the interface can be calculated with Fick's first law (eq 2.21) by differentiating C_{aq} with respect to x:[e]

$$\frac{1}{A_i}\frac{dn}{dt} = \sqrt{\frac{D_{aq}}{\pi t}}\left(C_{aq,\infty} - C_{aq,i}\right) \qquad (2.31)$$

The total moles transferred over an exposure time interval t_e (contact time) can be obtained by integrating eq 2.31 from t=0 to t=t_e:

---

[e] $\frac{d}{du}\mathrm{erf}(u) = \frac{2}{\sqrt{\pi}}e^{-u^2}$

$$n = 2A_i\left(C_{aq,\infty} - C_{aq,i}\right)\sqrt{\frac{D_{aq}t_e}{\pi}} \qquad (2.32)$$

The *average* flux over the time increment t_e can then be calculated as:

$$\frac{1}{A_i}\frac{n}{t_e} = 2\sqrt{\frac{D_{aq}}{\pi t_e}}\left(C_{aq,\infty} - C_{aq,i}\right) \qquad (2.33)$$

Analogy with eq 2.5 gives the expression for the aqueous phase mass transfer coefficient (eq 2.24) according to penetration theory.

The most appropriate model (i.e film theory or penetration theory) for the solvent microextraction system is chosen by independently measuring both β_{aq} and D_{aq} for a series of compounds to determine the functional relationship between these two parameters. While it is recognized that both models are approximations to the real situation, they are useful nevertheless in understanding the mechanism of mass transfer and predicting mass transfer rates. The determination of diffusion coefficients will be discussed in Chapter 3.

2.5 Analytical methodology

In an analysis, it is desired to evaluate $C_{aq,\ initial}$ for an aqueous sample solution based upon the measured value of C_o at some stirring time, t. Combining eqs 2.1 and 2.16 gives the expression

$$C_{aq,initial} = C_o\left(\frac{1+\kappa V_o/V_{aq}}{\kappa\left(1-e^{-kt}\right)}\right) \qquad (2.34)$$

The bracketed term will be a constant which can be evaluated by extracting a standard solution of known $C_{aq,\ initial}$ (or a series of calibration standards), provided that the concentrations are in the linear region of the distribution isotherm for both sample and standard (i.e. κ is constant), and provided that the following are the same for both sample and standard: A_i, V_o, V_{aq}, $\bar{\beta}_o$ (i.e. same stirring rate and temperature), and stirring time, t. Equation 2.34 shows that it is not necessary to stir until equilibrium is reached, provided that the stirring conditions and time are reproduced, though, of course, the closer the system is brought to equilibrium, the less critical are the stirring conditions and time.

In cases where the aqueous sample is plentiful, it would be possible to expose the organic drop to an "infinite bath" of sample (flowing stream or large stirred volume relative to the volume of the drop). In this way, the drop would continuously be in contact with aqueous sample having the initial analyte concentration. Such a situation is equivalent to setting V_{aq} equal to infinity in eqs 2.1, 2.7, 2.14, 2.17, and 2.34, and as a consequence, the organic phase analyte concentration would be approaching an equilibrium value of $\kappa C_{aq,\ initial}$.

If the extracting species are involved in labile homogeneous equilbria in the aqueous phase, the distribution equilibria and kinetics become more complex. This will be discussed in detail in Chapter 6.

Table 2.1 Concentrations immediately adjacent to the interface for the data in Figure 2.1, according to film theory.

	$\delta_{aq} = \delta_o = 10^{-3}$cm	$\delta_{aq}=10^{-3}$cm, $\delta_o=2\times10^{-3}$cm	$\delta_{aq}=2\times10^{-3}$cm, $\delta_o=10^{-3}$cm
$C_{aq,i}$	0.0244	0.0476	0.0123
$C_{o,i}$	0.976	1.90	0.494

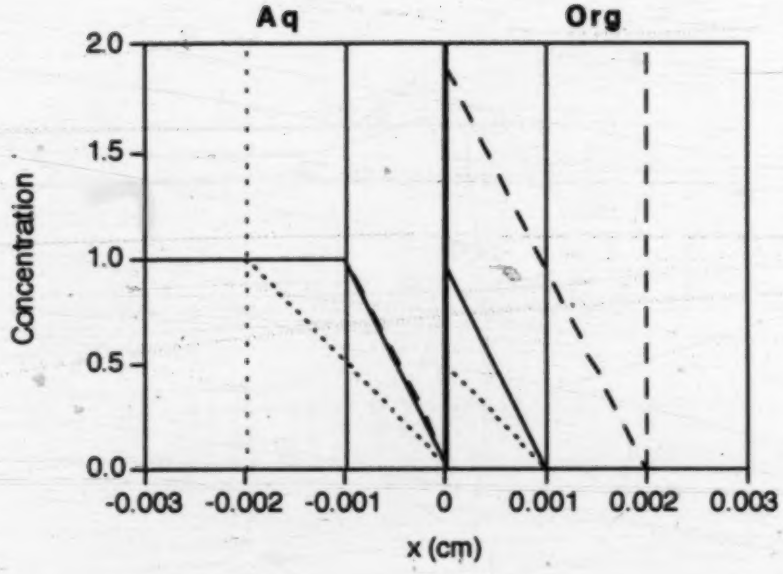

Figure 2.1 Concentration profiles near the interface according to film theory. The interface is represented by the thick vertical line at x=0. Solid lines are for $\delta_{aq} = \delta_o = 10^{-3}$cm. Dashed lines are for $\delta_{aq} = 10^{-3}$cm, $\delta_o = 2 \times 10^{-3}$cm. Dotted lines are for $\delta_{aq} = 2 \times 10^{-3}$cm, $\delta_o = 10^{-3}$cm. Other conditions are: $\kappa = 40$, $D_{aq} = D_o = 5 \times 10^{-6}$ cm^2/s, C_{aq} (bulk) = 1 (arbitrary units), C_o (bulk) = 0. Film thicknesses are indicated by vertical lines.

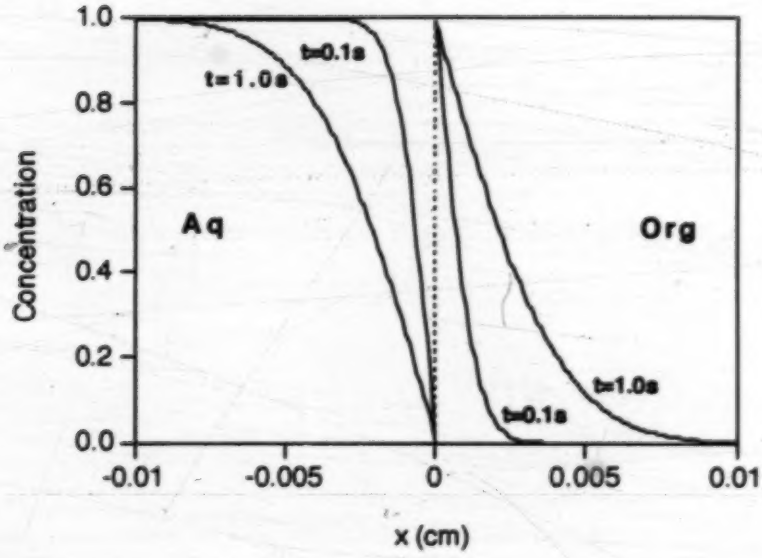

Figure 2.2 Concentration profiles near the interface according to penetration theory. The interface is represented by the dotted vertical line at x=0. The following conditions were chosen: $\kappa = 100$, $D_{aq} = D_o = 5 \times 10^{-6}\ cm^2/s$, $C_{aq,\infty} = 1$ (arbitrary units), $C_{o,\infty} = 0$. The concentration gradient at the interface (and hence the flux) changes with time. The average flux over a time interval t_e leads to an expression for the mass transfer coefficient.

Chapter 3

MEASUREMENT OF DIFFUSION COEFFICIENTS

3.1 The Taylor dispersion method

As was discussed in section 2.4, the treatment of the observed mass transfer kinetics with mass transfer models requires knowledge of the diffusion coefficient of the analyte molecule. The Taylor dispersion method of measuring diffusion coefficients was chosen because the apparatus is relatively simple to construct and use (components consist of commonly available HPLC equipment), results can be obtained in a short time (e.g. 30 minutes), and the method is reasonably accurate.

The method was originally described by Taylor[80, 81] in 1953-54 and by Aris[82] in 1956. While fluid (liquid or gas) is pumped slowly through a long, narrow tube, a sharp plug of dissolved sample is injected at the upstream end of the tube. As the narrow plug of sample flows through the tube under laminar flow conditions, bandbroadening occurs as a result of the non-uniform parabolic flow profile in the tube. The velocity of flow, U as a function of radial distance, r from the center of the tube is given by

$$U = 2\overline{U}\left(1-\left(\frac{r}{a}\right)^2\right) \qquad (3.1)$$

where $\overline{U}$ is the average linear velocity and a is the tube radius. Thus, at r=0 (center of the tube), $U=2\overline{U}$. At r=a (at tube wall), U=0. Molecules closer to the center of the tube will move faster than those near the walls. However, as a consequence of *radial diffusion* of sample components in the flow stream, sample molecules near the center of the tube will migrate towards the edge of the tube, and vice-versa (see Figure 3.1). Thus, the bandbroadening will be less than that from the parabolic flow profile,

depending on the magnitude of the sample molecule diffusion coefficient. This is the basis of the Taylor dispersion method.

Taylor showed that under certain conditions, the concentration of solute will be normally distributed according to[80,83,84]

$$C = \frac{1}{2} M a^{-2} \pi^{-3/2} (Kt)^{-1/2} \exp\left(\frac{-(x - \bar{U}t)^2}{4Kt}\right) \qquad (3.2)$$

where M is the total mass of solute injected, t is time, x is distance along the tube of radius a, and K is the Taylor *dispersion* coefficient, defined by

$$K = \frac{a^2 \bar{U}^2}{48D} \qquad (3.3)$$

where D is the diffusion coefficient.

If a detector is placed at the end of the tube to record a signal proportional to concentration (e.g. UV absorbance), a peak (signal versus time) will be obtained. Because the variance of the peak can be easily measured graphically, it is this parameter that is commonly used to determine the diffusion coefficient.[85-87] The variance of the distribution (in distance units) is given by[85-87]

$$\sigma_x^2 = \frac{a^2 \bar{U}^2 t}{24D} \qquad (3.4)$$

or, in units of time,

$$\sigma_t^2 = \frac{a^2 t}{24D} \tag{3.5}$$

Thus, diffusion coefficients can be calculated from eq 3.5 by measurement of the variance (σ_t^2) and elution time (t) of the peak.

There are three assumptions under which eqs 3.2 - 3.5 are valid.[80, 81, 83, 84] First, radial differences in concentration must be small compared to longitudinal differences. In other words, radial diffusion must be fast enough to smooth out radial differences in concentration before significant convective effects occur due to the parabolic flow profile. This can be achieved by using narrow tubing (small a) and either slow flow or long tubing. Mathematically, this condition is expressed as

$$\frac{a^2}{D \cdot t} \ll 1 \tag{3.6}$$

The second assumption is that *longitudinal* diffusion is negligible compared with dispersion due to the laminar flow profile. This is equivalent to saying that the diffusion coefficient, D is much smaller than the Taylor dispersion coefficient, K (eq 3.3), or

$$\frac{a^2 \overline{U}^2}{48D^2} \gg 1 \tag{3.7}$$

This assumption is generally valid in liquid systems where diffusion coefficients are small. The final assumption is that all solutions are dilute, which is appropriate for this study.

In addition to these theoretical assumptions, there are a number of practical limitations which must be borne in mind. The variance due to the injection plug width and the detector cell volume must be small compared to the variance of the peak. Also, a steady flow rate must be achieved. If the tubing is coiled, the diameter of the coil must be large compared to the diameter of the tubing to avoid "racetrack" and secondary flow effects.[85, 86] Finally, care must be taken to ensure that sample components do not sorb on the tubing walls, injector, etc.

3.2 Experimental details

Chemicals. Caffeine (Aldrich, Milwaukee, WI), 4-methylacetophenone (4-MAP; Kodak, Rochester, NY), 4-nitrotoluene (4-NT; Anachemia, Champlain, NY), and progesterone (Aldrich) were all reagent grade and used as received. Malathion was an analytical standard from AccuStandard Inc. (New Haven, CT), obtained through the distributor Chromatographic Specialties, Inc. (Brockville, ON, Canada). The malathion standard was certified to be 98.9% pure (by HPLC) by the manufacturer. Water was purified by the Nanopure system (Barnstead, Dubuque, IA).

Apparatus and Procedure. The experimental apparatus is shown in Figure 3.2. The Nanopure water which had passed through a 0.45-μm nylon filter was degassed for several minutes with He. A constant pressure pump[88] was used to pump water through the system at a constant flow rate using a pressure of ~10psi. Sample plugs were injected via a six-port stainless steel injection valve (Valco HP series, Houston, TX) with a 10-μL loop. The sample plug was passed through 446 ± 1 cm of loosely coiled (9-cm coil diameter) stainless steel tubing (0.02 inch i.d.) which was maintained at 25 ± 0.02 °C in a water bath (Lauda K-2, Brinkmann, Rexdale, ON, Canada). The eluting peak was detected with a Varian UV-50 flow cell detector, and the peak was plotted on a strip-chart recorder. All compression fittings were zero-dead

volume to minimize any "mixing chamber" effects. Before use, the stainless steel tubing was flushed with n-hexane to clean the tube and remove any traces of oil from the manufacturing process. The bandwidth of the detector was set to the smallest value (2 nm) to ensure adherence to Beer's Law. The absorbance range was optimized according to the molar absorptivity and concentration of the sample component.

The radius of the tubing was estimated by filling a known length of the tubing with water, collecting the water in a flask, and weighing. The radius can be calculated simply as

$$a = \sqrt{\frac{W/\rho}{\pi L}} \tag{3.8}$$

where W is the weight of water, ρ is the density of water, and L is the length of the tube. However, a small amount of water may adhere to the tubing wall after emptying the tubing, resulting in a slight underestimation of the radius. Therefore, the effective radius of the tubing was calculated by calibration with a sample component of known diffusion coefficient (caffeine) as described in the Results and discussion section.

To determine the optimal absorption wavelength, UV absorption spectra of dilute solutions of the sample components were obtained with a Hewlett-Packard HP 8451A diode array spectrophotometer.

A 0.21mM caffeine solution was used to calibrate the tubing radius. Solutions of 0.15mM 4-MAP, 0.17mM 4-NT, 0.019mM malathion, and 0.0022mM progesterone in water were prepared for the determination of the repective sample molecule diffusion coefficients.

3.3 Results and discussion

The wavelength of maximum absorption (λ_{max}) for progesterone is 240nm.[89, 90] Values of λ_{max} for 4-MAP and 4-NT were determined experimentally to be 258 and 286nm respectively. The absorbance of malathion was found to decrease steadily from 200 to 260nm; a wavelength of 210nm was chosen. Caffeine was measured at 254 nm.

The observed peaks were highly symmetrical, as can be seen from the typical peak shown in Figure 3.3. The elution time (t) of the peak was obtained by the intersection of the lines tangent to the points of inflection, and σ_t was taken as 1/4 the peak width at the baseline (obtained by the intersection of lines tangent to the points of inflection with the baseline).[86] Samples could be injected every 15-30 minutes without peak overlap.

Caffeine, with a known diffusion coefficient of 6.3×10^{-6} cm^2/s at 25°C,[91] was used to calibrate the system in terms of tubing radius via eq 3.5. The results are shown in Table 3.1. The average value of the tubing radius from caffeine calibration (a = 0.0263 ± 0.0004 cm) is slightly larger than the value obtained by direct measurement via eq 3.8 (a = 0.0253 ± 0.0001 cm). Since the directly measured value may be an underestimate as discussed above, the value obtained from caffeine calibration will be used to calculate D for the sample compounds.

The results for 4-NT, 4-MAP, malathion, and progesterone are shown in Table 3.2. The elution time (t), peak width (w_t) and variance (σ_t^2) are given in columns 3, 4, and 5. The diffusion coefficient, calculated from eq 3.5 using a = 0.0263cm, is given in column 6. Relative standard deviations (based on 3 replicate measurements) are in the range of 2-8%.

Several assumptions integrated into the Taylor dispersion method must be verified under these experimental conditions. First, the assumption that radial differences in concentration are small compared to longitudinal differences can be checked by eq 3.6. Second, the assumption that longitudinal diffusion is negligible can be verified with eq 3.7. Experimental values of the terms on the left-hand side of eqs 3.6 and 3.7 are given in Table 3.3. Clearly, these two assumptions are valid under the present experimental conditions.

A third condition is that the variance due to the width of the injection plug and the detector flow cell must be small compared to the overall variance. The characteristic time, τ_{inj} associated with the 10μL injection volume (assuming a "plug" distribution) is given by

$$\tau_{inj} = V_{inj}/F \qquad (3.9)$$

where V_{inj} is the injected volume (10^{-2} cm^3) and F is the volumetric flow rate (cm^3/s), which can be calculated by

$$F = \frac{\pi a^2 L}{t} \qquad (3.10)$$

The variance due to the injection plug can be calculated from moment analysis[92] and is given by

$$\sigma_{t,inj}^2 = \tau_{inj}^2/12 \qquad (3.11)$$

Thus, for t = 2000s, τ_{inj} = 21s, and $\sigma_{t,\,inj}^2 = 35\ s^2$. This is clearly small compared with the overall variances given in Table 3.2.

Similarly, the bandbroadening due to the finite volume of the detector flow cell must be small. The volume of the flow cell in the Varian UV-50 is 8μL, and the same argument presented above can be made to show that the volume of the flow cell is sufficiently small. The treatment of bandbroadening effects in the injector and detector with a "plug" model is reasonable beacuse of the symmetry of the observed peaks. If either the injector or detector behaved more like a "mixing chamber" in which any fluid entering the chamber (injector/detector) was mixed with the entire chamber volume, tailed peaks would be observed.[92]

A fourth condition which must be met is constant flow rate from the time of injection to elution. The elution times (and hence the flow rates) varied by about 27% over the course of all the measurements (~6 hours). Thus, in a typical 30 min run, the flow rate varied by only about 2%.

Table 3.1 Calibration of the tubing radius with caffeine ($D = 6.3 \times 10^{-6}$ cm^2/s)

Trial	Elution time t (s)	Peak width w_t (s)	Variance σ_t^2 (s^2)	Tubing radius[a] a (cm)
1	1736	356	7899	0.0262
2	1833	360	8111	0.0259
3	1898	379	8984	0.0268
Average				0.0263 ± 0.0004

[a] from equation 3.5

Table 3.2 Measurement of diffusion coefficients for 4-NT, 4-MAP, malathion, and progesterone in water at 25°C

Compound	Trial	Elution time t (s)	Peak width w_t (s)	Variance σ_t^2 (s^2)	Diffusion coeff.[a] D (cm^2/s) x 10^6
4-NT	1	1964	345	7434	7.61
	2	2033	344	7383	7.94
	3	2047	333	6934	8.51
	Ave.				**8.0 ± 0.5**
4-MAP	1	2062	354	7847	7.57
	2	2105	357	7952	7.63
	3	2137	354	7847	7.85
	Ave.				**7.7 ± 0.2**
malathion	1	2144	409	10440	5.92
	2	2165	436	11870	5.26
	3	2173	438	12000	5.22
	Ave.				**5.5 ± 0.4**
progesterone	1	2232	493	15160	4.24
	2	2251	504	15900	4.08
	3	2287	540	18210	3.62
	Ave.				**4.0 ± 0.3**

[a] from equation 3.5

Table 3.3 Verification of assumptions (equations 3.6 and 3.7) for the experimental conditions employed in the determination of diffusion coefficients

Compound	$\frac{a^2}{D \cdot t}$ [a, b]	$\frac{a^2 \overline{U}^2}{48D^2}$ [c, d]
caffeine	0.06	22000
4-NT	0.04	11000
4-MAP	0.04	11000
malathion	0.06	21000
progesterone	0.08	36000

[a] t taken from the average of the 3 trials for each compound

[b] must be << 1 for verification of eq 3.6

[c] $\overline{U} = L/t$

[d] must be >> 1 for verification of eq 3.7

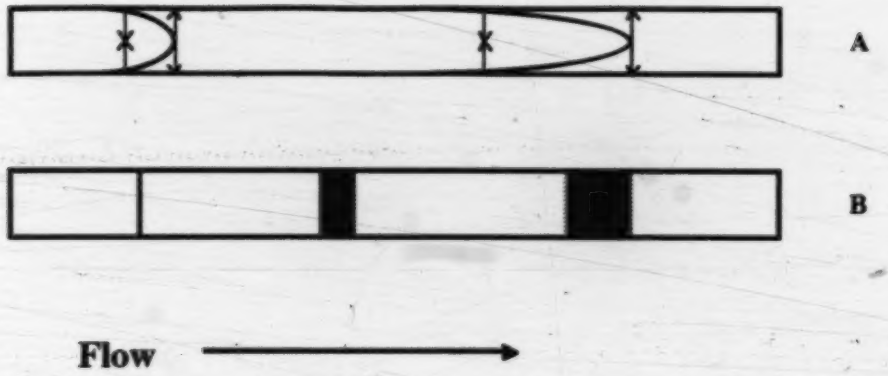

Figure 3.1 Taylor dispersion in laminar flow. The hypothetical case of no diffusion is represented by the parabolic concentration profiles in A. Radial diffusion, however, will relax this dispersion as molecules near the center of the tube diffuse towards the side of the tube, and vice versa (represented by arrows). The result is the observed concentration profile shown in B. Here, radial differences in concentration are minimal, and the sample disperses in a gaussian distribution as it flows through the tube.

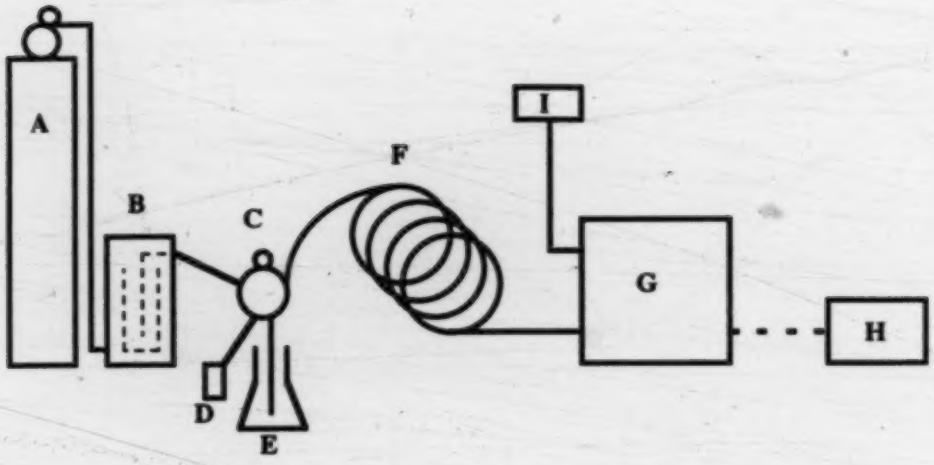

Figure 3.2 Experimental apparatus for the determination of diffusion coefficients. A: He tank, B: aluminum cylinder pump with solvent reservoir inside, C: 6-port injection valve with 10μL loop, D: syringe for loading sample, E: sample solution, F: 446cm, 0.02" i.d. stainless steel tubing (constant temperature bath not shown), G: UV detector, H: chart recorder, I: waste.

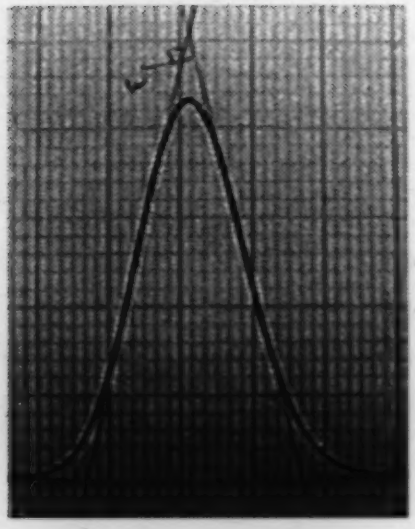

Figure 3.3 Typical 4-MAP peak from the Taylor dispersion apparatus. Also shown are manually drawn tangents to the inflection points and baseline construction. The x-axis is time, and the y-axis is absorbance. See text for details.

Chapter 4

TEFLON ROD SYSTEM*

4.1 Introduction

The solvent microextraction apparatus described in this chapter consists of a 1-mL vial which contains the aqueous sample and a rod-shaped Teflon probe hollowed out at one end and held in place by a washer and cap. The hollowed-out end of the Teflon probe is filled with 8 μL of organic solvent (n-octane) containing a fixed concentration of internal standard (n-dodecane). The probe is immersed in the aqueous sample which is stirred by a magnetic stirrer. After the desired stirring time, the Teflon probe is removed from the aqueous sample, and a 1-μL aliquot of the organic phase is taken by microsyringe and injected into a gas chromatograph (GC) for quantification.

The observed rate of solvent extraction (concentration in the organic phase, C_o versus stirring time, t) is in excellent agreement with the first order kinetic model (eq 2.16). Although maximum sensitivity and precision are obtained by stirring until equilibrium is reached, it is generally more convenient to stir for a fixed, short time period (e.g. 5 min) at a constant stirring speed. Analytically, the relative standard deviation of the method is 1.7% for a 5.00-min extraction of the analyte 4-methylacetophenone (4-MAP) into n-octane.

---

* A version of this chapter has been published. Jeannot, M.A.; Cantwell, F.F. 1996. Analytical Chemistry. 68: 2236-2240.

4.2 Experimental details

4.2.1 Chemicals

n-dodecane (Aldrich, Milwaukee, WI), 4-methylacetophenone (4-MAP; Kodak, Rochester, NY), and n-octane (BDH, Poole, England) were all reagent grade and used as received. Water was purified by the Nanopure system (Barnstead, Dubuque, IA).

4.2.2 Apparatus

The solvent microextraction apparatus is shown diagrammatically in Figure 4.1. The 1.0-mL minivial and stir bar were obtained from Alltech Associates (Deerfield, IL), stock no. 95010. The Teflon probe was fabricated in the chemistry department machine shop. A 1/8 inch (0.317$_5$ cm) drill bit with a rounded tip was used to machine out the hemispherical recess in one end of a 2.0-cm long x 0.40-cm diameter Teflon rod, to contain the organic solvent. The Teflon probe was held in place by a silicone septum with ~1/8 inch hole punched out at the center. The septum was held inside the minivial cap. Consistent placement of the probe within the cap/septum assembly was achieved by carefully aligning the top of the Teflon probe with the top of the cap using a flat surface.

The speed of the stir bar was measured with a strobe lamp (Strobe 5K, Strobe Automation Ltd., England) and adjusted to the appropriate value. Temperature was maintained at 25 ± 0.02 °C by a circulating water bath (Lauda K-4/RD, Brinkmann, Rexdale, ON, Canada). A 10-µL microsyringe (model 701 N, Hamilton, Reno, NV) was used to introduce 8.0 µL of organic phase into the probe and to sample and inject the organic phase into the GC after extraction. A Hewlett-Packard HP5840A gas chromatograph with packed column (Apiezon L stationary phase) and flame ionization

detector (FID) was used for quantification. Helium was used as carrier gas at a flow rate of 20 mL/min, and column temperature was 200 °C.

4.2.3 Extraction studies

The model compound 4-methylacetophenone (4-MAP) was extracted from water into n-octane which contained 2.2 mmol/L n-dodecane as internal standard. An aqueous 0.221 mmol/L solution of 4-MAP was used in the kinetic studies, while several aqueous solutions of 4-MAP in the concentration range 0.109 - 0.543 mmol/L were prepared for the analytical methodology studies.

The probe was first inverted (hemispherical recess facing up) and filled with 8.0 μL of n-octane/internal standard solution. The probe was then returned to its normal position (recess facing down) and transferred to the vial. After the solution was stirred for a known time, the probe was removed, inverted, and a 1-μL aliquot of the organic phase was taken with the microsyringe and injected into the GC for quantification. For the kinetic studies and isotherm measurement, the FID response was calibrated by injecting standard solutions of 4-MAP. This is not necessary, however, for routine analysis, as discussed later.

In all cases, a fixed concentration of n-dodecane was present in the organic phase as an internal standard in order to correct both for evaporation of n-octane after extraction and for variable injection volumes. The analytical signal was taken as the peak area ratio of 4-MAP to n-dodecane. In these cases, the *ratio* of 4-MAP to n-dodecane remains the same. Note that the internal standard does not correct for evaporation of solvent before the extraction while the filled probe is being transferred to the vial. The use of a relatively low volatility solvent such as n-octane and rapid transfer of the filled probe to the vial minimize pre-extraction evaporation of the drop. (After standing in air for 60 seconds, only about 7% of the n-octane drop evaporates.

Transfer to the vial is performed in 2-3 seconds, during which time a negligible amount of solvent would evaporate.)

4.3 Results and discussion

4.3.1 Flow pattern

In the apparatus shown in Figure 4.1, the aqueous phase is well stirred. The flow patterns in both the aqueous and organic phases were made visible to the eye by suspending charcoal powder in each phase while stirring only the aqueous phase. The circulatory flow in each phase consists of both a horizontal-rotational component and a vertical-toroidal component. The toroidal flow in each of the phases is shown diagramatically in Figure 4.2. The origin of such flow in the stirred aqueous phase is obvious. The reason for it in the organic phase is as follows: As the aqueous phase sweeps radially inward in a horizontal plane past the aqueous-organic interface, the frictional drag on the organic layer induces a parallel motion in the organic phase. When the flow streamlines in each phase converge at the central axis of the vial, they change direction and move vertically into their respective bulk phases. The situation is analogous to that which prevails in a liquid drop that is falling or rising through an immiscible liquid.[68, 93] Circulation in the organic phase will affect the rate of solvent extraction only if $1/\beta_o$ is not much smaller than κ/β_{aq} (eq 2.4); however, in any event, this circulation has the desirable effect of homogenizing the organic phase prior to gas chromatographic analysis.

4.3.2 Kinetics

The GC response was calibrated with standard solutions of 4-MAP in n-octane/internal standard solution, as shown in Figure 4.3. Since the concentration of internal standard (n-dodecane) was the same as that used in the extraction studies, this

calibration curve was used to calculate $[4\text{-MAP}]_o$ from peak area ratios in the various extraction studies.

Shown as data points in Figure 4.4 are plots of concentration vs time for extraction of 4-MAP from 1.00 mL of a 2.21×10^{-4} mol/L, stirred aqueous solution into an 8.0-μL droplet of n-octane. Four different stirring rates between 900 and 1800 rpm were employed. Slower stirring rates could not be measured with the strobe lamp, and faster stirring rates resulted in dislodgement of the organic drop from from the rod. The solid lines through the four sets of data points represent the fitting of eq 2.16 to the data using a nonlinear least-squares program in the software package KaleidaGraph.[94] Values of the fitting parameters $C_{o,eq}$ and k are presented in columns 2 and 3 of Table 4.1. Within experimental error, the equilibrium concentration $C_{o,eq}$ is independent of stirring rate, so κ, from eq 2.17, is also a constant, independent of stirring rate (column 4 in Table 4.1). Evidently, the rate constant k is constant at a fixed stirring rate, so $\bar{\beta}_o$, from eq 2.14, is also constant (column 5 in Table 4.1).[b] However, at higher stirring rates, k and $\bar{\beta}_o$ increase. The half-time of extraction (time required to reach half the equilibrium value) is given in the sixth column of Table 4.1.

To gain some insight into the nature of the extraction process, the mass transfer coefficient $\bar{\beta}_o$ may be interpreted in terms of a convective-diffusive mass transfer model. The popular Whitman two-film theory[68, 69, 72, 74] is employed.

Film theory postulates steady-state diffusion (after a short lag time) across stagnant solvent layers of thickness δ_o and δ_{aq} adjacent to the interface in the organic and aqueous phases, respectively. In either the organic or the aqueous phase, the mass transfer coefficient $\beta = D/\delta$, where D is the diffusion coefficient of the solute and δ is

---

[b] The interface was approximately flat. The interfacial area (required for evaluation of the mass transfer coefficient from eq 2.14) was estimated from the diameter of the recess (0.31_8 cm) to be 0.079 cm^2.

the film thickness in the appropriate phase. Thus, according to film theory, eq 2.4 can be written as

$$\frac{1}{\beta_o} = \frac{\delta_o}{D_o} + \frac{\kappa\delta_{aq}}{D_{aq}} \qquad (4.1)$$

If the two terms on the right hand side of eq 4.1 are comparable in magnitude, then simultaneous evaluation of both film thicknesses is not possible from studies of only one solute (i.e. only one κ). However, in the present case, κ is large, so the first term on the right in eq 4.1 can be neglected, and resistance to mass transfer in the aqueous phase is the rate-determining step for extraction. With this approximation, δ_{aq} can be evaluated since D_{aq} is independently known (Chapter 3). Calculated values are presented in the seventh column of Table 4.1.

The dashed line in Figure 4.4, shown for comparison, is the concentration vs time profile predicted for the case in which there is no stirring. This rate curve is based on a semiinfinite linear diffusion model.[71, 79] Assuming no interfacial turbulence, and assuming that the diffusing substance does not reach the end of the drop, eq 2.32 can be used with $D_{aq} = 7.7 \times 10^{-6}$ cm^2/s (Chapter 3) to calculate the total amount of substance diffusing across the interface as a function of time. The equation describing the dashed line is

$$C_o(t) = 0.053\text{mmol/L}\cdot\text{min}^{1/2}\sqrt{t(\text{min})} \qquad (4.2)$$

In such a stagnant system, after 30 min, the concentration in the organic phase would be ~0.29 mmol/L, compared with the equilibrium value of 6.72 mmol/L, or about 4%

of the way to equilibrium. Clearly, stirring produces a dramatic increase in the extraction rate compared to the stagnant case.

It has often been observed for solvent extraction systems that $\bar{\beta}_o$ is related to stirring rate s by an expression of the form[68]

$$\log \bar{\beta}_o = \text{const} + p \cdot \log s \qquad (4.3)$$

For the data in Table 4.1, a plot of log $\bar{\beta}_o$ vs log s is shown in Figure 4.5. The plot fits a straight line with a slope of 0.74 ± 0.06, an intercept of -6.1 ± 0.2, and a correlation coefficient $R^2 = 0.988$. The value of p = 0.74 is intermediate between the value of 1.0 that is often observed for the "Lewis cell", in which two immiscible liquids are stirred independently without disturbing the interface,[68, 95] and the value of 0.5 predicted by the Levich equation for a rotating disk and observed in the Albery rotated extractor.[96]

The values of δ_{aq} obtained in the microextraction system are somewhat smaller than those observed in the Lewis cell[95] ($\delta_{aq} \approx 5 \times 10^{-3}$ cm) and in the so-called "rapid-stir cell",[9, 97] ($\delta_{aq} \approx 3 \times 10^{-3}$ cm) in which droplets of one phase are dispersed in the other phase. This is because Lewis cells are stirred more slowly to avoid disturbing the interface, while in rapid-stir cells the shearing forces between the droplets and the continuous phase are limited because the dispersed droplets tend to move along with the continuous phase. Although δ_{aq} in the microextraction system is relatively small (i.e. $\bar{\beta}_o$ is relatively large), the small A_i/V_o ratio (eq 2.3) limits the rate of extraction compared to the rapid-stir cell.

The absolute values of $\bar{\beta}_o$ obtained in the microextraction system, while larger than those for other stirred systems, are comparable to those observed for falling and

rising drops. Laddha and Degaleesan[93] propose the following expression for the continuous phase mass transfer coefficient (β_{aq} in this case):

$$\beta_{aq} = \frac{0.023 U_t}{\sqrt{(Sc)_{aq}}} \qquad (4.4)$$

where U_t is the terminal velocity of the drop and $(Sc)_{aq}$ is the dimensionless Schmidt number for the aqueous phase, given by:

$$(Sc)_{aq} = \frac{\mu_{aq}}{\rho_{aq} D_{aq}} \qquad (4.5)$$

Here, μ_{aq} is the viscosity of water (0.890×10^{-2} g/cm·s at 25°C),[98] ρ_{aq} is the density of water (0.997 g/cm^3 at 25°C),[99] and D_{aq} is the diffusion coefficient in water (7.7×10^{-6} cm^2/s for 4-MAP at 25°C, from Chapter 3).

At a stirring rate of 1500 rpm, the angular velocity of water in the vicinity of the probe tip was measured to be 115 rad/s by observing the movement of a single charcoal particle with the aid of a strobe lamp. With a rotational radius of about 0.1 cm, this corresponds to a linear velocity of 12 cm/s. For a drop of n-octane rising through water with a terminal velocity, U_t, of 12 cm/s, eq 4.4 predicts continuous phase mass transfer coefficient $\beta_{aq} = 8 \times 10^{-3}$ cm/s. From eq 2.18, taking $\kappa = 40$ L/L for 4-MAP, $\bar{\beta}_o$ for the rising drop system would therefore be 2×10^{-4} cm/s. This is essentially the same as the value 1.9×10^{-4} cm/s reported in Table 4.1 at the appropriate 1500 rpm stirring rate.

4.3.3 Dissolution of n-octane

From eqs 2.1 and 2.14, it is clear that the volume of the drop has a direct influence on both the equilibrium and kinetic aspects of the extraction. Furthermore, the method is dependent on a fixed concentration of internal standard in the drop. For both of these reasons, it is essential that no significant amount of the solvent will dissolve in the water phase during the extraction.

The worst-case scenario is that both the water phase and the headspace become saturated with n-octane. The solubility of n-octane in water is low ($5.7_8 \times 10^{-6}$ mol/L)[100] so that a saturated 1-mL aqueous solution of n-octane would contain 5.8×10^{-9} mol of n-octane. This is negligible compared with the total of 4.9×10^{-5} mol of n-octane in the drop. The maximum number of moles of n-octane in the headspace, n, can be estimated from the vapor pressure, P of n-octane at 25°C (0.0184 atm),[100] assuming an ideal gas:

$$n = \frac{PV}{\Re T} \qquad (4.6)$$

where V is the headspace volume ($\sim 1 \times 10^{-4}$ L), $\Re$ is the gas constant (0.0821 L·atm/mol·K), and T is the temperature (298K). From eq 4.6, the maximum number of moles of n-octane in the headspace is $\sim 7.5 \times 10^{-8}$ mol. Again, this is very small compared to the total moles in the drop. Thus, no significant volume change in the drop will occur, even considering these "worst-case" conditions. This may not be true, however, for solvents that have a greater water solubility or volatility (see section 7.2).

The rate of dissolution of the drop may be estimated as follows: It may be assumed that the aqueous phase immediately adjacent to the interface is saturated with n-octane, and $C_{aq,i} = 5.7_8 \times 10^{-6}$ mol/L. Here, the "worst-case" condition for maximum

flux is that the concentration of octane in the bulk aqueous solution is zero (i.e. C_{aq} = 0). The flux is then given by:

$$\frac{1}{A_i}\frac{dn}{dt} = \frac{D_{aq}}{\delta_{aq}}\left(C_{aq,i} - C_{aq}\right) = \frac{D_{aq}}{\delta_{aq}}C_{aq,i} \qquad (4.7)$$

With $C_{aq,i} = 5.7_8 \times 10^{-9}$ mol/cm^3, assuming the interfacial area remains constant at 0.079 cm^2, and taking D_{aq} to be nominally 5.0×10^{-6} cm^2/s, and δ_{aq} to be 1.0×10^{-3}cm, the number of moles of octane dissolving per second is 2.3×10^{-12} mol/s. Thus, in 30 min, at most 4.1×10^{-9} mol of octane will have dissolved. Again, this is negligible compared with the total moles in the drop (4.9×10^{-5} mol).

4.3.4 Analytical methodology

4.3.4.1 Distribution isotherm

The equilibrium distribution isotherm was measured by the solvent microextraction technique using five aqueous solution concentrations of 4-MAP in the range 0.109 - 0.543 mmol/L. The aqueous phase was stirred at ~1800 rpm for 30 min. Equation 2.16 can be rearranged to calculate how close the system will be to equilibrium under these conditions:

$$\frac{C_o}{C_{o,eq}} = 1 - e^{-kt} \qquad (4.8)$$

Taking the rate constant k at 1800 rpm to be 2.7×10^{-3} s^{-1} (Table 4.1), after 30 minutes, the extraction is about 99% of the way to equilbrium.

The isotherm is shown in Figure 4.6. It is linear in this concentration range, with a slope of $\kappa = 38.5 \pm 1.7$ L/L, an intercept of zero (0.06 ± 0.46 mmol/L), and a correlation coefficient $R^2 = 0.994$. Equilibrium organic phase concentrations were measured by GC, and equilibrium aqueous phase concentrations were calculated with eq 2.7. At equilibrium, about 24% of the initial aqueous phase concentration has been extracted into the organic phase.

4.3.4.2 Calibration and precision

Since κ is constant, calibration using aqueous standards may be employed on the basis of eq 2.34. Since the GC signal (employing internal standard) is proportional to C_o, a plot of GC signal vs $C_{aq,\ initial}$ for a series of standard concentrations should yield a linear calibration curve. The same five aqueous 4-MAP solutions which were employed in measuring the distribution isotherm were each subjected to 5.00 min of stirring at a fixed stirring rate (~1800 rpm) in the microextraction apparatus, and the measured GC signals were plotted vs initial aqueous phase concentration of 4-MAP. The results are presented in Figure 4.7. This calibration curve is linear, with a slope of 4.88 ± 0.13 L/mmol, an intercept of zero (-0.001 ± 0.05), and a correlation coefficient $R^2 = 0.998$. After 5 min of stirring, the extraction is only slightly more than half way to equilbrium, and yet good precision is obtained for the calibration curve.

The precision was further tested by performing 5-min extractions and GC analyses on 10 replicate, 1.00 mL aliquots of the aqueous solution of $C_{aq,\ initial} = 0.177$ mmol/L. The results are shown in Table 4.2. The data in the table illustrate the importance of the internal standard. The peak areas of both internal standard and 4-MAP show some variation from trial to trial (4-5% rsd). However, run-to-run variations in the area of the internal standard peak coincide with proportional variations in the area of the 4-MAP peak. For example, trial 10 gave the highest areas for both

internal standard and 4-MAP. These variations are likely due to small differences in the injection volume and/or injection technique from run-to-run. By ratioing the peak areas, these errors cancel out. The relative standard deviation for the peak area *ratios* was 1.7%, which is quite acceptable for a solvent extraction GC method.

Table 4.1 Equilibrium and kinetic parameters for extraction of 4-MAP from water into 8.0 μL of n-octane at four stirring rates, plus diffusion film thickness in the water phase

Stirring rate (rpm)	$C_{o,eq}$ (mol/L) x 10^3	k (s^{-1}) x 10^3	κ (L/L)[a]	$\bar{\beta}_o$ (cm/s)[b] x 10^4	$t_{1/2}$ (min)[c]	δ_{aq} (μm)[d]
900	6.67 ± 0.07	1.61 ± 0.04	39.8 ± 0.6	1.24 ± 0.04	7.2	15.6
1200	6.69 ± 0.05	2.10 ± 0.05	39.9 ± 0.4	1.61 ± 0.04	5.5	12.0
1500	6.74 ± 0.03	2.42 ± 0.03	40.3 ± 0.2	1.85 ± 0.03	4.8	10.3
1800	6.77 ± 0.05	2.70 ± 0.05	40.6 ± 0.4	2.06 ± 0.04	4.3	9.2

[a] from eq 2.17

[b] from eq 2.14 with $A_i = 0.079$ cm², $V_{aq} = 1.00$ cm³, and $V_o = 8.00 \times 10^{-3}$ cm³

[c] Half-time calculated as $t_{1/2} = \ln 2/k$

[d] from eq 4.2 (neglecting the first term on the rhs), taking $D_{aq} = 7.7 \times 10^{-6}$ cm²/s (Chapter 3)

Table 4.2 GC data for replicate non-equilibrium (5-min) extractions of 0.177 mmol/L 4-MAP, illustrating the role of the internal standard (IS).

Trial	Peak area (IS)	Peak area (4-MAP)	Area ratio
1	120200	100100	0.8328
2	114800	91680	0.7986
3	110000	87300	0.7936
4	115500	93860	0.8126
5	120400	97440	0.8093
6	117100	95080	0.8120
7	108300	87440	0.8074
8	119200	97600	0.8188
9	119000	99180	0.8334
10	124000	103200	0.8323
% rsd	4.1	5.5	1.7

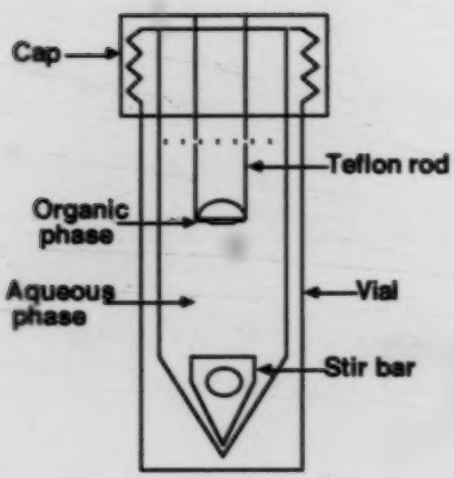

Figure 4.1 Side view illustration of the solvent microextraction system (approximately to scale). Magnetic stirrer not shown.

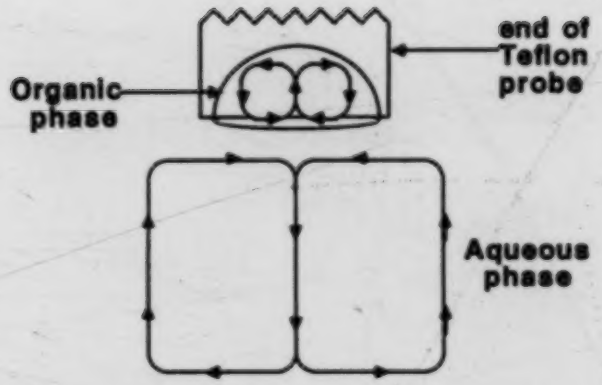

Figure 4.2 Enlarged view of the end of the Teflon probe showing the organic drop immersed in the aqueous phase. Fluid flow is illustrated conceptually with arrows (neglecting the rotational component for clarity), showing how circulation is induced in the organic phase.

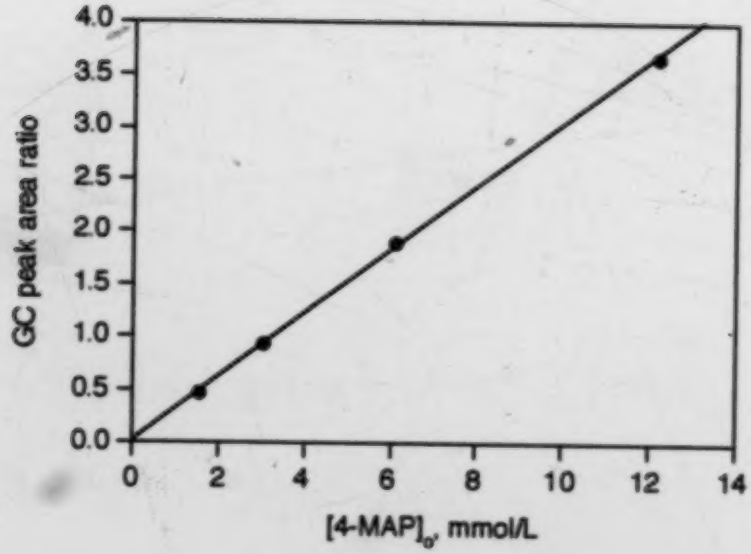

Figure 4.3 Calibration of GC response with standard solutions of 4-MAP in n-octane/internal standard solution. Each standard was measured in duplicate (points overlap on plot). Slope = 0.299 ± 0.002 L/mmol, intercept = 0.03 ± 0.02, R^2 = 1.000.

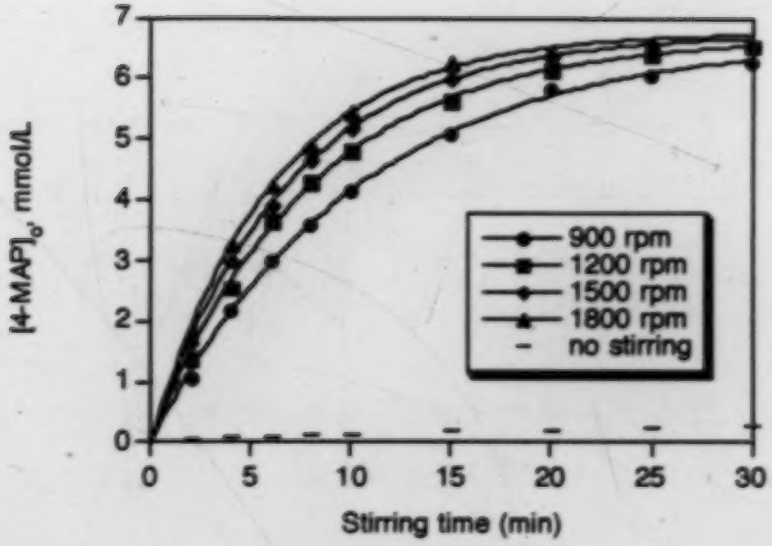

Figure 4.4 Plots of concentration of 4-methylacetophenone in n-octane versus stirring time at various aqueous phase stirring rates. Points indicate experimental data. Solid lines represent the fit to eq 2.16 with the parameters $C_{o,eq}$ and k given in Table 4.1. Dashed line represents extraction profile for the case of no stirring, as predicted by semiinfinite diffusion.

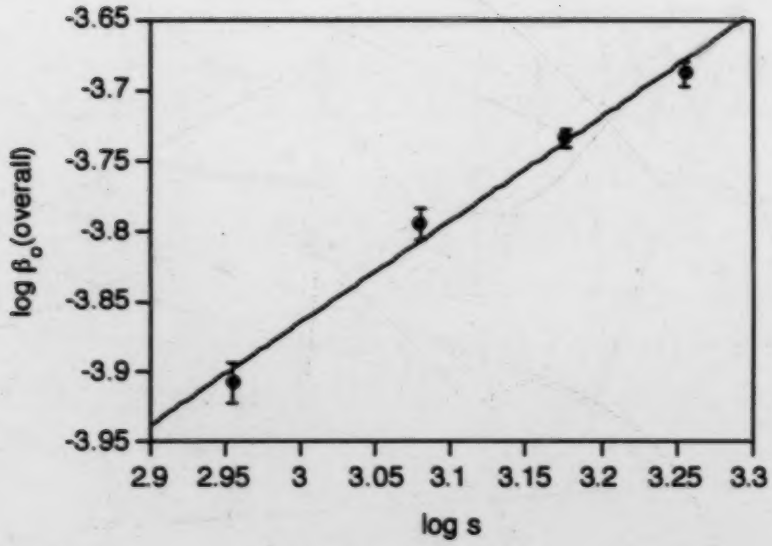

Figure 4.5 Plot of log $\bar{\beta}_o$ versus log s (s in rpm) for the data in Table 4.1. Points indicate experimental data. Line represents a linear least-squares fit to the data (slope = 0.74 ± 0.06, intercept = -6.1 ± 0.2, R^2 = 0.988). Error bars represent the estimated error in $\bar{\beta}_o$ at each stirring rate from the curve fits in Figure 4.4.

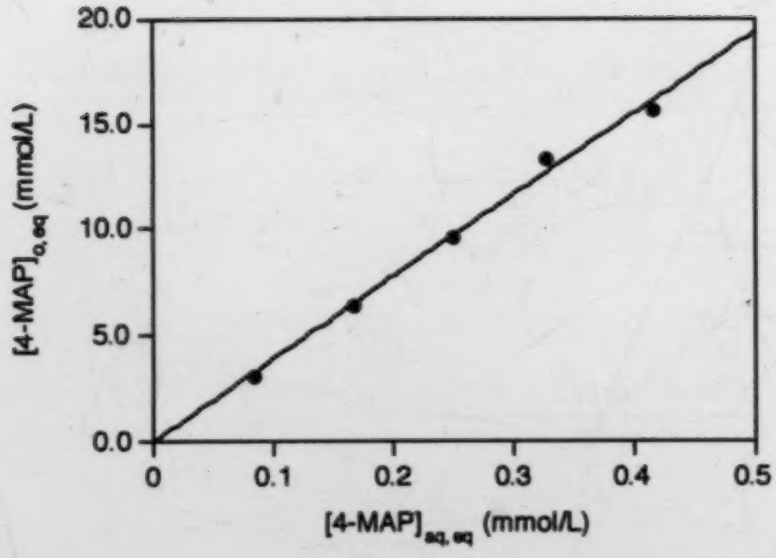

Figure 4.6 Equilbrium distribution isotherm for 4-MAP between water (aq) and n-octane (o). The isotherm is linear over this concentration range, as is normally observed for dilute solutions of simple organic solutes. Slope = κ = 38.5 ± 1.7 L/L, intercept = 0 (0.06 ± 0.46) mmol/L, R^2 = 0.994.

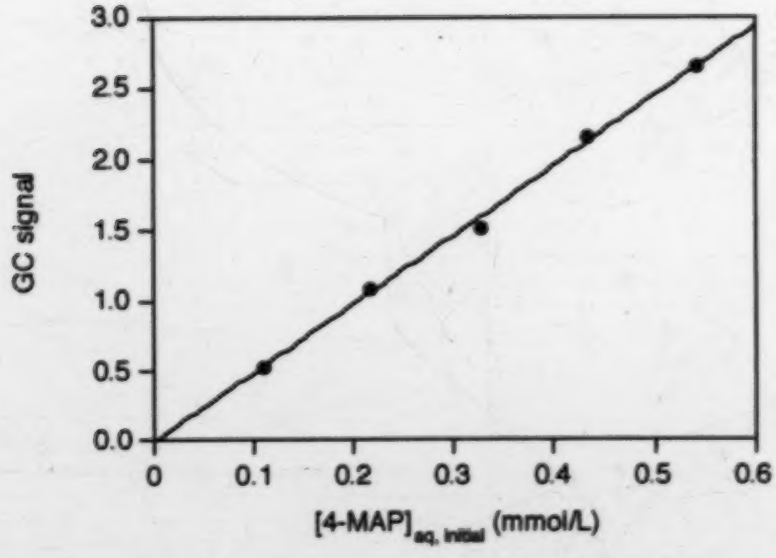

Figure 4.7 Calibration of the solvent microextraction system using aqueous standards. Standards are extracted for a short, non-equilibrium time (5.00 min). Slope = 4.88 ± 0.13 L/mmol, intercept = 0 (-0.001 ± 0.05), R^2 = 0.998.

Chapter 5

SYRINGE NEEDLE SYSTEM AND MASS TRANSFER MODEL[a]

5.1 Introduction

The 8-μL solvent microextraction system described in Chapter 4 is attractive in terms of sensitivity, precision, analysis time, and relative simplicity. However, the containment of the organic drop in a recess at the end of the Teflon rod is somewhat inconvenient because it requires filling the recess with the drop of solvent at the start of the experiment and sampling a portion of the drop with a microsyringe prior to injection into the gas chromatograph at the end of the experiment. In the present study, these manipulations are eliminated. Here, solvent microextraction is performed by suspending a 1-μL drop directly from the tip of a microsyringe needle immersed in the aqueous phase. The drop remains attached to the needle tip at stirring speeds up to 2000 rpm. Quantification of the amount of solute extracted into the 1-μL drop is performed by retracting the drop back into the needle, withdrawing the needle from the aqueous solution, and injecting directly into the GC. A second practical advantage of the 1-μL system over the Teflon rod system is a faster rate of extraction.

In the Teflon rod study, the mass transfer coefficient was tentatively interpreted in terms of film theory. However, no experiments were performed to test the validity of film theory. In the present study, the emphasis is on characterizing the mass transfer properties of the 1-μL system. In addition to establishing that the first-order rate law describes the extraction, the effects of stirring rate and of sample diffusion coefficient on the mass transfer coefficient are also investigated. Measurement of the dependence

---

[a] A version of this chapter has been published. Jeannot, M.A.; Cantwell, F.F. 1997. Analytical Chemistry. 69: 235-239.

of the mass transfer coefficient on diffusion coefficient is designed to reveal mechanistic information concerning the mass transfer process, specifically, whether film theory is an accurate model for the convective-diffusive mass transfer of the sample compound.

5.2 Experimental details

5.2.1 Chemicals

n-Dodecane (Aldrich, Milwaukee, WI), 4-methylacetophenone (4-MAP; Kodak, Rochester, NY), 4-nitrotoluene (4-NT; Anachemia, Champlain, NY), n-octadecane (Aldrich), n-octane (BDH, Poole, England), progesterone (Aldrich), and n-tetradecane (Kodak) were all reagent grade and used as received. Malathion was an analytical standard from AccuStandard Inc. (New Haven, CT), obtained through the distributor Chromatographic Specialties, Inc. (Brockville, ON, Canada). The malathion standard was certified to be 98.9% pure (by HPLC) by the manufacturer. Water was purified by the Nanopure system (Barnstead, Dubuque, IA).

5.2.2 Apparatus

The microextraction apparatus is similar to the one shown in Figure 4.1, modified as described. The Teflon rod and the cap insert which held it in place have been removed, and a silicone rubber septum of the type normally used with the 1-mL minivial has been placed in the cap. The minivial (No. 95010, Alltech Associates, Deerfield, IL) is clamped in a water-jacketed vessel and maintained at 25 ± 0.02 °C with a circulating water bath. During an extraction, a 5-μL microsyringe with Chaney adaptor (Model 7105 KH, Hamilton Co., Reno, NV) is clamped above the minivial such that the syringe needle passes through the rubber septum and the needle tip protrudes to a depth of about 5 mm below the surface of stirred 1.00 mL of aqueous

sample solution in the minivial. A 1-μL drop of the n-octane extracting solvent is suspended from the needle tip, and shown in the photograph in Figure 5.1.

In the type of microsyringe employed here, the plunger is a wire that is inside the needle itself. This particular needle has a no. 2 point style with a 22° bevel, and the plunger wire is bevelled and aligned to match the bevel of the needle tip (see Figure 5.1). The syringe is made leak-tight by tightening a ferrule near the junction of the needle and the glass barrel. The ferrule compresses the needle to form a tight seal with the plunger wire. The spacer on the end of the syringe barrel was cut to a length of 1" to allow sufficient penetration of the needle into the injection port of the GC.

In this type of syringe, the liquid is contained entirely within the needle. In this way, when the drop is dispensed from the syringe with the plunger wire, there is no solution remaining in the needle (except for a thin film between the plunger wire and needle wall, as discussed in the Results and Discussion). If an ordinary plunger-in-barrel syringe were used, the needle would be filled with solvent above the pendant drop. When the drop is retracted after extraction, it would mix in a non-reproducible way with the solvent in the needle.

The triangular Teflon-coated stirring bar (Alltech) is rotated at a constant speed by means of a Series H heavy-duty laboratory stirrer and motor controller (G.K. Heller Corp., Floral Park, NY). A feedback mechanism in the controller maintains the stirring rate at better than ±1% rsd, in spite of changes in line voltage or stirring load. The motor is inverted, and a rotating magnet assembly from a conventional plate-type magnetic stirrer is mounted in the motor chuck and centered underneath the water-jacketed vessel containing the minivial. The accuracy of the stirrer motor controller was checked with an optical tachometer; it was found to be accurate within about 1%.

Gas chromatographic determination of the amount of sample compound extracted into the n-octane drop was performed on a Model HP 5840A gas

chromatograph (Hewlett-Packard) using either an Apiezon L or an OV-1 packed column, helium carrier gas, and flame ionization detector (FID).

5.2.3 Extraction procedure

The aqueous phase in the minivial was 1.00 mL of one of the following aqueous sample solutions: either 1.50×10^{-4}, 2.06×10^{-4}, or 1.82×10^{-4} mol/L of 4-MAP; 2.4×10^{-6} mol/L of progesterone; 1.38×10^{-4} mol/L of 4-NT; or 1.86×10^{-5} mol/L of malathion. The organic phase was n-octane containing a fixed concentration of an internal standard. The internal standard was either n-tetradecane (for 4-MAP and 4-NT on OV-1 stationary phase), n-octadecane (for progesterone and malathion on OV-1), or n-dodecane (for 4-MAP on Apiezon L).

The extraction procedure, which follows, was always the same, though sample compounds, stirring rates, and stirring times were varied in the different studies. The Chaney adapter is set for a maximum volume of 2.00 μL and a delivery volume of 1.00 μL, using the stop button. After thoroughly rinsing the microsyringe with the appropriate n-octane/internal standard solution, 2.00 μL is taken up. While holding the needle tip in air, the plunger is depressed with the stop button activated. This leaves 1.00 μL of octane solution remaining in the needle and 1.00 μL of it as a drop suspended at the needle tip. The syringe is then clamped above the vial, and the clamped syringe is lowered so that the needle pierces the center of the septum and penetrates into the aqueous solution. In the process of piercing the septum, the suspended drop is wiped off the needle tip. (If the suspended drop is not present during transfer of the syringe to the vial, a portion of the 1.00 μL of solvent contained within the needle will evaporate during the transfer.) The plunger is next pushed to its fully depressed position, which dispenses the remaining 1.00 μL of octane solution and

leaves it suspended as a drop at the needle tip, as in Figure 5.1. Extraction will occur into this drop. Time zero in the extraction rate experiment is when the stirrer is turned on.

After stirring for the prescribed period of time, the plunger is withdrawn to its preset maximum of 2.00 µL while the needle is still immersed in the aqueous solution. (If the needle is withdrawn from the aqueous solution while the octane drop is still hanging, the drop leaves the needle tip and floats on the aqueous solution.) The microsyringe is then removed from the clamp, and the needle is withdrawn from the minivial. At this time, the needle contains all of the n-octane and, below it, a microliter of the aqueous sample solution. With the stop button activated, the plunger is depressed to the 1.00-µL position to expell the aqueous solution, and the needle is wiped with a tissue. The octane solution remaining in the needle is then injected into the gas chromatograph. To ensure leak-free operation of the GC septum with the larger-bore 7105 syringe, it is essential to make the septum retaining nut very tight and to inject in the same hole in the septum each time. Reproducible injections of the less-volatile solutes (e.g progesterone) are ensured by leaving the needle in the injection port for ~1s after injection.

The analytical signal is taken as the area ratio of the analyte peak to the internal standard peak. The GC response is calibrated using standard solutions containing both the sample compound and the internal standard in n-octane.

5.2.4 Carryover study

In order to determine the number of flushing cycles necessary to avoid contamination from previous solutions in the syringe, the following procedure was carried out: (1) The syringe was first flushed thoroughly and filled with 2 µL of n-dodecane / n-octane internal standard solution. 1 µL of this solution was dispensed and

wiped off with a tissue, and the other 1 μL was injected into the GC to measure the peak area of n-dodecane. (2) The syringe was then filled with 2 μL of n-octane alone; 1μL was dispensed and wiped off, and the other 1μL was injected into the GC to determine the peak area of residual n-dodecane (from step (1)). Step (2) was repeated until no trace of n-dodecane was detected.

5.3 Results and discussion

5.3.1 Practical considerations

The technique is capable of yielding a relative precision of 1-2%, provided that a few simple procedural details are employed. These steps are required as a consequence of the fact that there is, necessarily, a small but finite space between the side of the wire plunger and the inner wall of the syringe needle. This space will be occupied by a film of fluid, either air or liquid. Furthermore, the length, and thus the volume, of this film increases as the plunger is depressed and decreases as the plunger wire is retracted. There are three practical considerations arising from the existence of this film:

(i) When first using a *dry* microsyringe at the start of the day, it is necessary to flush it many times (e.g. 100 or more) with the n-octane/internal standard solution - drawing the plunger up slowly and depressing it rapidly each time - in order to replace all of the air in the film with liquid. If this is not done, air bubbles will appear as in Figure 5.1 in the 1-μL drop during extraction, changing the rate of extraction (different drop volume, shape). However, once this operation has been performed, the microsyringe may be used repeatedly for extractions and injections into the GC without air bubbles appearing.

Although air bubbles are undesirable, their occasional appearance was accompanied by their rapid movement within the drop during stirring. Thus, there is apparently significant circulation induced within the drop from the stirred aqueous solution, as was observed in the 8-μL system (Chapter 4).

(ii) The liquid film remaining in the needle after injection into the GC can cause carryover of sample compound to the next extraction if the syringe is not flushed well with the n-octane/internal standard solution prior to refilling it. A carryover study was performed to determine the number of cycles required to completely flush out old solution from the syringe, as described in section 5.2.4. The results are shown in Figure 5.2. After one flushing cycle with n-octane, the observed n-dodecane signal is about 3% of the original value. After 19 cycles, there is no detectable amount of n-dodecane remaining in the syringe. Therefore, 20 flushing cycles were deemed sufficient to avoid carryover.

(iii) When the 1-μL drop is drawn back into the needle to terminate the solvent extraction step, it mixes with the n-octane/internal standard solution from the portion of the film that is liberated by the retracting plunger. This represents a postextraction dilution of the drop with additional internal standard solution. It reduces the ratio of analyte compound to internal standard compound. When performing routine analytical determinations, this phenomenon *requires no compensation* because aqueous calibration standards of the analyte compound would be subjected to the same extraction procedure as the sample. When performing extraction rate measurements, as in the present case, the calibration standards are prepared directly in the n-octane/internal standard solution so that they do not experience the dilution effect from the film in the needle. Therefore, in the present case, the observed values of C_o are all erroneously low by a constant dilution factor. The value of $C_{o,eq}$(obsd), obtained by curve-fitting with eq 5.2 below, is also lower than the correct value by the same

dilution factor, but *the value of the rate constant k obtained from the curve fitting is the correct one.*

The magnitude of the concentration dilution factor can readily by calculated by employing eq 2.1, which relates the correct equilibrium concentration of sample compound in the organic phase to its initial concentration in the aqueous phase, as follows:

$$\text{dilution factor} = C_{o,eq}(\text{correct}) \,/\, C_{o,eq}(\text{obsd}) = \frac{\kappa C_{eq,initial}}{1+\kappa\left(V_o/V_{eq}\right)} \frac{1}{C_{o,eq}(\text{obsd})} \qquad (5.1)$$

Here, V_o is the volume of the organic solvent phase during the extraction (1.00μL) and V_{eq} is the volume of the aqueous phase (1.00 mL). For the compound 4-MAP, using the known values, κ = 40.2 L/L (Table 4.1), $C_{eq,\,initial}$ = 2.05(7) x 10^{-4} mol/L, and $C_{o,eq}$(obsd) = (6.65 ± 0.04) x 10^{-3} mol/L (from Table 5.1), the value of the dilution factor is 1.19 ± 0.01. The 1-μL drop is diluted with 0.19 μL from the film which is liberated as the plunger is retracted a distance of 2.4 cm (i.e. 2 μL, see Experimental details) in a needle that has a 0.033 cm i.d. This corresponds to an annular gap of 7.6-μm thickness between the plunger and the needle wall.

5.3.2 Kinetics

The GC response was calibrated by injecting standard solutions of 4-MAP in n-dodecane / n-octane solution. The calibration curve is linear, and is shown in Figure 5.3. Plots of observed concentration of extracted 4-MAP in the n-octane drop versus

stirring time, at four different stirring rates, are shown in Figure 5.4. Theory predicts that these extraction rate curves should be described by the expression

$$C_o(\text{obsd}) = C_{o,eq}(\text{obsd})\left(1-e^{-kt}\right) \qquad (5.2)$$

where k is a first-order extraction rate constant and $C_{o,eq}$(obsd) is the equilibrium concentration, which is reached after a long time. C_o(obsd) and $C_{o,eq}$(obsd) may be corrected as described above by multiplying them by the dilution factor 1.19. The solid lines in Figure 5.4 represent fits of the data points to eq 5.2, performed using the software package KaleidaGraph.[94] Evidently, eq 5.2 represents the extraction rate very well. Values of $C_{o,eq}$(obsd), $C_{o,eq}$(correct), and k are presented in Table 5.1.

The rate constant k is related to the overall mass transfer coefficient $\bar{\beta}_o$ by eq 2.14. The interfacial area of contact between the octane and water phases, A_i, is estimated as follows: If the shape of the drop is approximated as a prolate elipsoid with semi- major and minor axes l_1 = 0.15cm and l_2 = 0.04cm respectively, we obtain the volume and surface area as[101]

$$V \approx \frac{4}{3}\pi l_1 l_2^{\,2} = 1.0\text{x}10^{-3}\text{cm}^3 \qquad (5.3)$$

$$A_{drop} \approx 2\pi l_2^{\,2} + 2\pi\frac{l_1 l_2}{\varepsilon}\sin^{-1}\varepsilon \qquad (5.4)$$

where ε is the eccentricity of the ellipsoid, given by[102]

$$\varepsilon = \frac{\sqrt{l_1^2 - l_2^2}}{l_1} = 0.96, \qquad (5.5)$$

From eqs 5.4 and 5.5, the surface area of the drop is approximately 0.06_1 cm^2.

The area of contact with the needle tip can be estimated by treating the needle tip as an ellipse with semi- major and minor axes $l_1 = 0.15$cm and $l_2 = 0.04$cm respectively:

$$A_{\text{needle tip}} = \pi l_1 l_2 = 0.01_9 \text{cm}^2 \qquad (5.6)$$

Thus, the interfacial area can be estimated by subtracting the area of contact with the needle tip from the total area of the drop:

$$A_i \approx 0.06_1 \text{cm}^2 - 0.01_9 \text{cm}^2 = 0.04 \text{cm}^2 \qquad (5.7)$$

Although this estimation of A_i is somewhat crude, it is sufficient here, since we are concerned mainly with the functional dependence of $\bar{\beta}_o$ on stirring rate and diffusion coefficients, not the absolute values of $\bar{\beta}_o$. Calculated values of $\bar{\beta}_o$ using $A_i \approx 0.04\text{cm}^2$ are presented in Table 5.1.

Comparison of values in Table 5.1 for a 1-μL drop with the corresponding values in Table 4.1 for the 8-μL drop on the Teflon rod shows that, at a given stirring rate, k is larger for 1-μL than for 8-μL, but $\bar{\beta}_o$ is about the same for the two drop volumes. That is, $\bar{\beta}_o$ is approximately independent of drop size. The reason why k is larger for the 1-μL drop than for the 8-μL drop at a given stirring rate is that it has a

larger ratio of area to bulk phase volume, A_i/V_o. In terms of equilibrium considerations, the 1-μL system is also slightly more sensitive than the 8-μL system (V_o term in denominator of eq 2.1). (In both cases, 1 μL is injected.)

5.3.3 Mass transfer model

The chemical structures of the four compounds chosen for this study are shown in Figure 5.5. Criteria for the choice of compounds included the following: (1) Compounds must be relatively non-polar so that κ is large. (2) They must not be too volatile (loss of analyte into the headspace), but they must have sufficient volatility for GC analysis. (3) They must be UV absorbers for the determination of diffusion coefficients using the apparatus described in Chapter 3. (4) They must cover as wide a range of sizes (and hence diffusion coefficients) as possible.

Since 4-MAP is among the most volatile of the compounds under study, the loss of 4-MAP into the headspace may be considered as a worst-case scenario. The vapor pressure of pure *acetophenone* at 37°C is 1.0mmHg ($1.3(2) \times 10^{-3}$ atm).[109] Using the ideal gas law (eq 4.6), the number of moles of analyte lost to the headspace can be estimated as 5.2×10^{-9} mol. If we are working with 10^{-3}L of a 2×10^{-4} mol/L solution of 4-MAP, this represents a loss of $5.2 \times 10^{-9} / 2 \times 10^{-7}$ or ~3% of the 4-MAP into the headspace. However, the actual amount of 4-MAP lost will be even less than this, because (1) the vapor pressure used in the calculation was for the more volatile acetophenone, not 4-methylacetophenone, (2) the vapor pressure was for *pure* compound or saturated solution, not for a dilute, unsaturated solution, and (3) the temperature used in the calculation was 37°C, not 25°C. Therefore, loss into the headspace is insignificant for the compounds used in this study.

GC calibration curves for the four compounds using standard solutions in the appropriate n-octane / internal standard solution are shown in Figures 5.6 - 5.9. In all

cases, the plots are linear and there is little scatter. Shown in Figures 5.10 - 5.13 are extraction rate curves (observed concentration versus stirring time) for the four compounds 4-NT, 4-MAP, malathion, and progesterone obtained at a stirring rate of 1500 rpm using V_o = 1.00 μL of n-octane/internal standard solution and V_{aq} = 1.00 mL of aqueous sample solution. The solid lines represent fitting of the data with eq 5.2. Values of the fitting parameters $C_{o,aq}$(obsd), $C_{o,aq}$(correct), k, and of the distribution coefficient κ and the mass transfer coefficients $\bar{\beta}_o$ and β_{aq} are presented in Table 5.2. Distribution coefficients were calculated by means of the expression

$$\kappa = \frac{C_{o,aq}(\text{correct})V_{aq}}{C_{aq,\text{initial}}V_{aq} - C_{o,aq}(\text{correct})V_o} \qquad (5.8)$$

For all four of these compounds, κ is large so that the overall mass transfer rate is equal to the aqueous phase mass transfer rate:

$$\beta_{aq} \approx \kappa\bar{\beta}_o \qquad (5.9)$$

Experimentally determined distribution coefficients are in good agreement with data reported in the literature for hexane-water systems. Nasim et al[104] found κ to be 45.0 for 4-MAP at 27 ± 0.2 °C. Watanabe et al[105] measured the equilibrium distribution of progesterone between hexane and aqueous phosphate buffer at 25°C and found κ = 244.

Also shown in Table 5.2 are the experimentally measured aqueous phase diffusion coefficients, D_{aq}, for the four compounds of interest (from Table 3.2). A plot

of β_{aq} vs D_{aq} is presented in Figure 5.14. The straight line in this figure represents a linear least-squares fit of the data using an equation of the form $\beta_{aq} = (\text{const})D_{aq}$ to serve as a test of film theory, and the curved line represents a nonlinear least-squares fit to the data using an equation of the form $\beta_{aq} = (\text{const})D_{aq}^{1/2}$ to serve as a test of penetration theory. The linear fit is excellent. The slope is 936 ± 8 cm^{-1}, and the correlation coefficient $R^2 = 0.997$. The nonlinear fit is poor, with $R^2 = 0.750$. Thus, β_{aq} is well represented by film theory but poorly represented by penetration theory, so convective-diffusive mass transfer in the aqueous phase is quantitatively described in terms of film theory. From the reciprocal slope of the solid line in Figure 5.14, $\delta_{aq} = (10.7 \pm 0.1) \times 10^{-4}$ cm at 1500 rpm.

The linear dependence of β_{aq} on D_{aq} reported here is in contrast to most mass transfer correlations[74, 93, 106, 107] which predict an exponent of ~1/2 to ~2/3 on the diffusion coefficient for various systems, based on correlations of dimensionless numbers.[74] However, these correlations each apply strictly to a particular type of system, different from the single drop - microsyringe system. Furthermore, as pointed out by McManamey et al,[107] mass transfer correlations are often obtained by changing the liquid, and hence the viscosity, which in turn alters the diffusion coefficient of the sample molecule. Since the viscosity and the diffusion coefficient are interrelated, it is difficult to separate the effects of each parameter on the mass transfer coefficient. In this study, however, the diffusion coefficient alone was varied by changing the sample molecule.

According to film theory, β_{aq} increases with increasing stirring speed (s, in rpm) because faster stirring decreases δ_{aq}. Values of δ_{aq} at four different stirring rates

of 4-MAP are presented in column 7 of Table 5.1. A plot of δ_{aq} vs 1/s is shown in Figure 5.15. The solid line represents a linear least-squares fit. It has a slope of 1.48 ± 0.06, an intercept of zero (i.e. (3 ± 5) x 10^{-5}), and $R^2 = 0.997$. The linearity of this plot means that, for extraction into this pendant drop, the thickness of the diffusion film in the aqueous phase decreases linearly with an increase in stirring speed.

5.3.4 Analytical application

The above discussion reveals that extraction of analytes having relatively large κ's into a single drop at the tip of a syringe needle is well characterized in terms of kinetics and mass transfer processes. When designing an analytical determination by solvent extraction GC, a relatively large κ is generally a sought-for analyte property. Thus, the system which has been described and characterized in this study has great potential for use in routine analysis. In this connection, the syringe is a commonly used off-the-shelf model, requiring no modification, and the same is true for the vial and GC. Automation of this system using a conventional GC autosampler is an obvious possibility.

The use of compounds with *very large* κ's (e.g. 1000 or higher) is problematic for at least two reasons: (1) It is difficult to prepare aqueous solutions of known concentration using extremely hydrophobic (i.e. low water solubility) compounds, and (2) large errors in κ from eq 2.17 or 5.8 will result if the two terms in the denominator are very similar (i.e. ~quantitative extraction). However, κ need not be calculated in an analytical application (section 2.5) where simple calibration suffices.

In order to measure the precision that is routinely attainable with this system, 10 replicate extraction - GC measurements were performed for 1.00 min stirring time on a 1.82 x 10^{-4} mol/L 4-MAP solution at a stirring speed of 1500 rpm. The results are

shown in Table 5.3, again illustrating the role of the internal standard. Under these conditions, although the extraction is only 38% of the way to equilibrium, nevertheless the relative standard deviation of the peak area ratio of 4-MAP to internal standard was 1.5%. The system exhibits quite adequate reproducibility for use in routine analysis.

Table 5.1 Equilibrium and kinetic parameters for extraction of 2.06×10^{-4} mol/L 4-MAP from water into 1.00 μL of n-octane at four stirring rates

Stirring rate (rpm)	$C_{o,eq}$ (obsd) (mol/L) x 10^3	$C_{o,eq}$ (correct)[a] (mol/L) x 10^3	k (s^{-1}) x 10^3	$\bar{\beta}_o$[b] (cm/s) x 10^4	β_{aq}[c] (cm/s) x 10^3	δ_{aq}[d] (cm) x 10^4
900	6.68 ± 0.07	7.97 ± 0.08	$4.6_8 \pm 0.1_1$	1.12 ± 0.03	$4.5_3 \pm 0.1_5$	16.9 ± 0.7
1200	6.64 ± 0.06	7.92 ± 0.07	$6.4_2 \pm 0.1_7$	1.54 ± 0.04	$6.1_8 \pm 0.2_2$	12.4 ± 0.5
1500	6.61 ± 0.03	7.87 ± 0.03	7.98 ± 0.09	1.92 ± 0.02	$7.6_4 \pm 0.1_2$	10.1 ± 0.3
1800	6.69 ± 0.03	7.98 ± 0.03	$9.0_5 \pm 0.1_1$	2.18 ± 0.03	$8.7_8 \pm 0.1_4$	$8.7_5 \pm 0.2_2$

[a] $C_{o,eq}(\text{correct}) = (1.19)C_{o,eq}(\text{obsd})$, from eq 5.1

[b] from eq 2.14, with $A_i = 0.04_0$ cm^2, $V_{aq} = 1.00$ cm^3, and $V_o = 1.00 \times 10^{-3}$ cm^3

[c] from eq 2.18

[d] from eq 2.20, with $D_{aq} = 7.6_8 \times 10^{-6}$ cm^2/s

Table 5.2 Equilibrium and kinetic parameters for extraction of four compounds from water into 1.00 μL of n-octane at 1500 rpm, plus diffusion coefficients from Table 3.2

Solute	$C_{o,eq}$ (obsd) (mol/L) x 10^3	$C_{o,eq}$ [a] (correct) (mol/L) x 10^3	k (s^{-1}) x 10^3	κ [b] (L/L)	$\bar{\beta}_o$ [c] (cm/s) x 10^5	β_{eq} [d] (cm/s) x 10^3	D_{eq} (cm^2/s) x 10^6
4-NT	$12.1_1 \pm 0.3$	$14.4_4 \pm 0.3$	$2.9_1 \pm 0.1_8$	117 ± 3	$6.5_2 \pm 0.4_3$	$7.6_3 \pm 0.6_5$	$8.0_2 \pm 0.4_5$
4-MAP	$4.9_9 \pm 0.1_3$	$5.9_5 \pm 0.1_6$	$7.1_9 \pm 0.5_5$	$41._4 \pm 1._2$	$17._3 \pm 1._3$	$7.1_4 \pm 0.7_3$	$7.6_9 \pm 0.1_5$
mala-thion	2.83 ± 0.04	3.38 ± 0.05	1.12 ± 0.04	222 ± 4	2.29 ± 0.09	$5.0_8 \pm 0.2_6$	$5.4_6 \pm 0.3_9$
proges-terone	$0.36_3 \pm 0.01_3$	$0.43_3 \pm 0.01_5$	$0.78_4 \pm 0.06_3$	222 ± 10	$1.6_0 \pm 0.1_4$	$3.5_6 \pm 0.4_1$	$3.9_8 \pm 0.3_2$

[a] $C_{o,eq}(\text{correct}) = (1.19)C_{o,eq}(\text{obsd})$, from eq 5.1

[b] from eq 5.8

[c] from eq 2.14, with $A_i = 0.04_0\ cm^2$, $V_{eq} = 1.00\ cm^3$, and $V_o = 1.00 \times 10^{-3}\ cm^3$

[d] from eq 5.9

Table 5.3 GC data for replicate non-equilibrium (1-min) extractions of 0.182 mmol/L 4-MAP, illustrating the role of the internal standard (IS).

Trial	Peak area (IS)	Peak area (4-MAP)	Area ratio
1	80940	56930	0.7034
2	85100	61400	0.7215
3	91020	65040	0.7146
4	88360	62070	0.7025
5	92440	65480	0.7084
6	78580	54100	0.6885
7	95260	67460	0.7082
8	92620	64720	0.6988
9	88580	63710	0.7192
10	95080	66300	0.6973
% rsd	**6.4**	**6.8**	**1.5**

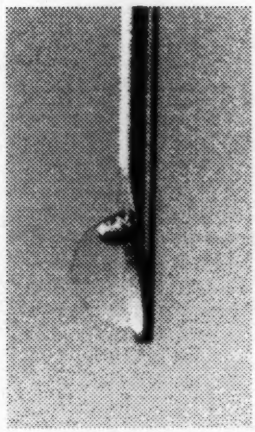

Figure 5.1 Photograph showing a 1-μL drop of n-octane suspended from the needle tip in aqueous solution. The drop contains an undesirable air bubble.

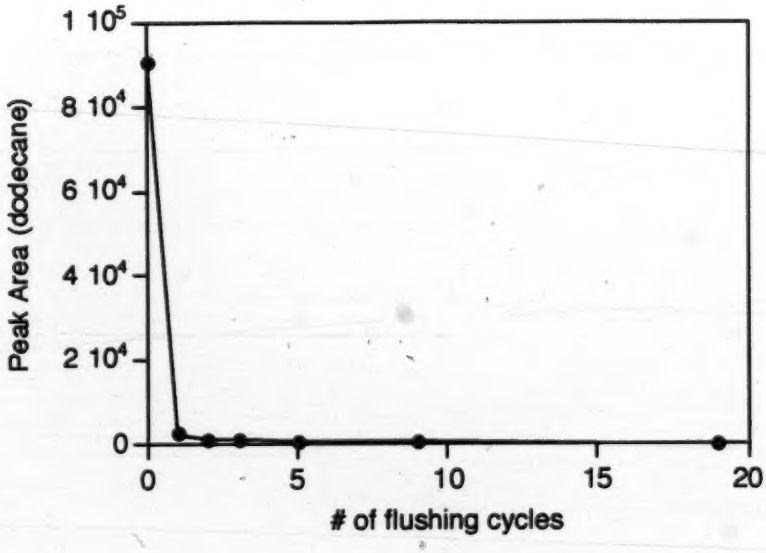

Figure 5.2 Carryover study to determine the number of syringe flushing cycles necessary to avoid contamination from one injection to the next.

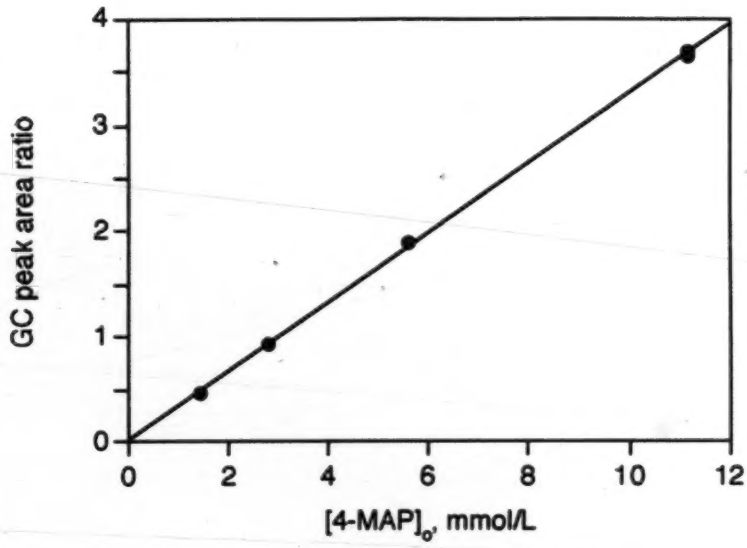

Figure 5.3 Calibration of GC response with standard solutions of 4-MAP in n-octane/internal standard solution. Slope = 0.326 ± 0.003 L/mmol, intercept = 0.04 ± 0.02, R^2 = 0.999.

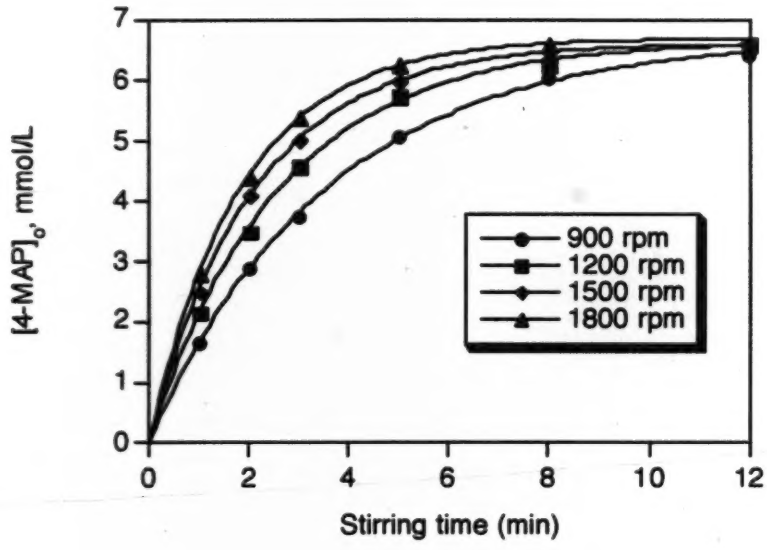

Figure 5.4 Plots of observed concentration of 4-MAP in n-octane versus stirring time at various stirring rates. Points indicate experimental data. Solid lines are fits to eq 5.2 with fitting parameters $C_{o,eq}$ and k given in Table 5.1.

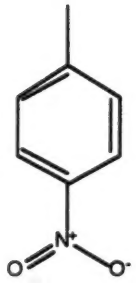

4-nitrotoluene (4-NT)

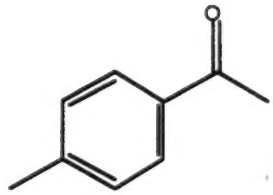

4-methylacetophenone (4-MAP)

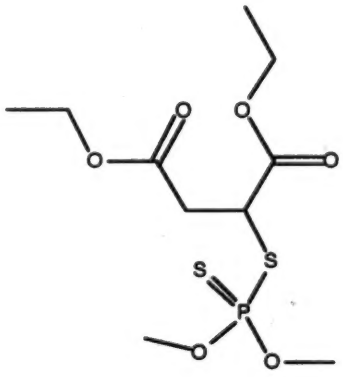

malathion

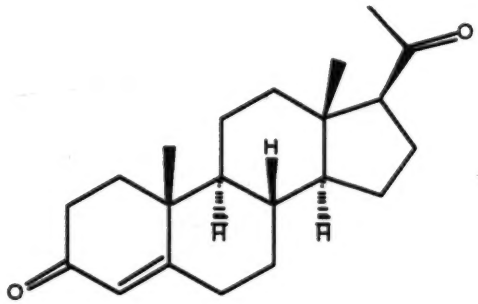

progesterone

Figure 5.5 Structures of the four compounds used in the mass transfer model study. All compounds are relatively non-polar, semi-volatile, and have no acid/base functional groups. They represent a relatively wide range of molecular sizes, and hence diffusion coefficients.

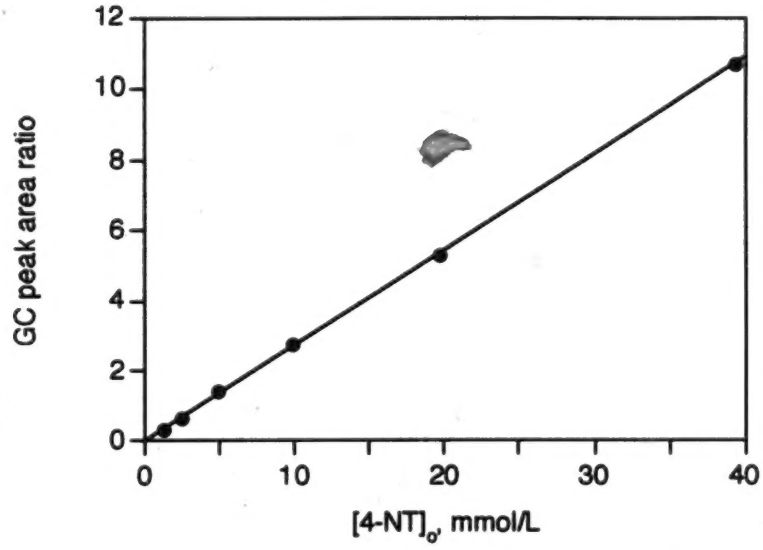

Figure 5.6 Calibration of GC response with standard solutions of 4-NT in n-octane/internal standard solution. Slope = 0.271 ± 0.001 L/mmol, intercept = 0.03 ± 0.02, R^2 = 1.000.

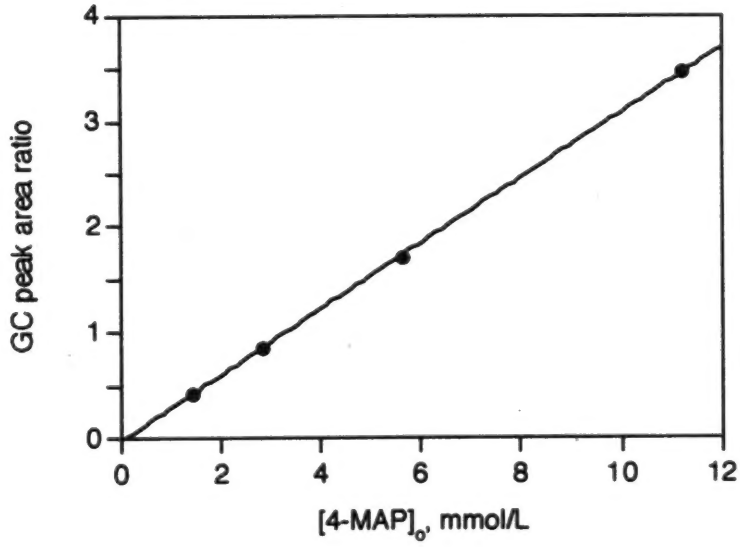

Figure 5.7 Calibration of GC response with standard solutions of 4-MAP in n-octane/internal standard solution. Slope = 0.309 ± 0.002 L/mmol, intercept = -0.02 ± 0.01, R^2 = 1.000.

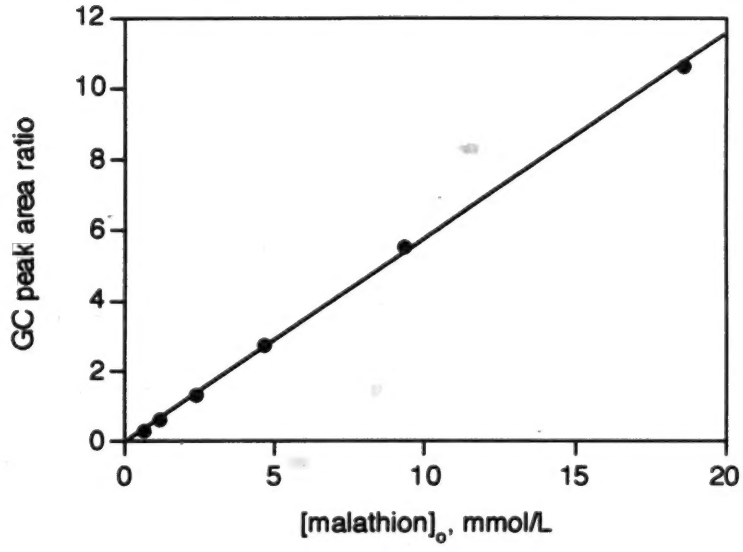

Figure 5.8 Calibration of GC response with standard solutions of malathion in n-octane/internal standard solution. Slope = 0.574 ± 0.007 L/mmol, intercept = 0.05 ± 0.06, R^2 = 0.999.

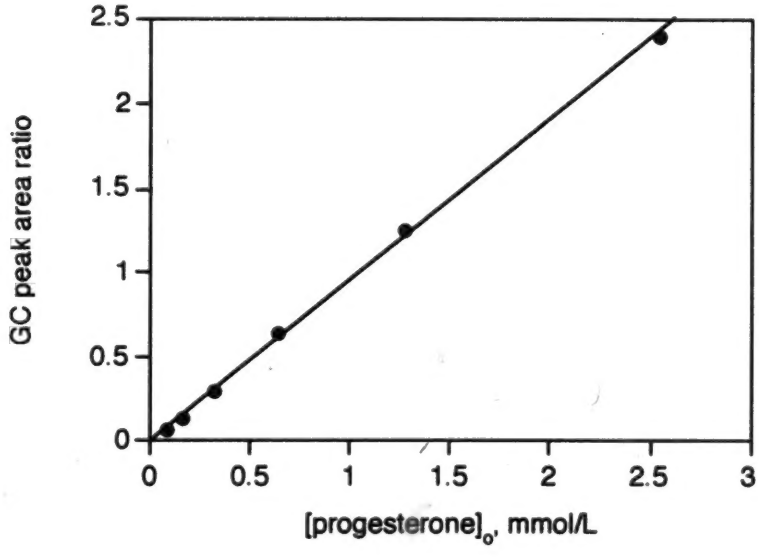

Figure 5.9 Calibration of GC response with standard solutions of progesterone in n-octane/internal standard solution. Slope = 0.95 ± 0.01 L/mmol, intercept = 0.003 ± 0.02, R^2 = 0.999.

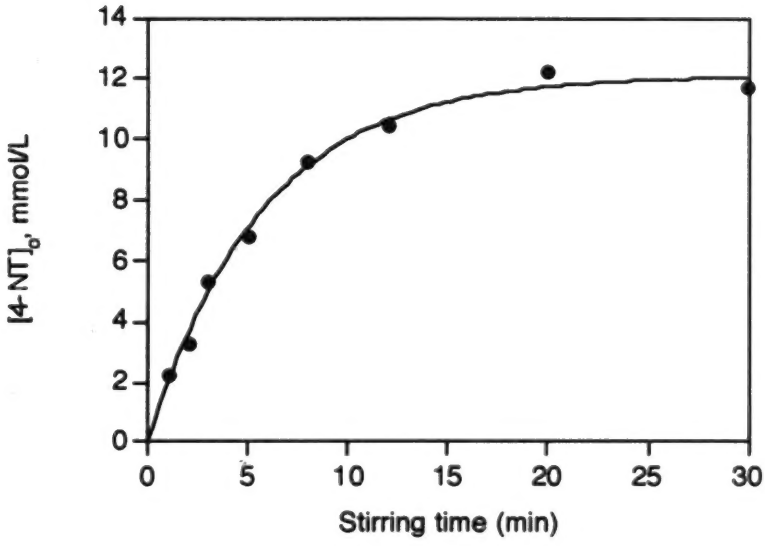

Figure 5.10 Plot of observed concentration versus stirring time at 1500 rpm for 4-nitrotoluene (4-NT). Points indicate experimental data. Solid lines are fits to eq 5.2 with fitting parameters $C_{o,eq}$ and k given in Table 5.2.

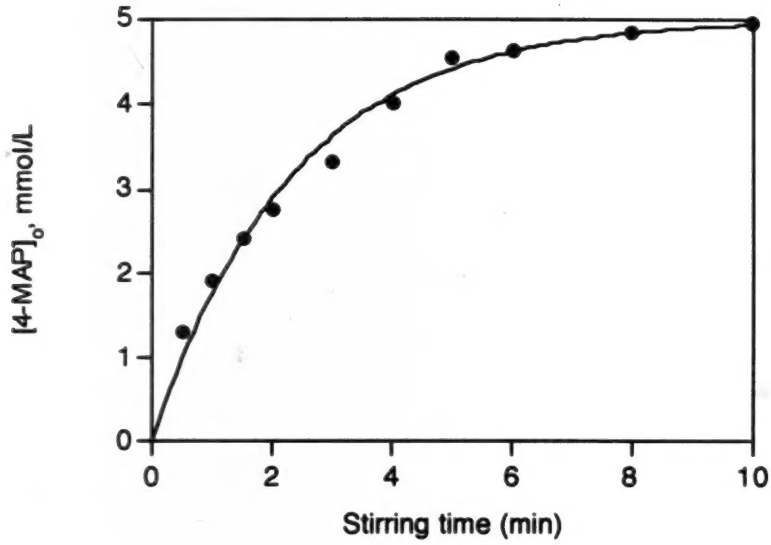

Figure 5.11 Plot of observed concentration versus stirring time at 1500 rpm for 4-methylacetophenone (4-MAP). Points indicate experimental data. Solid lines are fits to eq 5.2 with fitting parameters $C_{o,\,eq}$ and k given in Table 5.2.

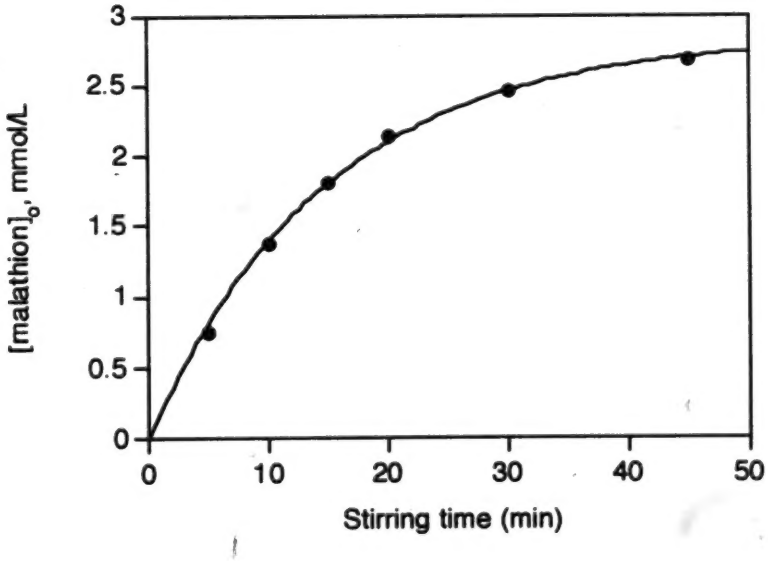

Figure 5.12 Plot of observed concentration versus stirring time at 1500 rpm for malathion. Points indicate experimental data. Solid lines are fits to eq 5.2 with fitting parameters $C_{o,\,eq}$ and k given in Table 5.2.

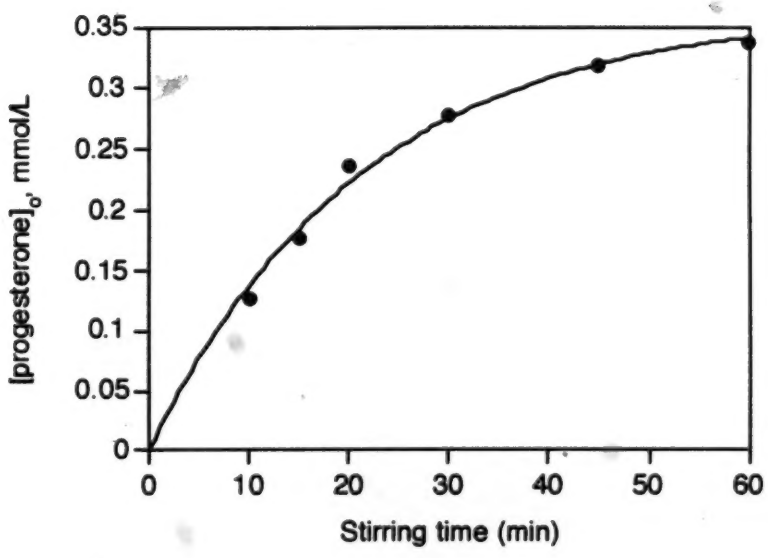

Figure 5.13 Plot of observed concentration versus stirring time at 1500 rpm for progesterone. Points indicate experimental data. Solid lines are fits to eq 5.2 with fitting parameters $C_{o,eq}$ and k given in Table 5.2.

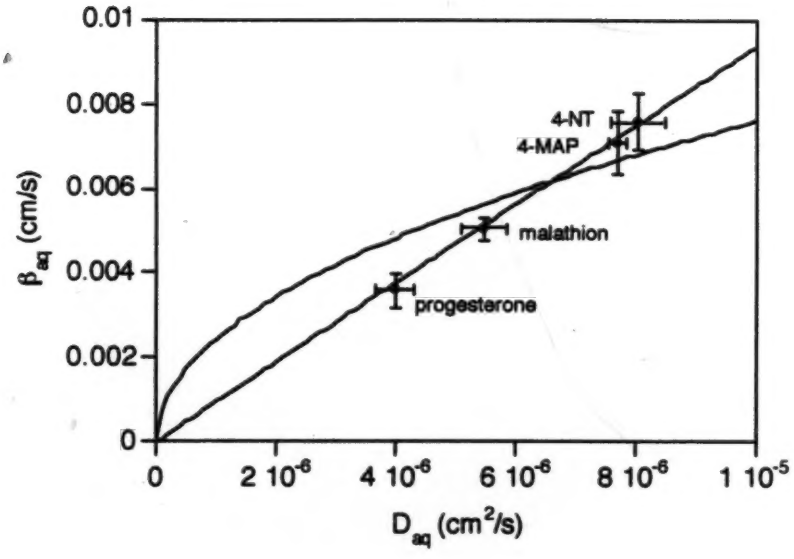

Figure 5.14 Plot of aqueous phase mass transfer coefficient β_{aq} versus aqueous phase diffusion coefficient D_{aq} for four compounds. Points indicate experimental data. Straight line is a fit to the film model (eq 2.20). Curved line is a fit to the penetration model (eq 2.24). Also shown are error estimates for both β_{aq} and D_{aq}.

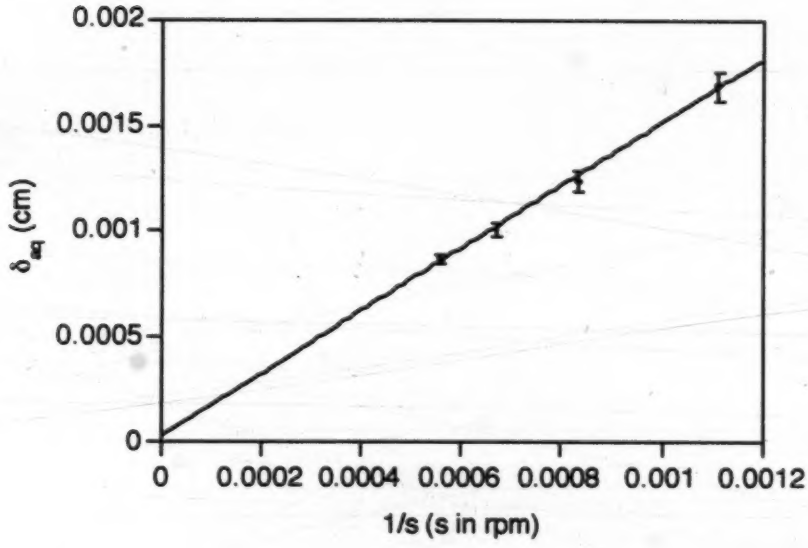

Figure 5.15 Plot of film thickness in the aqueous phase versus reciprocal stirring rate for the data in Table 5.1. Error bars represent the estimated error in δ_{aq}. Slope = 1.48 ± 0.06 cm/min, intercept = 0 ((3 ± 5) x 10^{-5}) cm, R^2 = 0.997.

Chapter 6

SPECIATION: DETERMINATION OF FREE PROGESTERONE IN A PROTEIN SOLUTION[a]

6.1 Introduction

Liquid-liquid extraction into microliter volumes of organic solvent has thus far been demonstrated for simple systems in which there are no complex equilibria in the aqueous phase. In particular, solvent extraction into a 1-μL drop of n-octane suspended at the tip of a microsyringe needle in a stirred aqueous solution has been shown to be a simple, inexpensive, and reproducible quantitative technique. In this chapter, the technique is extended to the extraction of a small solute molecule from an aqueous medium which contains a non-extractible macromolecule with which the solute forms a non-extractible complex. In the system chosen for study the steroid hormone progesterone is the solute and the protein bovine serum albumin (BSA) is the water soluble macromolecule. The effects which the binding of progesterone to protein exert on both the kinetic and equilbrium aspects of progesterone extraction are studied, as is the effect of the surface-active character of the protein.

When the extraction is performed with a very low phase ratio (e.g. V_o = 1 μL; V_{aq} = 500 mL) only a very small fraction of the progesterone is removed from the aqueous phase so that the binding equilibrium is not significantly perturbed. With this condition met, the concentration of the unbound (i.e. free) progesterone species can be determined directly. In addition, the binding constant can also be measured for the progesterone-protein complex. Furthermore, in order to minimize the time required for these measurements and because the extraction kinetics are so reproducible, the

---

[a] A version of this chapter has been accepted for publication. Jeannot, M.A.; Cantwell, F.F. 1997. Analytical Chemistry.

extraction may be performed for times that are far short of the time required for the attainment of equilibrium.

A large number of methods have previously been described for the study of steroid-protein interactions, the most popular of which is equilibrium dialysis.[108] Equilibrium solvent extraction methods have previously been described for measuring the binding of methyl orange,[109] testosterone,[110] and progesterone[105, 111, 112] to BSA. However, these extraction methods employ a very much greater phase ratio (organic/water) than is employed in the presently described method, with the consequence that the extraction of steroid from the aqueous phase significantly perturbs the binding equilibrium in that phase. Very recently, a non-perturbing solid-phase microextraction (SPME) technique has been used to measure the concentration of the unbound species of small-molecule solutes in an aqueous protein solution.[113]

6.2 Binding of steroids to protein

The mathematical treatment of the binding of steroids to protein generally involves some simplifying assumptions.[114-117] Although in principle a single protein molecule may contain many binding sites of different binding affinity, it is normally assumed that each protein molecule contains m binding sites of equal binding affinity. Furthermore, it is assumed that these sites are independent (i.e. the binding of a steroid molecule to one site does not affect the binding affinity of any other sites). Thus, the equilibrium may be represented by:

$$\text{Free Steroid} + \text{Protein Binding Site} \rightleftharpoons \text{Bound Steroid} \qquad (6.1)$$

The binding constant, K_a, for the binding of steroid to protein in aqueous (aq) solution is then given by the expression:

$$K_a = \frac{[S(\text{bound})]_{aq}}{[S]_{aq}\left(m[P]_{T,aq} - [S(\text{bound})]_{aq}\right)} \qquad (6.2)$$

where $[S(\text{bound})]_{aq}$ is the concentration of bound steroid (mol/L), $[S]_{aq}$ is the concentration of non-bound (free) steroid (mol/L), m is the number of binding sites per protein molecule, and $[P]_{T,aq}$ is the total molar concentration of protein, both with and without bound steroid (mol/L). The term in parenthesis in the denominator is simply the concentration of free protein binding sites.

If only a small fraction of the binding sites are occupied by steroid molecules, then $m[P]_{T,aq} \gg [S(\text{bound})]_{aq}$ and $[S(\text{bound})]_{aq} \approx [SP]_{aq}$ (i.e. species such as S_2P can be neglected, as discussed in section 6.6.4). Equation 6.2 reduces to:

$$mK_a \approx \frac{[SP]_{aq}}{[S]_{aq}[P]_{T,aq}} \qquad (6.3)$$

An independent evaluation of both m and K_a is not possible because these appear as a product. However, the new constant mK_a provides a useful measure of the binding affinity and serves as a basis for comparison with literature values.[114-116]

6.3 Modifications to the mass transfer model

In Chapter 5 it was shown that the rate of extraction of the steroid progesterone, and of other small molecules which have large distribution coefficients, can be quantitatively treated by film theory, according to which the aqueous phase mass transfer coefficient is given by the expression:

$$\beta_{S,aq} = \frac{D_{S,aq}}{\delta_{aq}}, \text{ cm/s} \qquad (6.4)$$

where $D_{S,aq}$ is the diffusion coefficient of the steroid in the aqueous phase (cm^2/s) and δ_{aq} is the thickness of the Nernst diffusion film in the aqueous phase (cm).

If the homogeneous rate constants for both complexation (binding) and decomplexation between progesterone and protein in aqueous solution are large, the kinetics of extraction of the steroid from an aqueous protein solution will also be controlled by mass transfer. The film model of mass transfer rate control can be adapted to this case. When there is a large excess of protein binding sites over the amount of steroid present, then eq 6.3 is valid.[114-117] The expression for the total flux of progesterone in the aqueous phase is:

$$\frac{1}{A_i}\frac{dn}{dt} = \beta_{S,aq}\left([S]_{aq} - [S]_{aq,i}\right) + \beta_{SP,aq}\left([SP]_{aq} - [SP]_{aq,i}\right) \qquad (6.5)$$

and the (equal) total flux of progesterone in the organic phase is:

$$\frac{1}{A_i}\frac{dn}{dt} = \beta_{S,o}\left([S]_{o,i} - [S]_o\right) \qquad (6.6)$$

Here, A_i is the interfacial area between the organic and aqueous phases, n is the number of moles of steroid being transferred in time t, $\beta_{S,aq}$ is the aqueous phase mass transfer coefficient for the free-steroid species (given by eq 6.4), $\beta_{SP,aq}$ is the aqueous phase mass transfer coefficient for the bound steroid species (cm/s), and $\beta_{S,o}$ is the organic phase mass transfer coefficient for the free-steroid species. The subscripts aq and o on

the bracketed species identify concentrations in the aqueous and organic phases, and the subscript i identifies concentrations immediately adjacent to, but not adsorbed on, the liquid-liquid interface.

There is no doubt that the free protein BSA adsorbs at surfaces and interfaces, and it is likely that this is true for BSA with steroid bound to it, as well. However, the rates of processes occuring at the interface will have no effect on the observed steady-state extraction rate, as will be discussed in section 6.6.5. Therefore, in eq 6.5 none of the rate terms includes interfacially adsorbed species.

Equation 6.5 for the aqueous phase mass transfer rate can be further altered by substitution for $[SP]_{aq}$ and $[SP]_{aq,i}$ from eq 6.3 and rearranging to give:

$$\frac{1}{A_i}\frac{dn}{dt} = \left[\beta_{S,aq} + mK_a[P]_{T,aq}\beta_{SP,aq}\right]\left([S]_{aq} - [S]_{aq,i}\right) \qquad (6.7)$$

Comparison of this equation with eq 2.5 shows that the term in square brackets may be considered to be an "effective" aqueous phase mass transfer coefficient for the steroid, $\beta_{S,aq,eff}$. It is larger than the mass transfer coefficient for the free steroid species alone because it includes not only the diffusion of free steroid but also the simultaneous diffusion of the steroid-protein complex.

Proceeding with the derivation as in Chapter 2, it is assumed that equilibrium prevails at the interface at all times:

$$K = \frac{[S]_{o,i}}{[S]_{aq,i}} \qquad (6.8)$$

where κ is the equilibrium distribution coefficient of the free-progesterone species. Equations 2.1 to 2.7, 2.14, and 2.16 to 2.19 apply here, with β_{aq} in these equations replaced by $\beta_{S,aq,eff}$. Thus, when κ is large and V_{aq} is *very much larger* than V_o, analogy with equations 2.4 and 2.14 leads to the following expression for the observed (first-order) rate constant for the solvent extraction of steroid when protein is present in the aqueous phase:

$$k_{BSA} \approx \frac{A_i \beta_{S,aq,eff}}{\kappa V_o} \tag{6.9}$$

In the absence of protein, the rate constant is simply:

$$k \approx \frac{A_i \beta_{S,aq}}{\kappa V_o} \tag{6.10}$$

According to film theory, which has been shown to apply quantitatively to single drop microextraction, $\beta_{S,aq}$ for the free steroid species is given by eq 6.4, and $\beta_{SP,aq}$ for the bound steroid species is given by:

$$\beta_{SP,aq} = \frac{D_{SP,aq}}{\delta_{aq}} \tag{6.11}$$

so that:

$$\beta_{S,aq,eff} = \left[\beta_{S,aq} + mK_a[P]_{T,aq}\beta_{SP,aq}\right] = \left(\frac{D_{S,aq}}{\delta_{aq}} + mK_a[P]_{T,aq}\frac{D_{SP,aq}}{\delta_{aq}}\right) \quad (6.12)$$

where $D_{SP,\,aq}$ is the diffusion coefficient for the protein-bound steroid species (cm^2/s).

In Figure 6.1 are diagramatically represented the concentration gradients of S and SP when steady-state diffusion has been established, at a time close to zero (anticipating the results from the last row of Table 6.1). Equation 6.3 is assumed to apply at all times and locations in the aqueous phase. The aqueous concentrations of S and SP immediately adjacent to the interface cannot be known accurately without knowledge of β_o, however, these concentrations will be very small, and can be estimated by combining eq 2.5 (with β_{aq} replaced by $\beta_{S,\,aq,\,eff}$) and 2.6 to obtain:

$$[S]_{aq,i} = \frac{\beta_{S,o}[S]_o + \beta_{S,aq,eff}[S]_{aq}}{\beta_{S,aq,eff} + \kappa\beta_{S,o}} \quad (6.13)$$

For large κ, the first term in the denominator may be neglected:

$$[S]_{aq,i} \approx \frac{[S]_o}{\kappa} + \frac{[S]_{aq}}{\kappa}\frac{\beta_{S,aq,eff}}{\beta_{S,o}} \quad (6.14)$$

Initially, $[S]_o = 0$, so the first term in eq 6.14 drops out. A crude estimate of $[S]_{aq,\,i}$ can be obtained by making the approximation $\beta_{S,\,aq,\,eff} \sim \beta_{S,\,o}$, leaving

$$[S]_{aq,i} \sim \frac{[S]_{aq}}{\kappa} \quad (6.15)$$

Thus, if $[S]_{aq} = 3.2 \times 10^{-6}$ mol/L, and $\kappa \approx 222$ (Chapter 5), $[S]_{aq,i} \sim 1 \times 10^{-8}$ mol/L (very small compared with $[S]_{aq}$). $[SP]_{aq,i}$ can be estimated from eq 6.3 to be $\sim 6 \times 10^{-8}$ mol/L (again very small compared with $[SP]_{aq} = 12.9 \times 10^{-6}$ mol/L). It should be emphasized here that this crude estimate of $[S]_{aq,i}$ and $[SP]_{aq,i}$ is used only in the construction of Figure 6.1, whose purpose is illustrative.

As the extraction proceeds, the concentration of S and SP immediately adjacent to the interface in the aqueous phase will increase, approaching bulk concentrations as equilibrium is attained. Diffusion of both S and SP contribute to the total flux of steroid to the interface, resulting in a rate enhancement compared to what would be observed with S alone. A concentration gradient of free protein equal and opposite to that of SP (not shown in Figure 6.1) will result in diffusion of free protein away from the interface back into bulk aqueous solution.

6.4 Drop-volume method of interfacial tension measurement

The interfacial tension (γ) between two immiscible fluids can be measured relatively easily by the drop-volume method.[118-123] In this method, drops of one liquid are formed slowly and allowed to detach from the tip of a vertically-mounted narrow tube that is immersed in the second fluid. The drop must either completely wet the tip (without rising up the outside of the tube), or alternatively, it must not wet the tip at all. At the point of drop detachment, the interfacial tension is given by

$$\gamma = \frac{V \Delta \rho g F'}{a} \qquad (6.16)$$

where V is the drop volume, $\Delta\rho$ is the difference in density between the two fluids (0.29_5 g/cm^3 for water/octane), g is the acceleration due to gravity (981 cm/s^2), a is the inner or outer radius of the tube, and F′ is a correction factor which is a function of ($a/V^{1/3}$). Values of F′ are tabulated in the literature.[122]

6.5 Experimental details

6.5.1 Chemicals

Acetone (BDH, Poole, England), 4-methylacetophenone (4-MAP; Kodak, Rochester, NY), n-octadecane (Aldrich, Milwaukee, WI), n-octane (BDH), progesterone (Aldrich), sodium chloride (A&C American Chemicals, Ville St. Laurent, PQ, Canada), and n-tetradecane (Kodak) were all reagent grade and used as received. Sodium dodecyl sulfate (SDS; Fisher, Fair Lawn, NJ) was laboratory grade. Bovine serum albumin (BSA) was obtained from Sigma (St. Louis, MO), cat. no. A-9647. Water was purified by the Nanopure system (Barnstead, Dubuque, IA).

6.5.2 Extraction apparatus and procedure

The microsyringe with a two-stop Chaney adapter, the GC, and the 25°C thermostatting water bath have been described in section 5.2.2. The aqueous phase was contained in a flat-bottom, 500-mL water-jacketted glass vessel. A one-inch glass-covered magnetic stir bar was stirred at 500 rpm (400 rpm in the equilibrium extractions) using the stirrer motor described in section 5.2.2. Although the stirring rate is slower here than with the 1-mL vial (1500 rpm, Chapter 5), the degree of agitation is at least as great on the basis of the stirring Reynolds number (Re):[71]

$$Re = \frac{sL^2\rho}{\mu} \qquad (6.17)$$

where s is the stirring rate (rps), L is the tip-to-tip length of the stirrer blades (cm), ρ is the density of water (1.0 g/cm^3), and μ is the viscosity of water (8.9 x 10^{-3} g/cm· s). Thus, for the 1-mL vial with ~0.5 cm stir bar stirred at 1500 rpm (25 rps), the Reynolds number is ~700. For the 500-mL vial with 2.54 cm stir bar stirred at 500 rpm (8.3 rps), the Reynolds number is ~6000. The similarity of the extraction rate constants for progesterone in water (7.8 x 10^{-4} s^{-1} for the 1-mL system (Table 5.2) and 6.6 x 10^{-4} s^{-1} for the 500-mL system (anticipating the results from section 6.6.1)) suggests that the hydrodynamics near the drop (i.e. δ_{aq}) are similar for the two systems.

After flushing the syringe thoroughly, 1.00 µL of n-octane containing a fixed concentration of internal standard (n-octadecane for progesterone and n-tetradecane for 4-MAP) was taken up (plunger stop on Chaney adapter set at 1.00 µL), and the syringe was quickly transferred to the aqueous solution and held in place with a clamp. The needle tip penetrated about 1 cm into the aqueous solution, and was located about 2 cm from the side of the 500-mL vessel (diameter = 9 cm). It was oriented so that the bevel of the needle tip was facing the horizontal-rotational flow component of the stirred solution at a 45° angle. The second stop on the Chaney adapter was set at 0.1 µL. Thus, when the stop button was held as the plunger was depressed, a volume of 0.9 µL of solvent was dispensed as a drop suspended in solution from the needle tip and 0.1 µL remained inside the needle. After extraction, the 0.9-µL drop was withdrawn

into the needle and all of the 1.00 μL of n-octane was injected into the GC. The reason for leaving 0.1 μL inside the needle during the extraction will become clear later on.

This procedure is somewhat simpler than that used with the 1-mL vial (Chapter 5). With the 1-mL vial, it took several seconds to align the needle with the hole in the vial septum, necessitating the use of the hanging 1μL drop to prevent evaporation from the 1μL of solvent inside the needle. With the 500mL vessel, the needle can be transferred very quickly, and there is no need to leave a 1μL drop of solvent hanging from the needle tip during transfer to prevent evaporation. A different "dilution factor" (eq 5.1) will result. However, since all calibrations are performed by extracting aqueous solutions, this dilution factor will become part of the calibration, as discussed in section 5.3.1.

Gas chromatography was performed on an OV-1 packed column, with column, injector, and detector (FID) temperatures of 275, 280, and 300°C (progesterone), and 175, 230, and 250°C (4-MAP), respectively. The GC signal was taken as the peak area ratio of analyte to internal standard. Since depletion of analyte in the aqueous phase was negligible, the same aqueous solution could be used for a series of extractions.

6.5.3 Interfacial tension measurements

Interfacial tension between aqueous solution and n-octane was measured by the drop-volume method at 25 ± 1°C.[118-123] A 2.0-mL Gilmont micrometer buret (Roger Gilmont, Greak Neck, NY) with a Teflon tip (0.166 cm i.d.) was used to slowly form aqueous drops in n-octane. The drops did not wet the Teflon tip. Measurements were performed in triplicate.

6.5.4 Solutions

Aqueous 1% (w/v) BSA solutions were prepared by dissolving 4.675 g of NaCl in ~400 mL of water, followed by the addition of 5.000 g of BSA. After dissolution, the solution was made up to 500.0 ± 0.5 mL final volume ([NaCl] = 0.16 mol/L). The pH of this solution was 7.1 ± 0.1.

Progesterone was added by pipetting an appropriate volume (<100 μL) of a concentrated solution of progesterone in acetone. SDS was added by pipetting microliter volumes of a 0.500 mol/L stock solution.

6.6 Results and discussion

6.6.1 Extraction rate curves

Shown in Figure 6.2 are typical extraction rate curves, plotted as GC responses R, normalized to their respective aqueous phase total steroid concentrations $[S]_{T,aq}$, versus time, both in the absence and in the presence of 1.00% BSA in the aqueous phase. The solid lines represent subsequently-normalized fits of the experimental points by the first-order rate equation:

$$R = R_{eq}\left(1 - e^{-kt}\right) \qquad (6.18)$$

where R_{eq} is the equilibrium value of the GC response at $t = \infty$ and k is the first-order extraction rate constant.

The extraction rate constant has a value of $(1.4 \pm 0.1) \times 10^{-3}$ s^{-1} in the presence of 1% BSA, which is greater than its value of $(6.6 \pm 0.4) \times 10^{-4}$ s^{-1} in the absence of BSA. This result agrees with the theoretical predictions embodied in eqs 6.9 and 6.10

(to be discussed quantitatively in section 6.6.4), and it is consistent with the enhanced mass transfer rate for progesterone in the presence of BSA which was observed in a liquid-membrane type extraction apparatus.[111]

A second, obvious difference between the curves in Figure 6.2 is the greater equilibrium organic-phase concentration of progesterone in the absence of BSA than in its presence. This results from the fact that the protein-bound fraction of progesterone is not extractable, and it serves as the basis for the equilibrium extraction method for determining the concentration of free-progesterone, as described in the next section.

6.6.2 Equilibrium extractions

Although stirring to equilibrium is a time-consuming way to measure free-steroid concentration in the presence of protein, it has the advantage that variables related to the rate of extraction are eliminated from the analysis. In this study, solutions of 3.07×10^{-6} mol/L of progesterone in 0.16 mol/L NaCl, both in the absence of BSA and in the presence of 1.00% BSA, were extracted to equilibrium at a stirring speed of 400 rpm (the 500 rpm stirring speed used in the other studies occasionally resulted in drop dislodgement after stirring for a long time; 400 rpm was chosen here to ensure that the drop adhered to the needle tip over the course of the long equilibrium stirring time). Extraction times of 1.25 hours and 2.5 hours were sufficient to reach ≥99% of extraction equilibrium for solutions containing 1% BSA and no BSA, respectively. At equilibrium, the distribution coefficient for the free-progesterone species between n-octane and 0.16 mol/L NaCl has the same value, both in the presence and in the absence of BSA:

$$\kappa = \frac{[S]_{o,eq}}{[S]_{aq,eq}} \qquad (6.19)$$

R_{eq} values from eq 6.18 are proportional to $[S]_{o,\,eq}$, both with and without BSA present. Also, since the phase ratio V_o/V_{aq} is very small, then in the absence of BSA, $[S]_{aq,\,eq}$ is equal to the initial concentration of progesterone (i.e. 3.07×10^{-6} mol/L). Thus, the concentration of free progesterone at equilibrium in the BSA-containing aqueous sample is given as:

$$[S]_{aq,eq}(\text{with BSA}) = \frac{R_{eq,\,BSA}}{R_{eq,\,no\ BSA}}\left(3.07\text{x}10^{-6}\ \text{mol/L}\right) \qquad (6.20)$$

Because of the very small phase ratio this is also equal to the initial concentration in the unextracted sample solution. In the present case $R_{eq,\,BSA} = 0.60 \pm 0.05$ and $R_{eq,\,no\ BSA} = 2.81 \pm 0.09$ so that $[S]_{aq}$ (with BSA) = $(6.6 \pm 0.6) \times 10^{-7}$ mol/L. That is, 21% of the progesterone is present in the free form in 1% BSA solution.

The binding constant mK_a can be calculated from $[S]_{aq}$ (with BSA) via eq 6.3. The value of $[SP]_{aq}$ is equal to (3.07×10^{-6} - $[S]_{aq}$ (with BSA)) and the value of $[P]_{T,\,aq}$ is 1.54×10^{-4} mol/L for 1.00% BSA, giving a value of $mK_a = (2.4 \pm 0.3) \times 10^4$ L/mol. This value is in agreement with previously reported values of 3.0×10^4 L/mol and $(2.7 \pm 0.1) \times 10^4$ L/mol which were obtained at pH 7.4 by equilibrium (macro-scale) solvent extraction,[105, 112] and 2.9×10^4 L/mol which was obtained at pH 8.0 by equilibrium dialysis.[124] Batch-to-batch variations in the fatty acid content of BSA may account for some of the small differences among the reported values.[105, 112, 114, 124]

It can easily be shown that the fraction of free progesterone remaining in the aqueous phase after one equilibrium extraction with 1-μL of n-octane is given by

$$f_{aq} = \frac{1}{1 + \kappa \dfrac{V_o}{V_{aq}}} \qquad (6.21)$$

Thus, for $\kappa \approx 222$ (Table 5.2), 99.96% of the free progesterone remains in the aqueous phase at equilibrium.

Given that the solubility of n-octane in water is 5.8×10^{-9} mol/cm^3 at 25°C[100] and that a 1-μL drop contains 6.1×10^{-6} mol of n-octane, it is evident that when solubility equilibrium is reached about 47% of the drop will be dissolved in 500 cm^3 of water. Furthermore, the presence of a biological macromolecule such as BSA would be expected to raise the solubility of n-octane in the aqueous phase. However, as discussed below, the rate of dissolution of n-octane is both expected and observed to be very slow, so that during a typical microdrop solvent extraction experiment a negligible fraction of the drop will dissolve.

Theoretically, the initial rate of dissolution of n-octane in water may be calculated from film theory by the expression:

$$\frac{dn}{dt} = A_i \frac{D_{aq}}{\delta_{aq}} C_{aq,i} \approx 1._2 \times 10^{-12} \text{ mol/s} \qquad (6.22)$$

where $A_i = 0.04$ cm^2 for the drop, D_{aq} is about 5×10^{-6} cm^2/s, δ_{aq} is about 1×10^{-3} cm, and $C_{aq,i}$ is 5.8×10^{-9} mol/cm^3. The amount of n-octane dissolved in water after one hour of stirring would be about 4×10^{-9} mol, or less than 0.07% of the n-octane drop. In the presence of 1% BSA the solubility of n-octane in the aqueous phase is increased to $C_{aq,i} \approx 3 \times 10^{-7}$ mol/cm^3, based on ref. 125, and the diffusion coefficient of the octane-BSA complex is $D_{aq} \approx 1 \times 10^{-6}$ cm^2/s (i.e. about the same as that of the progesterone-BSA complex, $D_{SP,aq}$, see below). Substituting these values for $C_{aq,i}$ and D_{aq} in equation 6.22 gives an initial rate of about $1._2 \times 10^{-11}$ mol/s for dissolution of n-octane. Thus, after 1 hour of stirring in 1% BSA only about 0.7% of the 1-μL drop of

n-octane is expected to have dissolved. Consistent with this, it is observed experimentally that after more than one hour of stirring in a 1% BSA solution there is no perceptable decrease in the volume of the drop, as can be seen when withdrawing the drop back into the needle.

Although it might be expected that n-octane bound to BSA may compete with progesterone for binding sites, this is apparently not the case, since this study and others employing solvent extraction[105, 112] give binding data that are in agreement with data from equilibrium dialysis.[124] Furthermore, as the number of extractions using the same progesterone/BSA solution increases (and the amount of dissolved n-octane presumably increases slightly), there is no systematic trend in the data which would reflect increasing competition for binding sites.

6.6.3 Non-equilibrium extractions

Determination of $[S]_{aq}$ was performed more rapidly by stirring for a fixed, short (non-equilibrium) time at 500 rpm. A calibration curve of GC response, R versus $[S]_{T,aq}$ was obtained by subjecting in duplicate a series of five solutions of progesterone in the concentration range (1.23 to 6.14) x 10^{-6} mol/L in 0.16 mol/L NaCl to an extraction for 10.0 min. The calibration curve is shown in Figure 6.3. It is linear with slope = (3.9 ± 0.2) x 10^5 L/mol, zero intercept (0.01 ± 0.09) and correlation coefficient R^2 = 0.974. In 10.0 min the extraction of progesterone from BSA-free standard solution is 33% of the way to equilibrium, while extraction from a 1% BSA solution is 56% of the way to equilibrium (Figure 6.2). Therefore, for use with a 10.0 min extraction time of progesterone from a 1% BSA sample solution, the calibration curve must be corrected for the faster extraction rate in 1% BSA. For small phase ratios eq 6.18 can be rewritten as:

$$R = \left[\text{const} \cdot \kappa\left(1 - e^{-k \cdot t}\right)\right]\left\{\frac{1 - e^{-k_{BSA} \cdot t}}{1 - e^{-k \cdot t}}\right\}[S]_{aq} \qquad (6.23)$$

where, for a fixed stirring time t, the term in square brackets is a constant, equal to the slope of the calibration curve. The term in braces is a correction factor equal to 1.7 ± 0.1. The rate constants k_{BSA} and k are obtained from extraction rate curves (Figure 6.2).

As samples, five progesterone solutions containing (3.21 to 16.0) x 10^{-6} mol/L progesterone in 0.16 mol/L NaCl + 1% BSA were analyzed in triplicate for free progesterone using 10.0-min extractions, as described above. The results are presented in Table 6.1. Column 1 is the total (added) steroid concentration in the aqueous phase $[S]_{T,aq}$, and column 2 is the free steroid concentration $[S]_{aq}$, calculated from eq 6.23. Column 3 is the fraction of total steroid in the free form. Within experimental error, this fraction is constant over the concentration range studied. The concentration of bound steroid $[SP]_{aq}$ shown in the fourth column is calculated as the difference between $[S]_{T,aq}$ and $[S]_{aq}$. The ratio of bound steroid to total protein concentration is given in column 5. The product mK_a calculated from eq 6.3 is given in column 6. The agreement between the average value of mK_a = (2.6 ± 0.1) x 10^4 L/mol obtained in this non-equilibrium study and the value of mK_a = (2.4 ± 0.3) x 10^4 L/mol from the equilibrium study described above is good. This demonstrates that a large reduction in analysis time for $[S]_{aq}$ in protein-containing solution can be realized without any significant loss in accuracy.

The constancy of the values mK_a and $[S]_{aq}/[S]_{T,aq}$, and the small magnitude of the fraction $[SP]_{aq}/[P]_{T,aq}$ are consistent with the assumption that only a small fraction of the binding sites are occupied by S. Furthermore, this assumption has been shown to be reasonable even for higher values of $[SP]_{aq}/[P]_{T,aq}$ in studies of progesterone binding to both BSA[112, 124] and HSA (human serum albumin).[126]

If the *total* concentration of progesterone is of interest, a standard-addition approach may be used where the protein solution is spiked with known increments of progesterone, and the GC response is plotted versus total added progesterone. The total progesterone present in the *original protein solution* can be determined from the negative x-intercept of the plot. The standard addition method relies on the assumption that a *constant fraction* of the progesterone added to the protein solution is bound by protein.[127] This will be the case as long as there is a large excess of protein binding sites relative to the amount of progesterone in the system, which has been demonstrated to be true in the present case. A standard addition plot for the data in Table 6.1 is shown in Figure 6.4. The plot is linear with a correlation coefficient $R^2 = 0.976$, slope of $(1.33 \pm 0.06) \times 10^5$ L/mol, zero x-intercept ($(1 \pm 4) \times 10^{-7}$ mol/L), indicating that no progesterone was present in the original BSA solution.

6.6.4 Agreement with modified mass transfer model

The predicted rate enhancement, k_{BSA}/k, can be shown from eqs 6.4, 6.9, 6.10, and 6.12 to be given by:

$$\frac{k_{BSA}}{k} = \frac{\beta_{S,aq,eff}}{\beta_{S,aq}} = 1 + mK_a[P]_{T,aq}\frac{D_{SP,aq}}{D_{S,aq}} \qquad (6.24)$$

Equating this to the observed rate enhancement of $k_{BSA}/k = 2.1 \pm 0.2$ and taking $D_{S,aq} = (4.0 \pm 0.3) \times 10^{-6}$ cm²/s (Table 3.2), permits the evaluation of $D_{SP,aq} = (1.0 \pm 0.2) \times 10^{-6}$ cm²/s. Since progesterone is a small molecule compared with BSA, $D_{SP,aq}$ is expected to be approximately equal to $D_{P,aq}$, the diffusion coefficient of the BSA molecule in aqueous solution. Literature values for $D_{P,aq}$ in various aqueous media,[128-130] corrected to 25°C by means of the Wilke-Chang equation,[131] are in the range $(0.69 \pm 0.02) \times 10^{-6}$ cm²/s, which is close to the observed value of $D_{SP,aq}$.

It has been assumed that there is a maximum of one steroid molecule bound per protein molecule (i.e. species such as S_2P have been neglected). It is conceivable that diffusion of species such as S_2P (which was neglected in the model) may account for the slightly higher diffusion coefficient which emerges from the model compared with literature values. However, it can be argued on statistical grounds that the concentration of S_2P is very small compared with SP, as follows:

To understand why $[S_2P]$ is negligible, the association equilbria must be viewed from a microscopic point of view, as in Figure 6.5. The microscopic equilibrium constants (k_1, k_2, k_{12}, k_{21}) and the macroscopic equilibrium constants (K_1, K_2) are defined as follows:

$$k_1 = \frac{[SP]}{[S][P]} \tag{6.25}$$

$$k_2 = \frac{[PS]}{[S][P]} \tag{6.26}$$

$$K_1 = \frac{[SP]+[PS]}{[S][P]} \tag{6.27}$$

$$k_{12} = \frac{[S_2P]}{[SP][S]} \tag{6.28}$$

$$k_{21} = \frac{[S_2P]}{[PS][S]} \tag{6.29}$$

$$K_2 = \frac{[S_2P]}{([SP]+[PS])[S]} \tag{6.30}$$

From the definitions of the microscopic and macroscopic equilibrium constants, it is obvious that

$$K_1 = k_1 + k_2 \tag{6.31}$$

$$\frac{1}{K_2} = \frac{1}{k_{12}} + \frac{1}{k_{21}} \tag{6.32}$$

For $k_1 = k_2 = k_{12} = k_{21}$ (i.e. both sites equivalent and independent),

$$K_1 = 2k_1 \tag{6.33}$$

$$K_2 = \frac{1}{2}k_1 \tag{6.34}$$

From eqs 6.27, 6.30, 6.33, and 6.34 we can write

$$\frac{K_1}{K_2} = \frac{([SP] + [PS])^2}{[P][S_2P]} = \frac{[SP]_T^2}{[P][S_2P]} = 4 \tag{6.35}$$

where $[SP]_T$ is the sum of [SP] and [PS]. Thus, for [P] = 1.5×10^{-4} mol/L and $[SP]_T$ = 1.0×10^{-5} mol/L, the concentration of S_2P would be 1.7×10^{-7} mol/L. Thus, neglecting S_2P in the model is a reasonable approximation. The more general treatment of Klotz[117] shows that this approximation is valid for any number of binding sites, with the number on the right-hand-side of eq 6.35 approaching 2 as the number of binding sites becomes large.

Also implicit in the model is the assumption of fast rates of association and dissociation of the steroid-protein complex in the Nernst diffusion films. Although these rates are generally assumed to be fast,[114] there is little quantitative published data. The first order rate constant for dissociation of progesterone from HSA was determined[132] to be 2.2 ± 0.5 s^{-1} at 37°C, corresponding to a half-life of 0.3 s. However, measurements used to obtain this value were made at 1-s intervals, with each measurement taking a full second to complete. According to the authors, the true dissociation rate may be significantly faster. In any event, its dissociation half-life is shorter than the root-mean-square time of 0.7 s which is required for a BSA-progesterone complex to diffuse across a nominal Nernst diffusion film of 10 μm, as estimated from the Einstein equation $\left(\sqrt{2D_{SP,aq}t}\right)$.

6.6.5 Protein adsorption at the liquid-liquid interface

During extractions from protein solutions, the drop of n-octane did not wet the needle tip or plunger wire tip, presumably because of BSA adsorption on the stainless steel. As a consequence, to prevent drop dislodgment, 0.10 μL of the 1.00 μL drop of n-octane was retained within the needle bore as described in section 6.5.2. The resulting drop had a slightly different shape than when BSA was absent. In addition the adsorption of BSA at the liquid-liquid interface and the resultant lowering of interfacial tension is apparently responsible for significant drop oscillatons which were observed in the presence of BSA.

In order to determine whether differences in drop shape and oscillation were partially responsible for the increased rate of extraction in the presence of BSA, extraction rate studies were performed on a system with similar interfacial tension as 1% BSA, but with no analyte complexation in the aqueous phase. In these studies, the

rate of extraction of 4-methylacetophenone (4-MAP) in the presence of various concentrations of sodium dodecylsulfate (SDS) surfactant was measured.

The measured interfacial tension between n-octane and a 1% BSA solution is $\gamma = 25 \pm 1$ dynes/cm. The measured interfacial tension between n-octane and pure water is $\gamma = 53 \pm 1$ dynes/cm, which agrees well with the literature value of 50.8 dynes/cm (measured at 20°C).[118] The interfacial tensions between n-octane and a series of SDS solutions having concentrations of SDS between 0.01 and 0.50 mmol/L were measured and are shown in Table 6.2. These concentrations of SDS are well below its critical micelle concentration. At [SDS] = 0.20mM, the interfacial tension is similar to that of a 1% BSA solution.

Extraction rates of 4-MAP were measured in the presence of 0 to 0.20 mmol/L of SDS and extraction rate constants were calculated via eq 6.18. R was measured at 2.00 min, and R_{eq} was measured at a long stirring time (15 min was sufficient for 4-MAP). As the concentration of SDS approached 0.20 mmol/L, drop oscillation and shape approached that observed in 1% BSA solutions. However, the rate of extraction was not enhanced, even at 0.20 mmol/L SDS (average k's at 0, 0.02, 0.06, and 0.20 mmol/L SDS were 0.40, 0.43, 0.42, and 0.38 min^{-1} respectively). Thus, the drop shape change and drop oscillation induced by lowering the interfacial tension do not affect the rate of extraction.

At higher concentrations of SDS, the drop is unstable and dislodges either as soon as it is formed, or after stirring commences. This suggests that there is a limitation to the micro-drop extraction system. While moderately surface-active solutions (e.g. 0.20mM SDS, 1% BSA) are compatible with the system, solutions of high concentrations of surfactants cannot be used. Solid-phase microextraction (SPME), where the organic phase is a solid polymer, would be preferred in this case.

Clearly, BSA adsorbs at the octane/water interface. At BSA concentrations in the range of 1%, adsorption of protein occurs at the oil-water interface in two different ways.[133-135] There is some irreversible adsorption of BSA at the interface, in which state at least some of the protein is unfolded from its native conformation. Additionally, there is reversible adsorption in secondary and subsequent layers in which the protein retains its native conformation. Thus, adsorbed BSA is capable of binding progesterone. The surface concentration of BSA at 1% solution concentration is estimated to be 1.5×10^{-11} mol/cm^2 at either the water-toluene or water-decane interface at 22°C.[134] With an interfacial area of about 0.04 cm^2 for a 1-μL drop (section 5.3.2), there are ~6×10^{-13} mol of BSA adsorbed at the interface. This is small in comparison with the ~6×10^{-12} mol BSA in the Nernst diffusion film adjacent to the interface (taking δ_{aq} = 10 μm), and, in any event the mass transfer model which was experimentally verified above suggests that there is no resistance to mass transfer at the interface itself. Thus, diffusion of progesterone through the adsorbed protein film and adsorption/desorption of progesterone by adsorbed BSA are apparently fast processes relative to aqueous phase mass transfer.

Table 6.1 Speciation and binding constant data for the steroid progesterone (S) in the presence of 0.16 mol/L NaCl + 1% BSA

$[S]_{T,aq}$ (mol/L) x 10^6	$[S]_{aq}$ [a] (mol/L) x 10^6	$\frac{[S]_{aq}}{[S]_{T,aq}}$	$[SP]_{aq}$ (mol/L) x 10^6	$\frac{[SP]_{aq}}{[P]_{T,aq}}$ [b]	mK_a [c] (L/mol) x 10^{-4}
3.21	0.66 ± 0.08	0.20 ± 0.03	2.55 ± 0.08	0.0166 ± 0.0005	2.5 ± 0.4
6.42	1.2 ± 0.1	0.19 ± 0.02	5.2 ± 0.1	0.034 ± 0.001	2.8 ± 0.4
9.63	1.9 ± 0.2	0.20 ± 0.02	7.7 ± 0.2	0.050 ± 0.001	2.6 ± 0.3
12.8	2.6 ± 0.4	0.21 ± 0.03	10.2 ± 0.4	0.066 ± 0.002	2.5 ± 0.4
16.0	3.2 ± 0.3	0.20 ± 0.02	12.9 ± 0.3	0.083 ± 0.002	2.6 ± 0.3

[a] standard deviations are based on triplicate determinations of R with error propogation from calibration slope and correction factor (eq 6.23)

[b] $[P]_{T,aq} = 1.54 \times 10^{-4}$ mol/L (BSA: 65 000 g/mol)

[c] calculated from eq 6.3

Table 6.2 Interfacial tension data for aqueous - octane systems using the drop-volume method

Aqueous solution	Trial	V_{drop} (cm^3)	$a/V^{1/3}$	F^{-a}	γ (dyn/cm)[b]
water only	1	0.076	0.19_6	0.20	$52._9$
	2	0.074	0.19_8	0.20	$51._5$
	3	0.078	0.19_5	0.20	$54._3$
	ave.				**53 ± 1**
0.01mM SDS	1	0.066	0.20_6	0.20	$45._9$
	2	0.066	0.20_6	0.20	$45._9$
	3	0.066	0.20_6	0.20	$45._9$
	ave.				**46 ± (0)**
0.05mM SDS	1	0.054	0.22_0	0.21	$39._4$
	2	0.054	0.22_0	0.21	$39._4$
	3	0.054	0.22_0	0.21	$39._4$
	ave.				**39 ± (0)**
0.10mM SDS	1	0.044	0.23_6	0.21	$32._1$
	2	0.042	0.23_9	0.21	$30._7$
	3	0.042	0.23_9	0.21	$30._7$
	ave.				**31 ± 1**
0.20mM SDS	1	0.030	0.26_8	0.21	$21._9$
	2	0.030	0.26_8	0.21	$21._9$
	3	0.028	0.27_4	0.21	$20._5$
	ave.				**21 ± 1**
0.50mM SDS	1	0.018	0.31_7	0.22	$13._8$
	2	0.016	0.33_0	0.22	$12._3$
	3	0.016	0.33_0	0.22	$12._3$
	ave.				**13 ± 1**
1% BSA	1	0.034	0.25_7	0.21	$25._5$
	2	0.034	0.25_7	0.21	$25._5$
	3	0.032	0.26_2	0.21	$24._0$
	ave.				**25 ± 1**

[a] correction factor using $a/V^{1/3}$ from column 4 (ref. 122)

[b] from eq 6.16

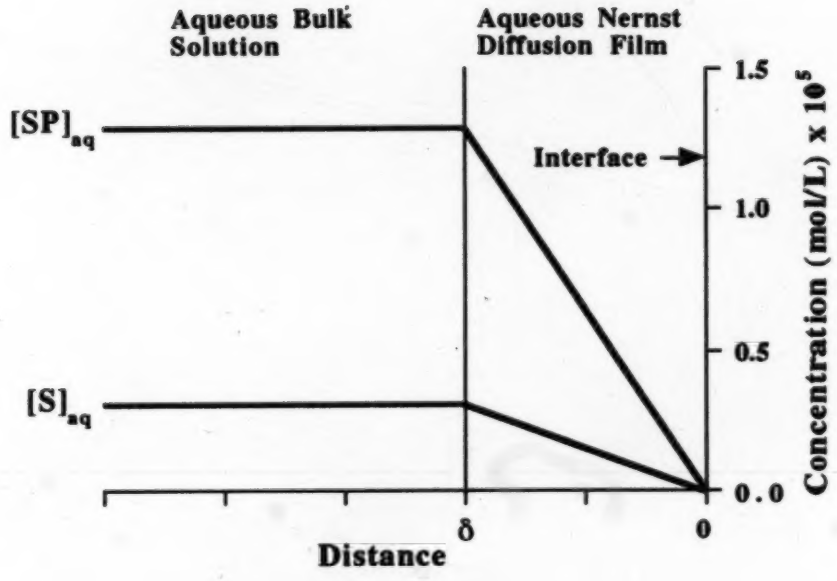

Figure 6.1 Sketch of the steady-state concentration profiles for S and SP at a total aqueous phase steroid concentration of 1.60×10^{-5} mol/L, early in the extraction experiment. Concentrations of both species immediately adjacent to the interface are very small, and the ratio $[SP]_{aq}/[S]_{aq}$ is constant everywhere, as required by eq 6.3.

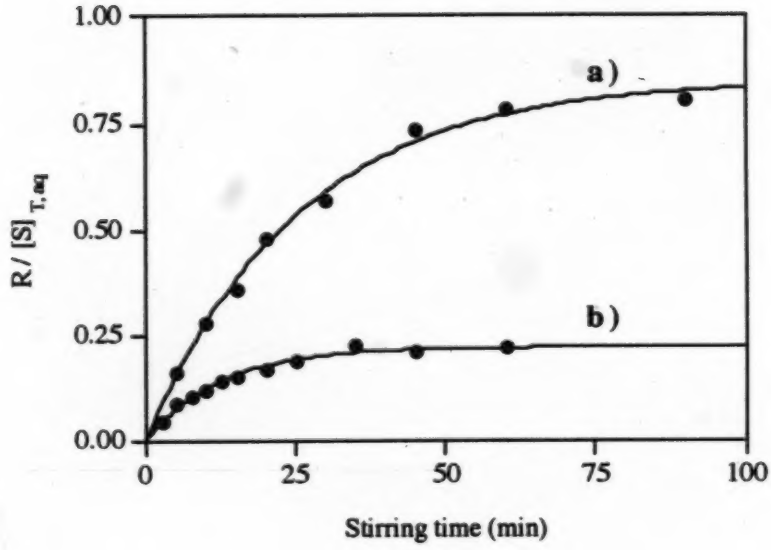

Figure 6.2 Normalized extraction rate curves for: (a) $[S]_{T,eq}$ = 2.5 µmol/L progesterone in 0.16 mol/L NaCl, and (b) $[S]_{T,eq}$ = 6.1 µmol/L progesterone in 0.16 mol/L NaCl + 1.00% BSA. Points are experimental GC response divided by $[S]_{T,eq}$ and solid lines are non-linear least squares curve fits of eq 6.18 to the data. Stirring rate = 500 rpm.

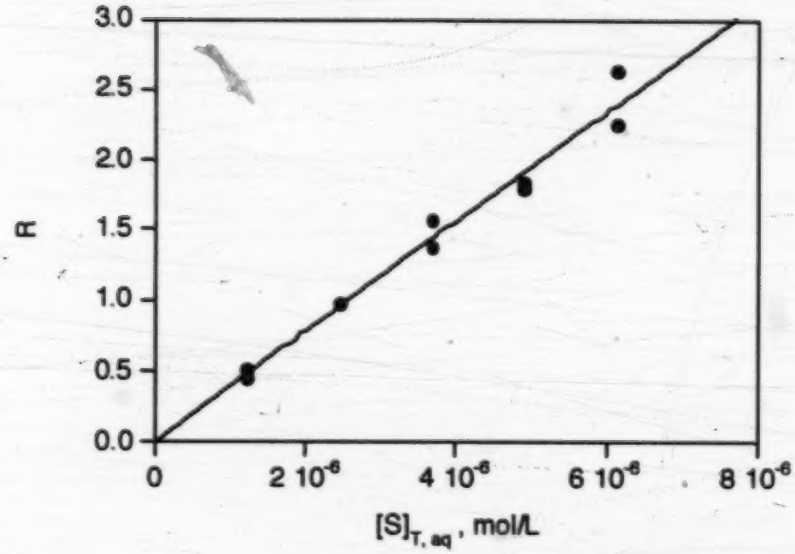

Figure 6.3 Calibration curve for the determination of free progesterone. Calibration standards are BSA-free progesterone solutions which are extracted for a short, non-equilibrium time (10.0 min) at 500 rpm. For use with a 10.0 min extraction time of progesterone from a 1% BSA sample solution, the calibration curve must be corrected for the faster rate of extraction in 1% BSA as discussed in the text. Slope = $(3.9 \pm 0.2) \times 10^5$ L/mol, intercept = 0 (0.01 ± 0.09), $R^2 = 0.974$.

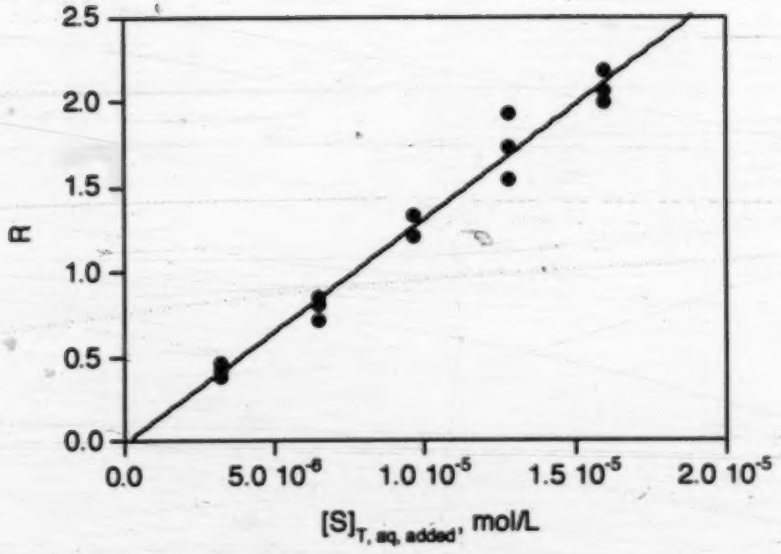

Figure 6.4 Standard addition plot for the data in Table 6.1. The zero x-intercept ($(1\pm4) \times 10^{-7}$ mol/L) indicates that no progesterone was present in the original BSA solution. Slope = $(1.33 \pm 0.06) \times 10^5$ L/mol, $R^2 = 0.976$.

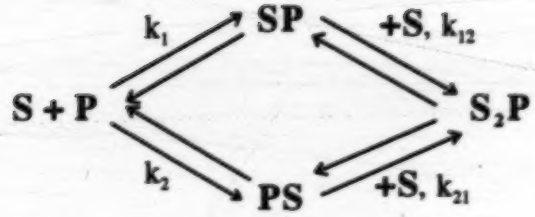

Figure 6.5 Microscopic association scheme for steroid (S) and protein (P) with two protein binding sites.

Chapter 7

CONCLUSIONS AND FUTURE WORK

7.1 Conclusions

The analytical technique which has been described has several distinct advantages over conventional sample preparation techniques:

(1) The system is convenient and inexpensive. Since it requires only equipment commonly found in a typical analytical laboratory, the feasibility of this method for a particular analysis can be studied at low cost.

(2) The 1-μL microsyringe system is amenable to automation with a GC autosampler. Such automation has been demonstrated for solid-phase microextraction (SPME).[29]

(3) There is negligible solvent consumption compared to conventional liquid-liquid extracton and other techniques. This is important, since the use of large volumes of solvents creates a costly disposal problem.

(4) Unlike conventional liquid-liquid extraction, there is no droplet dispersion and therefore no phase coalescence step required after extraction. Coalescence can be a problem in some systems, particularly those which contain surface active components (e.g proteins) and tend to form stable emulsions.

(5) The interfacial area is approximately independent of stirring rate, facilitating the study of mass transfer kinetics.

(6) Because the phase ratio (V_o/V_{aq}) can be made very small, the extraction can be performed under non-perturbing conditions (i.e. where a negligible amount of solute is extracted from the aqueous solution). In this way, the extraction system behaves like a "probe" similar to, for example, a pH electrode which measures [H^+] without altering the solution composition significantly. This aspect of the system has been exploited in

the speciation studies of progesterone/BSA compelex (Chapter 6) in which case the extraction does not perturb homogeneous aqueous phase equilibria.

(7) The methodology is simple, and analysis times are relatively short.

(8) Good precision can be obtained, even under non-equilbrium conditions.

Care must be taken with the microsyringe system to avoid air bubbles, since even a very tiny air bubble at the start will grow considerably over the course of the extraction, presumably as a result of outgassing from the solvent. The microextraction system is also limited by high concentrations of surface active material which can cause the drop to dislodge or break up into tiny droplets during the extraction.

Since solid-phase microextraction (SPME) is becoming a widely-used alternative to other sample preparation methods, it is of interest to compare the solvent microextraction method described here with SPME. The two techniques appear to be comparable in terms of precision, sensitivity, and analysis time.[26] SPME has the advantage that there is no solvent peak in the GC. However, this advantage is offset by the cost of a somewhat more elaborate and expensive apparatus than is employed in solvent microextraction and by the fact that analyte desorption from the polymer in the GC injector is slower than conventional solvent evaporation which can lead to analyte peaks showing greater tailing. Acceleration of the desorption rate using an elaborate injection system has been demonstrated.[34] A second advantage of SPME is its ready adaptability to headspace analysis, although Dasgupta and co-workers have successfully demonstrated the use of a liquid droplet for the sampling of gas streams.[60-63]

SPME has recently been applied to the determination of free-species in the presence of protein[113] and humic organic matter[136] using a large volume of aqueous solution to avoid perturbing aqueous phase equilibria. The micro-drop solvent extraction technique (Chapter 6) and the SPME technique both have advantages with respect to one another. The main advantage of the micro-drop technique is the fact that

a completely renewed solvent drop is used for each extraction, rather than having the same polymer film cycled through many extraction and high temperature thermal desorption steps. In some cases this cycling leads to polymer film destruction due to thermal degradation of adsorbed high molecular weight sample components (e.g. humic acid),[137] although with a polyacrylate film, adsorption of BSA seems not to occur.[113] An advantage of the SPME technique, employing an 85-μm thick polyacrylate film, is the fact that if the stirring rate is very fast, the extraction rate is found to be controlled by diffusional mass transfer in the polymer film, rather than in the aqueous phase, even for relatively hydrophobic solutes.[31] Thus, the calibration curve for the non-equilibrium measurement of free solute concentration does not have to be corrected for co-diffusion of the protein-bound complex. However, this type of correction, which is required in the micro-drop solvent extraction technique, can be predicted at any protein concentration by eq 6.24.

7.2 Future work

The low sensitivity of the packed column / FID detector GC system used in this study limited the analyses to relatively high concentrations of solute. The use of a more sensitive detection system (e.g. capillary GC/MS) would permit the extension of the extraction system to trace analysis of very low concentrations of sample components (e.g. low concentrations of pesticides in natural waters). For example, the micro-drop system could be used to measure the free concentration of a pesticide in the presence of naturally occuring ligands (e.g. humic acid, clays) at naturally ocurring concentrations. This type of speciation data is important in the study of the transport and degradation of pesticides in water and soil.

The principles of micro-drop extraction can be applied to a solvent double-extraction system for sample cleanup and preconcentration. The system shown in

Figure 7.1 employs a 1-μL drop of an aqueous buffer (inner aqueous phase or acceptor) suspended at the tip of a microsyringe needle. The 1-μL aqueous drop is contained within a 10-μL drop of n-octane which is housed at the end of a Teflon rod. The combined assembly is immersed in a stirred aqueous solution (outer aqueous phase or donor) which is buffered at a different pH than the inner aqueous phase. The system may be used for the analysis of amine drugs, for example, if the outer aqueous phase is buffered at a high pH (neutral drug molecule) and the inner aqueous phase is buffered at a low pH (protonated drug molecule). The organic phase behaves as a liquid membrane which prevents other matrix components from entering the inner aqueous phase. Preconcentration or enrichment is achieved by "trapping" the drug molecule in the inner aqueous phase at low pH, and by using a very small ratio of inner to outer aqueous phase volume. Analysis can be performed by injecting the 1-μL drop into an HPLC or FIA system.

Micro-drop extraction could also be applied to metal ion speciation in aqueous solution. For example, a 1-μL drop of n-octane containing a hydrophobic ligand could be used to extract free metal ion species in the presence of its kinetically labile complexes, under non-perturbing conditions (i.e. small phase ratio). Analysis of the drop by electrospray mass spectrometry is an obvious possibility.

Since film theory has been shown to apply quantitatively to the 1-μL microsyringe system, it would be possible to estimate aqueous diffusion coefficients of hydrophobic (i.e. large κ) compounds using solvent microextraction. In the simplest type of experiment, extraction rate constants (k) could be obtained from eq 2.16 by extracting at a fixed stirring rate for (1) a non-equilibrium time, t (to obtain C_o), and (2) a long time, sufficient to reach equilibrium (to obtain $C_{o,eq}$). A standard with a known

diffusion coefficient $D_{aq,\,std}$ would first be used to calibrate the system in terms of δ_{aq} by measuring the observed extraction rate constant k_{std}. By combining eqs 2.14, 2.18, and 2.20, the following expression is obtained for δ_{aq}:

$$\delta_{aq} = \frac{D_{aq,std} A_i \left(\kappa_{std} V_o / V_{aq} + 1\right)}{k_{std} V_o \kappa_{std}} \tag{7.1}$$

A similar extraction study using a compound of unknown diffusion coefficient $D_{aq,\,unk}$ would yield k_{unk}, and then $D_{aq,\,unk}$ could be calculated by combining eqs 2.14, 2.18, 2.20, substituting eq 7.1 for the film thickness:

$$D_{aq,\,unk} = \frac{k_{unk}}{k_{std}} \frac{\kappa_{unk}}{\kappa_{std}} \frac{\kappa_{std} V_o / V_{aq} + 1}{\kappa_{unk} V_o / V_{aq} + 1} D_{aq,\,std} \tag{7.2}$$

By calibrating in this way, the interfacial area A_i (which can only be estimated) need not be known. The distribution coefficients (κ) may be calculated from $C_{o,\,eq}$ by eq 2.17.

As was mentioned in section 4.3.3, solvents that are less immiscible with water than n-octane may dissolve significantly during extraction. However, this problem could be avoided by placing a wick soaked with the solvent in the headspace above the aqueous solution. Prior to extraction, the aqueous phase could be saturated with the solvent by stirring in the presence of the wick in a closed system for a sufficient length of time. In this way, no dissolution of the solvent drop would occur during the extraction, since the aqueous phase would already be saturated with the solvent.

Normally, the needle tip wets reasonably well with n-octane. However, with protein or SDS solutions (Chapter 6), n-octane did not wet the needle tip, presumably because of adsorption of surfactant material (protein, SDS) on the needle. Such

adsorption apparently makes the needle tip more hydrophilic. It would be interesting to see the effect of altering the surface chemistry of the needle tip (e.g. by coating it with Teflon). It is possible that such a coating may prevent adsorption of surface-active material on the needle tip, and therefore maintain the hydrophobicity and solvent-wetting characteristics of the needle.

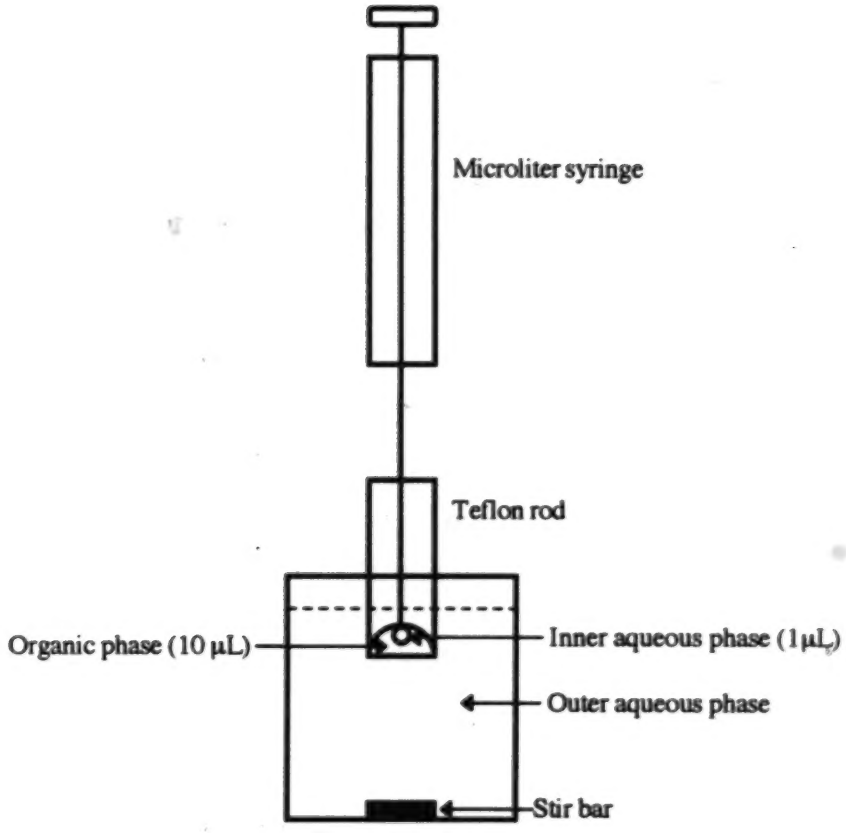

Figure 7.1 Microliter drop solvent double-extracton apparatus (not to scale).

Bibliography

1. Namiesnik, J.; Gorecki, T.; Biziuk, M.; Torres, L. *Anal. Chim. Acta.* **1990**, 237, 1-60.
2. Poole, S.K.; Dean, T.A.; Oudsema. J.W.; Poole, C.F. *Anal. Chim. Acta.* **1990**, 236, 3-42.
3. Poole, C.F.; Schuette, S.A. *J. High Resolut. Chromatogr.* **1983**, 6, 526-549.
4. Karasek, F.W.; Clement, R.E.; Sweetman, J.A. *Anal. Chem.* **1981**, 53, 1050A-1058A.
5. Laitinen, H.A.; Harris, W.E. *Chemical Analysis*, 2nd ed.; McGraw-Hill: New York, 1975; Chapter 23.
6. Sekine, T.; Hasegawa, Y. *Solvent Extraction Chemistry*; Marcel Dekker: New York, 1977.
7. Irving, H.; Williams, R.J.P. In *Treatise on Analytical Chemistry, Part 1, Theory and Practice*; Kolthoff, I.M.; Elving, P.J., Eds.; Interscience: New York, 1961; Vol. 3, Chapter 31.
8. Morrison, G.H.; Freiser, H. *Solvent Extraction in Analytical Chemistry*; Wiley: New York, 1957.
9. Amankwa, L.; Cantwell, F.F. *Anal. Chem.* **1989**, 61, 1036-1040.
10. Kuban, V.; Ingman, F. *Crit. Rev. Anal. Chem.* **1991**, 22, 491-518.
11. Valcarcel, M.; Luque de Castro, M.D. *J. Chromatogr.* **1987**, 393, 3-23.
12. Karlberg, B.; Thelander, S. *Anal. Chim. Acta* **1978**, 98, 1-7.
13. Bergamin, H.; Medeiros, J.X.; Reis, B.F.; Zagatto, E.A.G. *Anal. Chim. Acta* **1978**, 101, 9-16.
14. Nord, L.; Backstrom, K.; Danielsson, L.-G.; Ingman, F.; Karlberg, B. *Anal. Chim. Acta* **1987**, 194, 221-233.
15. Lucy, C.A.; Cantwell, F.F. *Anal. Chem.* **1989**, 61, 101-107.

16. Lucy, C.A.; Cantwell, F.F. *Anal. Chem.* **1989**, 61, 107-114.

17. Lucy, C.A.; Yeung, K.K.-C. *Anal. Chem.* **1994**, 66, 2220-2225.

18. Dressler, M. *J. Chromatogr.* **1979**, 165, 167-206.

19. Renberg, L.; Lindstrom, K. *J. Chromatogr.* **1981**, 214, 327-334.

20. Rostad, C.E.; Pereira, W.E.; Ratcliff, S.M. *Anal. Chem.* **1984**, 56, 2856-2860.

21. Wells, M.J.M.; Michael, J.L. *J. Chromatogr. Sci.* **1987**, 25, 345-350.

22. Junk, G.A.; Richard, J.J. *Anal. Chem.* **1988**, 60, 451-454.

23. Hagen, D.F.; Markell, C.G.; Schmitt, G.A. *Anal. Chim. Acta.* **1990**, 236, 157-164.

24. Kraut-Vass, A.; Thoma, J. *J. Chromatogr.* **1991**, 538, 233-240.

25. Arthur, C.L.; Pawliszyn, J. *Anal. Chem.* **1990**, 62, 2145-2148.

26. Zhang, Z.; Yang, M.J.; Pawliszyn, J. *Anal. Chem.* **1994**, 66, 844A-853A.

27. Pawliszyn, J. *Trends Anal. Chem.* **1995**, 14, 113-122.

28. Gorecki, T.; Boyd-Boland, A.; Zhang, Z.; Pawliszyn, J. *Can. J. Chem.* **1996**, 74, 1297-1308.

29. Arthur, C.L.; Killam, L.M.; Buchholz, K.D.; Pawliszyn, J. *Anal. Chem.* **1992**, 64, 1960-1966.

30. Louch, D.; Motlagh, S.; Pawliszyn, J. *Anal. Chem.* **1992**, 64, 1187-1199.

31. Vaes, W.H.J.; Hamwijk, C.; Ramos, E.U.; Verhaar, H.J.M.; Hermens, J.L.M. *Anal. Chem.* **1996**, 68, 4458-4462.

32. Ai, J. *Anal. Chem.* **1997**, 69, 1230-1236.

33. Dewulf, J.; Van Langenhove, H.; Everaert, M. *J. Chromatogr.* **1997**, 761, 205-217.

34. Gorecki, T.; Pawliszyn, J. *Anal. Chem.* **1995**, 67, 3265-3274.

35. Zhang, Z.; Pawliszyn, J. *Anal. Chem.* **1993**, 65, 1843-1852.

36. Chen, J.; Pawliszyn, J. *Anal. Chem.* **1995**, 67, 2530-2533.

37. Drozd, J.; Novak, J. *J. Chromatogr.* **1979**, 165, 141-165.

38. Nunez, A.J.; Gonzalez, L.F.; Janak, J. *J. Chromatogr.* **1984**, 300, 127-162.

39. Kepner, R.E.; Maarse, H.; Strating, J. *Anal. Chem.* **1964**, 36, 77-82.

40. Drozd, J.; Novak, J. *J. Chromatogr.* **1977**, 136, 37-44.

41. Drozd, J.; Novak, J. *J. Chromatogr.* **1978**, 152, 55-61.

42. Michael, L.C.; Erickson, M.D.; Parks, S.P.; Pellizzari, E.D. *Anal. Chem.* **1980**, 52, 1836-1841.

43. Novak, J.; Zluticky, J.; Kubelka, V.; Mostecky, J. *J. Chromatogr.* **1973**, 76, 45-50.

44. Bellar, T.A.; Lichtenberg, J.J. *J. Am. Water Works Assoc.* **1974**, 66, 739-744.

45. Wasik, S.P. *J. Chromatogr. Sci,* **1974**, 12, 845-848.

46. Bertsch, W.; Anderson, E.; Holzer, G. *J. Chromatogr.* **1975**, 112, 701-718.

47. Grob, K. *J. Chromatogr.* **1973**, 84, 255-273.

48. Grob, K.; Grob, G. *J. Chromatogr.* **1974**, 90, 303-313.

49. Grob, K.; Grob, K. Jr.; Grob, G. *J. Chromatogr.* **1975**, 106, 299-315.

50. Grob, K.; Zurcher, F. *J. Chromatogr.* **1976**, 117, 285-294.

51. Lunte, S.M.; Lunte, C.E. In *Advances in Chromatography*; Brown, P.R.; Grushka, E., Eds.; Marcel Dekker: New York, 1996; Vol. 36, Chapter 8.

52. Janle, E.M.; Kissinger, P.T. In *Advances in Food and Nutrition Research*; Coburn, S.P.; Townsend, D.W., Eds.; Academic: San Diego, 1996; Vol. 40, Chapter 11.

53. Audunsson, G. *Anal. Chem.* **1986**, 58, 2714-2723

54. Jonsson, J.A.; Lovkvist, P.; Audunsson, G.; Nilve, G. *Anal. Chim. Acta.* **1993**, 277, 9-24.

55. Thordarson, E.; Palmarsdottir, S.; Mathiasson, L.; Jonsson, J.A. *Anal. Chem.* **1996**, 68, 2559-2563.

56. Pratt, K.F.; Pawliszyn, J. *Anal. Chem.* **1992**, 64, 2101-2106.

57. Pratt, K.F.; Pawliszyn, J. *Anal. Chem.* **1992**, 64, 2107-2110.

58. Yang, M.J.; Harms, S.; Luo, Y.Z.; Pawliszyn, J. *Anal. Chem.* **1994**, 66, 1339-1346.

59. Yang, M.J.; Pawliszyn, J. *Anal. Chem.* **1993**, 65, 2538-2541.

60. Liu, S.; Dasgupta, P.K. *Anal. Chem.* **1995**, 67, 2042-2049.

61. Cardoso, A.A.; Dasgupta, P.K. *Anal. Chem.* **1995**, 67, 2562-2566.

62. Dasgupta, P.K.; Kar, S. *Anal. Chem.* **1995**, 67, 3853-3860.

63. Liu, H.; Dasgupta, P.K. *Anal. Chem.* **1995**, 67, 4221-4228.

64. Liu, H.; Dasgupta, P.K. *Anal. Chem.* **1996**, 68, 1817-1821.

65. Murray, D.A.J. *J. Chromatogr.* **1979**, 177, 135-140.

66. van Rensburg, J.F.J.; Hassett, A.J. *J. High. Resolut. Chromatogr. Chromatogr. Commun.* **1982**, 5, 574-576.

67. Attygalle, A.B.; Morgan, E.D. *Anal. Chem.* **1986**, 58, 3054-3058.

68. Danesi, P.R.; Chiarizia, R. *CRC Crit. Rev. Anal. Chem.* **1980**, 10, 1-126.

69. Laddha, G.S.; Degaleesan, T.E. *Transport Phenomena in Liquid Extraction*; Tata McGraw-Hill: New Delhi, 1976; Chapter 3.

70. Tarasov, V.V.; Yagodin, G.A. In *Ion Exchange and Solvent Extraction*; Marinsky, J.A.; Marcus, Y., Eds.; Marcel Dekker: New York, 1988; Vol. 10, Chapter 4.

71. Davies, J.T.; Rideal, E.K. *Interfacial Phenomena*; Academic Press: New York, 1961; Chapter 7.

72. Pratt, H.R.C. In *Handbook of Solvent Extraction*; Lo, T.C.; Baird, M.H.; Hanson, C., Eds.; Wiley: New York, 1983; Chapter 3.

73. Hanna, G.J.; Noble, R.D. *Chem. Rev.* **1985**, 85, 583-598.

74. Cussler, E.L. *Diffusion: Mass Transfer in Fluid Systems*; Cambridge University Press: Cambridge, UK, 1984; Chapters 1, 2, 9, 11.

75. Nernst, W. *Z. Phys. Chem.* **1904**, 47, 52.

76. Lewis, W.K.; Whitman, W.G. *Ind. Eng. Chem.* **1924**, 16, 1215-1220.

77. Higbie, R. *Trans. AIChE* **1935**, 31, 365-389.

78. Danckwerts, P.V. *Ind. Eng. Chem.* **1951**, 43, 1460-1467.

79. Crank, J. *The Mathematics of Diffusion*, 2nd ed.; Clarendon Press: Oxford, UK, 1975; Chapter 3.

80. Taylor, G. *Proc. R. Soc. A* **1953**, 219, 186-203.

81. Taylor, G. *Proc. R. Soc. A* **1954**, 225, 473-477.

82. Aris, R. *Proc. R. Soc. A* **1956**, 235, 67-77.

83. Cussler, E.L. *Diffusion: Mass Transfer in Fluid Systems*; Cambridge University Press: Cambridge, UK, 1984; Chapters 4, 5.

84. Crank, J. *The Mathematics of Diffusion*, 2nd ed.; Clarendon Press: Oxford, UK, 1975; Chapter 10.

85. Grushka, E.; Kikta, E.J. Jr. *J. Phys. Chem.* **1974**, 78, 2297-2301.

86. Ouano, A.C. *Ind. Eng. Chem. Fundam.* **1972**, 11, 268-271.

87. Pratt, K.C.; Slater, D.H.; Wakeham, W.A. *Chem. Eng. Sci.* **1973**, 28, 1901-1903.

88. Fossey, L.; Cantwell, F.F. *Anal. Chem.* **1982**, 54, 1693-1697.

89. Cyan, E.D. In *CRC Handbook of Chemistry and Physics*, 70th ed.; Weast, R.C.; Lide, D.R., Eds.; CRC Press: Boca Raton, FL, 1989; p C-703.

90. van der Molen, H.J. In *Hormones in Blood*, 3rd ed.; Gray, C.H.; James, V.H.T., Eds.; Academic Press: London, UK, 1979; Vol. 3, Chapter VIII.

91. Liley, P.E.; Reid, R.C.; Buck, E. In *Chemical Engineers' Handbook*, 6th ed.; Perry, R.H.; Green, D.W., Eds.; McGraw-Hill: New York, 1984; Chapter 3, pp258-259.

92. Sternberg, J.C. In *Advances in Chromatography*; Giddings, J.C.; Keller, R.A., Eds.; Marcel Dekker: New York, 1966; Vol. 2, Chapter 6.

93. Laddha, G.S.; Degaleesan, T.E. *Transport Phenomena in Liquid Extraction*; Tata McGraw-Hill: New Delhi, 1976; Chapters 6,7.

94. KaleidaGraph 3.0, Synergy Software, Reading, PA.

95. Higuchi, T.; Michaelis, A.F. *Anal. Chem.* **1968**, 40, 1925-1931.

96. Albery, W.J.; Burke, J.F.; Leffler, E.B.; Hadgraft, J. *J. Chem. Soc., Faraday Trans.* **1976**, 72, 1618-1626.

97. Cantwell, F.F.; Freiser, H. *Anal. Chem.* **1988**, 60, 226-230.

98. *CRC Handbook of Chemistry and Physics*, 70th ed.; Weast, R.C.; Lide, D.R., Eds.; CRC Press: Boca Raton, FL, 1989; p F-40.

99. *CRC Handbook of Chemistry and Physics*, 70th ed.; Weast, R.C.; Lide, D.R., Eds.; CRC Press: Boca Raton, FL, 1989; p F-4.

100. Riddick, J.A.; Bunger, W.B. *Organic Solvents. Physical Properties and Methods of Purification*, 3rd ed.; Wiley-Interscience: New York, 1970.

101. Fogiel, M. *Handbook of Mathematical Formulas, Tables, Functions, Graphs, Transforms*; Research and Education Association: New York, 1983.

102. Burington, R.S. *Handbook of Mathematical Tables and Formulas*, 5th ed.; McGraw-Hill: New York, 1973.

103. *CRC Handbook of Chemistry and Physics*, 70th ed.; Weast, R.C.; Lide, D.R., Eds.; CRC Press: Boca Raton, FL, 1989; p D-198.

104. Nasim, K.; Meyer, M.C.; Autian, J. *J. Pharm. Sci.* **1972**, 61, 1775-1780.

105. Watanabe, S.; Tani, T.; Watanabe, S.; Seno, M. *Lipids* **1990**, 25, 633-638.

106. Harriot, P. *Can. J. Chem. Eng.* **1962**, 40, 60-69.

107. McManamey, W.J.; Davies, J.T.; Woollen, J.M.; Coe, J.R. *Chem. Eng. Sci.* **1973**, 28, 1061-1069.

108. Westphal, U. *Steroid-Protein Interactions*; Springer-Verlag: New York, 1971; Chapter IV.

109. Karush, F. *J. Am. Chem. Soc.* **1951**, 73, 1246-1252.

110. Schellman, J.A.; Lumry, R.; Samuels, L.T. *J. Am. Chem. Soc.* **1954**, 76, 2808-2813.

111. Watanabe, S.; Tani, T.; Watanabe, S.; Seno, M. *Biochim. Biophys. Acta.* **1991**, 1073, 275-284.

112. Watanabe, S.; Sato, T. *Biochim. Biophys. Acta.* **1996**, 1289, 385-396.

113. Vaes, W.H.J.; Ramos, E.U.; Verhaar, H.J.M.; Seinen, W.; Hermens, J.L.M. *Anal. Chem.* **1996**, 68, 4463-4467.

114. Westphal, U. *Steroid-Protein Interactions*; Springer-Verlag: New York, 1971.

115. Westphal, U. In *Mechanism of Action of Steroid Hormones*; Ville, C.A.; Engel, L.L., Eds.; Permangon: New York, 1961; pp. 33-89.

116. Sandberg, A.A.; Slaunwhite, W.R. Jr.; Antonades, H.N. In *Recent Progress in Hormone Research*; Pincus, G., Ed.; Academic Press: New York, 1957; Volume XIII; Chapter 6.

117. Klotz, I.M. *Arch. Biochem.* **1946**, 9, 109-117.

118. Shaw, D.J. *Introduction to Colloid and Surface Chemistry*, 3rd ed.; Butterworth: Boston, 1980; Chapter 4.

119. Davies, J.T.; Rideal, E.K. *Interfacial Phenomena*, 2nd ed.; Academic: New York, 1963; Chapter 1.

120. Harkins, W.D.; Brown, F.E. *J. Am. Chem. Soc.* **1919**, 41, 499-524.

121. Boucher, E.A.; Evans, M.J.B. *Proc. R. Soc. Lond A.* **1975**, 346, 349-374.

122. Lando, J.L.; Oakley, H.J. *J. Coll. Interface Sci.* **1967**, 25, 526-530.

123. Amankwa, L.; Cantwell, F.F. *Can. J. Chem.* **1991**, 69, 88-93.

124. Ryan, M.T.; Chopra, R.K. *Biochim. Biophys. Acta.* **1976**, 427, 337-349.

125. Mohammadzadeh-K., A.; Feeney, R.E.; Smith, L.M. *Biochim. Biophys. Acta* **1969**, 194, 246-255.

126. Westphal, U.; Ashley, B.D.; Selden, G.L. *J. Am. Chem. Soc.* **1958**, 80, 5135-5138.

127. Fulton, R.B.; Kratochvil, B. *Anal. Chem.* **1980**, 52, 546-552.

128. Creeth, J.M. *Biochem. J.* **1952**, 51, 10-17.

129. Wagner, M.L.; Scheraga, H.A. *J. Phys. Chem.* **1956**, 60, 1066-1076.

130. Stern, K.G.; Singer, S.; Davis, S. *J. Biol. Chem.* **1947**, 167, 321-330.

131. Wilke, C.R.; Chang, P. *A.I.Ch.E.J.* **1955**, 1, 264-270.

132. Mendel, C.M.; Miller, S.B.; Siiteri, P.R.; Murai, J.T. *J. Steroid Biochem. Molec. Biol.* **1990**, 37, 245-250.

133. Graham, D.E.; Phillips, M.C. *J. Coll. Interface Sci.* **1979**, 70, 403-414.

134. Graham, D.E.; Phillips, M.C. *J. Coll. Interface Sci.* **1979**, 70, 415-426.

135. Graham, D.E.; Phillips, M.C. *J. Coll. Interface Sci.* **1979**, 70, 427-439.

136. Poerschmann, J.; Zhang, Z.; Kopinke, F.-D.; Pawliszyn, J. *Anal. Chem.* **1997**, 69, 597-600.

137. Zhang, Z.; Poerschmann, J.; Pawliszyn, J. *Anal. Communications* **1996**, 33, 219-221.

APPENDIX

This appendix contains tabulated (x-y) experimental data for the plots shown throughout the thesis.

Data for Figure 4.3:

$[4\text{-MAP}]_o$, mmol/L	GC peak area ratio
1.525	0.4756
1.525	0.4636
3.050	0.9340
3.050	0.9382
6.100	1.892
6.100	1.900
12.20	3.665
12.20	3.666

Data for Figure 4.4:

Stirring time (min)	$[4\text{-MAP}]_o$, mM 900 rpm	$[4\text{-MAP}]_o$, mM 1200 rpm	$[4\text{-MAP}]_o$, mM 1500 rpm	$[4\text{-MAP}]_o$, mM 1800 rpm
2	1.05	1.39	1.65	1.84
4	2.16	2.55	3.00	3.26
6	2.97	3.64	3.90	4.23
8	3.59	4.27	4.65	4.87
10	4.12	4.82	5.17	5.43
15	5.09	5.63	6.01	6.25
20	5.82	6.15	6.36	6.46
25	6.04	6.39	6.55	
30	6.27	6.53		

Data for Figure 4.5:

log s (s in rpm)	log $\bar{\beta}_o$ ($\bar{\beta}_o$ in cm/s)
2.954	-3.907 ± 0.014
3.079	-3.794 ± 0.011
3.176	-3.733 ± 0.007
3.255	-3.687 ± 0.009

Data for Figure 4.6:

$[4\text{-MAP}]_{aq,\ eq}$ (mmol/L)	$[4\text{-MAP}]_{o,\ eq}$ (mmol/L)
0.0834	3.15
0.166	6.45
0.249	9.54
0.328	13.3
0.417	15.7

Data for Figure 4.7:

$[4\text{-MAP}]_{aq,\ initial}$ (mmol/L)	GC signal
0.109	0.5351
0.217	1.082
0.326	1.526
0.434	2.158
0.543	2.646

Data for Figure 5.2:

# of flushing cycles	Peak Area (dodecane)
0	90560
1	2467
2	1199
3	1063
5	653
9	443
19	0 (not integrated)

Data for Figure 5.3:

$[4\text{-MAP}]_o$, mmol/L	GC peak area ratio
1.397	0.4649
1.397	0.4717
2.790	0.9466
2.790	0.9414
5.588	1.896
5.588	1.889
11.18	3.688
11.18	3.629

Data for Figure 5.4:

Stirring time (min)	$[4\text{-MAP}]_o$, mM 900 rpm	$[4\text{-MAP}]_o$, mM 1200 rpm	$[4\text{-MAP}]_o$, mM 1500 rpm	$[4\text{-MAP}]_o$, mM 1800 rpm
1	1.64	2.14	2.48	2.80
2	2.89	3.49	4.10	4.40
3	3.73	4.59	5.02	5.41
5	5.06	5.75	6.00	6.26
8	6.05	6.25	6.46	6.58
12	6.41	6.60		

Data for Figure 5.6:

$[4\text{-NT}]_o$, mmol/L	GC peak area ratio
1.230	0.3357
2.461	0.6717
4.922	1.379
9.844	2.761
19.69	5.337
39.38	10.70

Data for Figure 5.7:

$[4\text{-MAP}]_o$, mmol/L	GC peak area ratio
1.405	0.4238
2.810	0.8575
5.620	1.708
11.24	3.467

Data for Figure 5.8:

$[malathion]_o$, mmol/L	GC peak area ratio
0.5819	0.3286
1.164	0.6753
2.328	1.360
4.655	2.734
9.310	5.583
18.62	10.64

Data for Figure 5.9:

$[progesterone]_o$, mmol/L	GC peak area ratio
0.07938	0.06430
0.1588	0.1350
0.3175	0.2940
0.6350	0.6398
1.270	1.254
2.540	2.402

Data for Figure 5.10:

Stirring time (min)	$[4\text{-NT}]_o$, mmol/L
1	2.24
2	3.28
3	5.28
5	6.77
8	9.23
12	10.4
20	12.2
30	11.7

Data for Figure 5.11:

Stirring time (min)	$[4\text{-MAP}]_o$, mmol/L
0.5	1.31
1	1.93
1.5	2.43
2	2.77
3	3.34
4	4.01
5	4.55
6	4.64
8	4.84
10	4.96

Data for Figure 5.12:

Stirring time (min)	$[malathion]_o$, mmol/L
5	0.758
10	1.37
15	1.81
20	2.14
30	2.46
45	2.68

Data for Figure 5.13:

Stirring time (min)	$[progesterone]_o$, mmol/L
10	0.126
15	0.177
20	0.236
30	0.278
45	0.318
60	0.338

Data for Figure 5.14:

Compound	D_{aq} (cm^2/s) x 10^6	β_{aq} (cm/s) x 10^3
progesterone	3.98 ± 0.32	3.60 ± 0.40
malathion	5.46 ± 0.39	5.08 ± 0.26
4-MAP	7.68 ± 0.15	7.14 ± 0.73
4-NT	8.02 ± 0.45	7.63 ± 0.65

Data for Figure 5.15:

1/s (s in rpm) x 10^4	δ_{aq} (cm) x 10^4
5.556	8.75 ± 0.22
6.667	10.1 ± 0.3
8.333	12.4 ± 0.5
11.11	16.9 ± 0.7

Data for Figure 6.2:

Stirring time (min)	$R/[S]_{T,eq}$ a) no BSA	$R/[S]_{T,eq}$ b) 1% BSA
2.5		0.04336
5	0.1622	0.08718
7.5		0.1040
10	0.2791	0.1160
12.5		0.1376
15	0.3544	0.1492
20	0.4784	0.1681
25		0.1893
30	0.5698	
35		0.2215
45	0.7351	0.2065
60	0.7820	0.2169
90	0.8053	

Data for Figure 6.3:

$[S]_{T,aq}$ (mol/L) x 10^6	R (GC Response)
1.227	0.4530
1.227	0.5164
2.455	0.9771
2.455	0.9686
3.682	1.375
3.682	1.562
4.910	1.836
4.910	1.791
6.137	2.632
6.137	2.252

Data for Figure 6.4:

$[S]_{T,\ eq.\ added}$ (mol/L) x 10^6	R (GC Response)
3.21	0.4739
3.21	0.4319
3.21	0.3949
6.42	0.8119
6.42	0.8450
6.42	0.7183
9.63	1.216
9.63	1.215
9.63	1.334
12.8	1.548
12.8	1.935
12.8	1.727
16.0	2.176
16.0	2.064
16.0	1.996